ZFP423 Coordinates Notch Pathway, Bmp Signaling and EBF/COE Transcription Factors to Regulate *Hes5* Gene Expression

Thesis

oro.open.ac.uk

Giacomo Masserdotti

ZFP423 coordinates Notch Pathway, Bmp Signaling

and EBF/COE Transcription Factors to regulate

Hes5 Gene Expression

Doctor of Philosophy in

Molecular and Cellular Biology

DIBIT

April 2010

Date of Submission: 13 April 2010
Date of Award: 10 May 2010

ProQuest Number: 13837638

ProQuest 13837638

Abstract

Zinc finger protein 423 encodes a 30 Zn-finger transcription factor involved in cerebellar and olfactory development. ZFP423 is a known interactor of SMAD1-SMAD4 and of Collier/Olf-1/EBF proteins, and acts as a modifier of retinoic acid-induced differentiation. In this thesis, we show that ZFP423 interacts functionally and molecularly with the Notch1 intracellular domain (NICD) in mammalian cell lines and in Xenopus laevis neurula embryos, to activate the expression of the Notch1 target Hes5 / ESR1. This effect is antagonized by EBF transcription factors, both in cultured cells and in Xenopus laevis embryos, and amplified in vitro by BMP4, the morphogen triggering the activation of SMAD1-SDMAD4 complex.

Taken together, the data presented in this thesis suggest that ZFP423 acts to integrate BMP- and Notch signaling, selectively promoting their convergence onto the Hes5 gene promoter.

Table of Contents

To Chiara

Introduction

From fertilization to neural tube formation

In mammals, fertilization occurs in the ampulla of the oviduct, a region close to the ovary. After fertilization, the first cleavage begins about one day later and is a normal meridional division; in the second cleavage, one of the blastomeres divides meridionally, and the other divides equatorially, in process called *rotational cleavage* (Gulyas, 1975). Mammalian blastomeres do not all divide at the same time, so that they do not increase exponentially from 2 to 4- to 8-cell stage, but frequently contain an odd number of cells. Mouse embryo proper derives from the *inner cell mass* (ICM), which originates from a small group of internal cells at the *morula* stage (16-cell), and, by 64-cell stage, becomes separated by the *trophoblast*, composed by the external cells in the morula.

The inner cell mass forms two layers, the hypoblast, and the epiblast. The former will give rise to the extrambryonic endoderm, which forms the yolk sac; the latter is split by small cells that coalesce to separate the embryonic epiblast from the other epiblast cells that line the amniotic cavity.

At the beginning of the *gastrulation*, epiblast cells located at one region around the circumference of the egg cylinder adjacent to the extra-embryonic ectoderm undergo an epithelial-to-mesenchymal transition to form a transient structure called *the primitive streak*. At the interior end of the primitive streak lies the *node*, an organizer that has a bi-laminar organization with a dorsal and a ventral cell layer. Mammalian embryos appear to have two signaling centers: one in the node, the other one in the anterior visceral endoderm (AVE). The node is responsible for the formation of all the body, and the two signaling centers work together to form the anterior region of the embryo. The *notochord* forms by the dorsal infolding of the ciliated cells of the node, and will secrete Sonic Hedgehog (SHH), while the AVE expresses several molecules necessary for the head formation, such as *Lim1* and *Otx2*, and the paracrine factor *Cerberus*.

During gastrulation, three germ layers are generated: the endoderm, the mesoderm and the ectoderm. The endoderm will form the gut, associated organs, and the lungs. The mesoderm will give rise to most of the embryonic mesenchyme and to the notochord; the latter plays a central role in the induction of overlying neural tissue and is the precursor of the vertebrate column. The ectoderm forms the outer epithelium of the body and the neural tube, from

which the nervous system develops.

Neurulation is the process through which a portion of the dorsal ectoderm is induced to become neural ectoderm, the so-called neural plate, which, then, will form the neural tube. During neural induction, the neural-inducing signals, such as fibroblast growth factors (FGFs) (Streit et al., 2000; Wilson et al., 2000), are released by the organizer, and counteract Bone Morphogenic Proteins (BMP) molecules, secreted by non-neural ectoderm, to generate the neural plate. The early neural plate is initially rostral, and more rostral regions form as a result of the caudal regression of the Organizer.

Decades of studies have contributed to shed light on the mechanisms underlying neural tube formation: studies conducted mainly in *Xenopus laevis* embryos, but also in other model systems, have demonstrated that the ectoderm is naturally fated to become neuroectoderm, but BMP signaling represses this default fate, causing the ectoderm to become epidermis. The natural tendency of the ectoderm to develop into neuroectoderm is defined as *neural induction default model*. The node is essential to induce the formation of the neural plate, because it secretes BMP antagonists, such as Chordin and Noggin.

The neural plate is shaped by the movements of the epidermal and the lateral neural plate regions, and lengthens along the anterior-posterior axis. Initially, the ectodermal cells of the forming neural plate increase in height, undergo pseudo-stratification and begin to express unique molecular markers. Subsequently, the neural plate starts to bend, and this process involves the formation of hinge regions – one median and two dorso-lateral – where the neural plate contacts surrounding tissues. The median hinge point (MHP) is attached to the prechordal plate, and the paired dorso-lateral hinge points (DLHP) are attached to adjacent epidermal ectoderm. After MHP forms, the neural plate on each side undergoes dorsal elevation around the longitudinal axis centered at the midline furrow. This results in the formation of the neural groove, an initially V-shaped space extending the length of the neural plate, flanked bilaterally by the incipient neural folds. Finally, the neural folds fuse, the detached neuroepithelial layers from both sides fuse together deep to the epidermal ectoderm, establishing the roof plate of the neural tube (**Fig. 1.1A-F**).

The cavity of the neural tube gives rise to the ventricular system of the central nervous system, while the epithelial cells that line the walls of the neural tube constitute the *neuroepithelium*, which will generate all the neurons and glial cells of the Central Nervous

System (CNS).

From Neuroepithelial cells to Radial glial cells

Structurally, the neuroepithelium (NE) is a pseudo-stratified layer. That is, although there may be up to 10 layers of nuclei, the cytoplasm of each cell extends to contact both the apical and basal surface of the wall, resulting in a bipolar cellular morphology up to 100 μm long (Fig. 1.1G). Progenitor cells are born at the apical surface of the NE and their nuclei move toward the basal side of the NE during the G1-phase of the cell cycle. After completing the S-phase, the nuclei return to the apical surface, where they undergo division as their parent cells did. Thus, the location of any given progenitor cell during this interkinetic nuclear migration reflects the progression of the cell along the cell cycle (Fig. 1.1H). This phenomenon was firstly suggested by Sauer (1935), and later verified by experiments in which 3H-thymidine uptake from the basal half of the NE was measured shortly after injection, and found to accumulate in the apical surface (Sauer and Walker, 1959; Sidman et al., 1959).

The apical-basal polarity of neuroepithelial cells is demonstrated by the differential localization of certain proteins, such as CD133 (Prominin-1), selectively expressed in the apical plasma membrane (Weigmann et al., 1997), or intergrin-α6 (Wodarz and Huttner, 2003), concentrated in the basal plasma membrane. Even within the lateral plasma membrane, a gradient of transmembrane proteins in the apical-basal direction can be detected, such as those of N-cadherin (Aaku-Saraste et al., 1996) or ephrin B1 (Stuckmann et al., 2001), more concentrated towards the apical end.

Historically, neuroepithelial cells in the neural tube were believed to produce two separate pools of glial and neuronal progenitors (His, W., 1889): this concept remained predominant for a century, although in 1935 Sauer had already shown that the two presumptive progenitors were indeed the same cell at different cell cycle stages. Only in late eighties of the last century accumulated evidence convinced researchers that glia and neurons arise from a common progenitor (Galileo et al., 1990; Temple, 1989).

Neuroepithelial cells are stem cells, accordingly to the criteria of self-renewal and multipotency: they undergo symmetric cell division to expand the pool of cells, and they can give rise to neurons and glia. Although some old reports indicated that neurons can originate

from neuroepithelial cells, the current view is that *neurogenesis*, that is the generation of cells fated to become neurons, takes place when neuroepithelial cells transform into self renewing progenitors cells, referred to as radial glia. This transition occurs around embryonic day E9-E12 in mouse embryos, and corresponds to the onset of the neurogenic phase, during which most of the neurons are generated.

To permit a full comprehension of the literature concerning neuroepithelial cell proliferation, differentiation, and its relationship with radial glial cells, it is important here to underline that many reports before the late nineties (e.g. Williams and Price, 1995) referred to neuroepithelial cells as the progenitor cells located in the VZ, and others do not distinguish between neuroepithelial cells and radial glial cells (for instance (Haubensak et al., 2004; Iacopetti et al., 1999)). In the latter case, they prefer to talk about neuron-generating neuroepithelial cells, that are radial glial cells.

Radial glial cells retain many features of neuroepithelial cells, such as the apical-basal polarity, the apical localization of Prominin-1 (Weigmann et al., 1997), and interkinetic nuclear migration, with their nuclei undergoing mitosis at the apical surface of the ventricular zone (VZ) - the most apical cell layer that lines the ventricle and contains most of the progenitor cell bodies. In contrast to neuroepithelial cells, radial glial cells show several astroglial properties: astrocyte-specific markers such as glutamate transporter (GLAST), the Ca2+-binding protein S100β, glial fibrillary acidic protein (GFAP), vimentin, glycogen granules and brain-lipid-binding-protein (BLBP) start to appear in most cells located in the ventricular zone during, but not before, neurogenesis (Campbell and Gotz, 2002; Gotz, 2003).

Radial glial cells differ from neuroepithelial cells in two essential features: they switch from symmetric to asymmetric cell division, and their differentiation potential seems to be restricted.
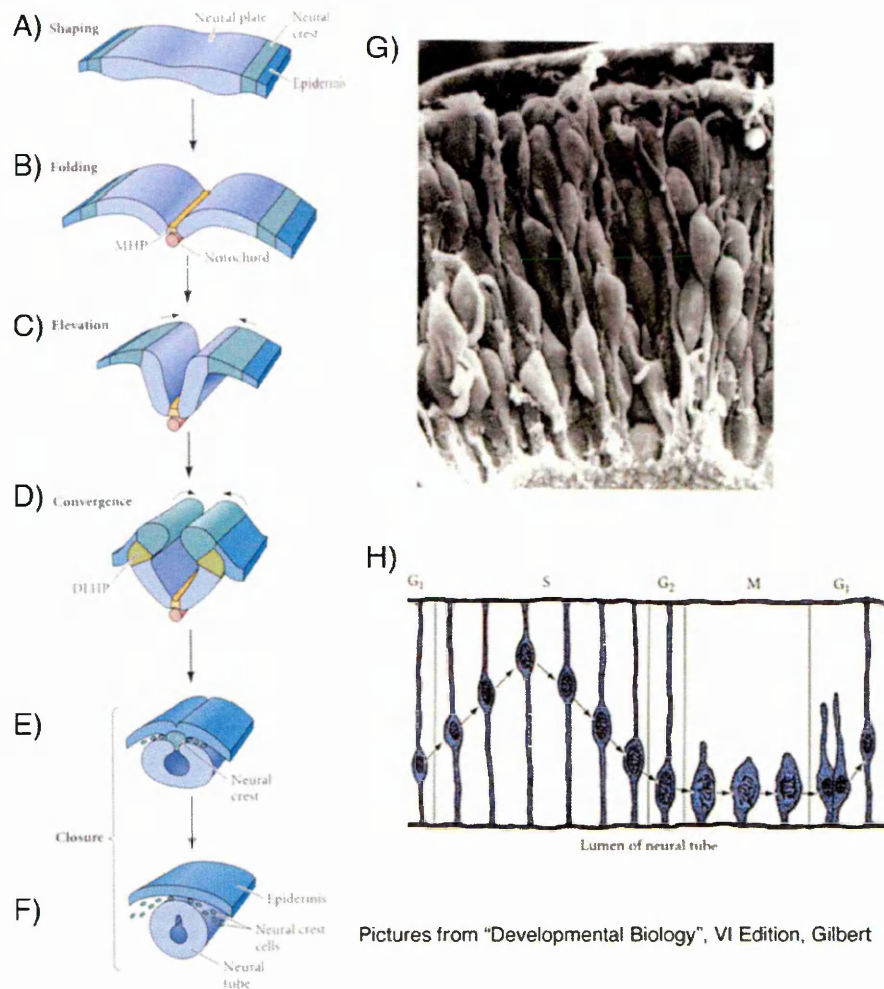
Figure 1.1 – Neural tube folding, pseudo-stratified neuroepithelium and interkinetic nuclear migration. A-F) Schematic representation of neural tube folding. **G)** High magnification of pseudo-stratified neuroepithelium. **H)** Sketch of interkinetic nuclear migration occurring in the developing neuroepithelium. Pictures from "Developmental Biology", VI edition, Gilbert.

Symmetric and asymmetric cell division

Traditionally, symmetric cell division has been defined as a division that generates two identical daughter cells, while asymmetric cell division produces two daughter cells with different fate. More recently, these definitions have been revised, being asymmetric cell division preferentially associated with an unequal distribution of cellular components between the resulting two daughter cells. Evidence for the distribution-defined asymmetric division has been obtained by monitoring cell division in intact tissue using time-lapse microscopy, analysis of mitotic cells *in vivo*, as well as identifying molecular markers.

By analogy to the proliferative versus neurogenic divisions in *Drosophila melanogaster*,

14

the orientation of the cleavage plane during mitosis was proposed to determine the fate of the cells: if vertical with respect to the VZ layer, the cleavage results in symmetric, proliferative division of neuroepithelial and radial glial cells, because of an equal distribution of apical and basal constituents. On the other hand, cleavage plane parallel to the surface of VZ results in asymmetric, neurogenic division, because one daughter cell will inherit the apical membrane constituents while the other will inherit and the basal ones (Chenn and McConnell, 1995). Against this simplistic hypothesis were two major observations: firstly, horizontal cleavages are too rare (Chenn and McConnell, 1995) to explain the high rate of neuron generation, and, secondly, the apical membrane of radial glial cells represent a small fraction of the total membrane (Kosodo et al., 2004), thus unable to generate one of the two daughter cells. Huttner and collaborators hypothesized (Huttner and Brand, 1997) and then demonstrated (Kosodo et al., 2004) that vertical cleavage planes can generate either two identical daughter cells or two distinct daughter cells, depending on the inheritance of the apical plasma membrane and the junctional complexes found in the most apical end of the lateral plasma membrane. If the apical plasma membrane is equally distributed between the two daughter cells, division is symmetric; otherwise, it is asymmetric (Kosodo et al., 2004). The anti-proliferative gene *Tis21* (Iacopetti et al., 1994; Iacopetti et al., 1999; Lim et al., 1987; Rouault et al., 1996) was used as marker to distinguish proliferative versus neurogenic division (Kosodo et al., 2004). *Tis21* mRNA, in fact, is transiently expressed in G1/S phase of cells undergoing neurogenic division, and the cell that starts to differentiate inherits TIS21 protein (Iacopetti et al., 1999). Progenitor cells undergoing proliferative/symmetric division do not express *Tis21*. Analysis of knock-in embryos that express GFP from the *Tis21* locus showed that more than 80% of mitotic neuroepithelial cells (= radial glial cells) that distribute the apical plasma membrane to both daughter cells do not express *Tis21* and undergo proliferative divisions. On the other hand, almost 90% of mitotic neuroepithelial cells that distribute the apical plasma membrane to only one daughter cell express *Tis21* and undergo neurogenic divisions (Kosodo et al., 2004). Specifically, the daughter cell that inherit the apical membrane remains uncommitted, thus maintaining the pool of proliferating cells, while the daughter cell which does not inherit it is fated to neuronal differentiation. Importantly, other molecules have been found to be differentially segregated between daughter cells after asymmetric division, such as PAR3 (Kosodo et al., 2004) – a protein localized to the apical membrane and implicated in cell

15

polarity (Lin et al., 2000) – and SNARE proteins (soluble N-ethylmaleimide-sensitive fusion protein (NSF) attachment protein receptor proteins) (Chae et al., 2004; Low et al., 2003), whose members are proximal either to the basal or the apical membrane.

Another type of neuronal progenitor has been recently described, the basal progenitor cell (Haubensak et al., 2004; Noctor et al., 2004). Basal progenitors originate from the mitosis of radial glial cells at the apical surface of neuroepithelium, are TIS21 positive (Haubensak et al., 2004), but they can be distinguished for their localization, and for the expression of specific markers. In fact, when basal progenitors are in S-phase and their nuclei are close to the basal side of the VZ, called sub-ventricular zone (SVZ), they retract their extension to the apical membrane and divide symmetrically, giving rise to two post-mitotic neurons. Unlike radial glial cells, they express the transcription factor TBR2 (Englund et al., 2005), the vesicular glutamate transporter VGlut2 (Schuurmans et al., 2004), the non-coding RNA Svet1 (Tarabykin et al., 2001), and, at some stages, higher levels of the bHLH transcription factor Neurogenin2 (*Neurog2*, see later) (Miyata et al., 2004).

In *D.melanogaster*, asymmetric segregation of Numb protein has been linked with cell-fate choice (Bodmer et al., 1989; Rhyu et al., 1994) during development. Numb is a plasma-membrane-associated cytoplasmatic protein that antagonizes Notch signaling (Frise et al., 1996) (see later). In mammals, Numb is located at the apical side of the mitotic cells (Zhong et al., 1996), and early in development it may act as an inhibitor of progenitor differentiation (Zhong et al., 2000), while later as permissive protein for neuronal differentiation. In 80% of cell divisions that produce one progenitor and one neuron, Numb is asymmetrically distributed, while it is symmetrically distributed when cell division generates two identical daughter cells, either progenitor cells or neurons (Shen et al., 2002).

Whatever cell division occurs within progenitor compartment, the inheritance of radial glial fibers is still a matter of discussion. Several observations suggest that one daughter cell inherits the radial process, implying that the other one has to extend a new radial process (Hartfuss et al., 2003; Tamamaki et al., 2001). Noctor and colleagues reported that the daughter cell that inherits the radial process remains as radial glia cell within the VZ, while the other daughter cell never inherits the long radial process (Noctor et al., 2001; Noctor et al., 2004); in contrast, Miyata observed that in about 50% of all division the differentiating cell inherits radial glial process and loses only the apical ventricular process while migrating towards the

basal cortical plate (Miyata et al., 2001). This process, referred to as nuclear translocation, as the migrating cells maintain the basal contact while retracting the basal fiber (Nadarajah and Parnavelas, 2002), has been observed in various regions of the developing CNS, and with different techniques (Tamamaki et al., 2001). Taken together, these results indicate that radial fiber inheritance may not be correlated to a specific cell fate, as inheritance of the basal process occurs in post-mitotic neurons as well as radial glial cells.

Differentiation potential of radial glial cells

The second main feature that distinguishes radial glial cells from neuroepithelial cells is the ability to generate both neurons and glia. A growing amount of data, both *in vivo* and *in vitro*, indicates a high rate of heterogeneity among radial glial cells, both in time and space.

Early evidence came from lineage analysis of virally infected VZ precursors (Grove et al., 1993; Walsh and Cepko, 1993): upon retroviral infection, the viral genome is integrated into post-replicational DNA of the host genome, thereby inherited by only one daughter cell, and, eventually, by all the progeny of this daughter cell. Infection of VZ, constituted almost essentially by radial glial cells at the stages the experiments were performed, demonstrated *in vivo* that the majority of cells generated a single cell-type (either neurons or glia) while a minority of the clones contained a mix of both (McCarthy et al., 2001).

In vitro studies confirmed and further extend the notion of heterogeneity of radial glial cells: using transgenic mice carrying green fluorescent protein (GFP) cDNA under the control of the human GFAP (hGFAP) promoter, Malatesta and collaborators isolated radial glial cells from developing cerebral cortex by fluorescence-activating cell sorting (FACS) (Malatesta et al., 2003; Malatesta et al., 2000). Firstly, they verified that sorted cells were GLAST, BLBP or RC2 positive to confirm the glial origin; then, they plated the isolated radial glial cells at low density *in vitro*, and followed the progeny of individual cell. They performed the experiment at three different prenatal stage, E14, E16 and E18; they found that, both at E14 and E16, the largest population (60-70%) of radial glial cells gave rise to neurons only, a small subset generated radial glial cells only, and even a smaller population generated both neurons and glia, either radial glial cells, astrocytes or oligodendrocyte. On the contrary, radial glial cells isolated at E18 generated mainly glia (about 70%) and only a

30% of pure neuronal population. These data confirmed the observations made by *in vivo* lineage-tracing experiments, that (I) different subtypes of radial glial cells coexist at a given developmental stage in cerebral cortex, (II) most precursors are restricted in their potential, and, at the end of neurogenesis, (III) gliogenic radial glial cells proceed to generate glia.

From progenitors to neurons: neurogenesis at a glance

Neurogenesis, namely the differentiation of progenitor cells towards a neuronal fate, is the outcome of a complex program that directs the expression of specific genes within individual cells. This program is the result of a dynamic interplay between the environment where the cells reside, referred to as extrinsic determinants, and cellular properties, namely intrinsic determinants, which define the competence of the cell for responding to the environmental pathways at a given time and the degree of commitment towards specific developmental pathways.

The best-studied example of the neuronal commitment as a result of the interaction between extrinsic and intrinsic factors is the early regionalization of the neural tube. The position occupied by cells along the dorso-ventral and rostro-caudal axes define their future identities, through exposure to regionally restricted signaling factors.

Extrinsic signals

As mentioned before, during neural induction, secreted molecules contribute to generate the neural plate. The initial dorso-ventral (DV) and anterior-posterior (AP) patterning are set up by the action of several extracellular signaling molecules: FGF8, retinoic acid (RA), Wingless-related integration site (WNT), Sonic Hedgehog (SHH) and Bone Morphogenesis Proteins (BMP).

Fibroblast growth factor signaling

Fibroblast growth factors (FGFs) are a large family of secreted proteins composed of at least 23 members, some of which exist in different isoforms. FGFs are known to activate a

set of receptor tyrosine-kinases called Fibroblast Growth Factor Receptors (FGFRs). FGF binding leads to FGFR dimerization, which causes the trans-phosphorylation of the receptors and the activation of the multiple signaling pathways typical of the tyrosine-kinase receptor, such as mitogen-activated protein kinase (MAPK), phopshatidyl inositol-3-kinase (PI3K) and phospholipase C-gamma (PKCγ) pathway (**Fig. 1.2A**).

During neural tube formation, FGF8 is produced by the node and, then, by a caudal stem zone. *Fgf8* is expressed at highest level posteriorly: newly formed tissues degrade slowly *Fgf8* mRNA. Maintenance of caudal progenitors in this stem zone requires FGF signaling while the attenuation of FGF is necessary for neuronal differentiation. FGF8 is expressed also in the midbrain-hindbrain boundary, marking the Isthmic Organizer (IsO), and plays an important role in defining cerebellar development (see later).

Retinoic Acid

Retinoic acid (RA) is the most biologically active naturally occurring member of a family of molecules called retinoids, all of which derive from vitamin A. Once in the cells, vitamin A is enzymatically converted, first to retinal by the retinol or alcohol dehydrogenases (roDH or ADHs), and then to RA by the retinaldehyde dehydrogenases (RALDHs). Two cytocrome P450 enzymes – CYP26A1 and CYP26B1 (Sonneveld et al., 1999; White et al., 2000) – metabolize RA to inactive products.

When RA is synthesized, it enters into the cell and binds RA receptors, which act as transcription factors. There are two classes of RA receptors, retinoic acid receptors (RAR) and retinoid X receptor (RXR). Both receptors act as heterodimers, and recognize consensus sequences known as RA-responsive elements (RAREs) (**Fig. 1.2B**).

The role of RA during development has been studied in detail with different techniques – embryo treatment with RA (Avantaggiato et al., 1996), administration of RA synthesis inhibitors (Maden, 1996), dominant-negative form of the receptors (Blumberg et al., 1997): the data clearly showed that RA has a positive effect on posteriorization and dorsalization of tissues. Embryos treated with an excess of RA lose anterior structures such as the forebrain and eyes, while the hindbrain and the spinal cord expand and compensate; genes expressed more rostrally, such as *Otx2, Emx1* and *Dlx1*, are repressed, and posterior genes such as

Krox2, Pax2 and various Hox (*Hoxb4* and *Hoxb8* (Dekker et al., 1994)) are up-regulated and extend more anteriorly. Along the DV axis, RA treatment induces the differentiation of certain subsets of interneurons, characterized by the expression of homeobox genes such as *Dbx1, Dbx2, Evx1* and *Evx2* (Pierani et al., 1999), while ventral populations (positive, for instance, for the genes *Shh* and *Nkx6.1*) had expanded at the expense of dorsal population in RA-deficient quail embryos (Wilson et al., 2004).

Wnt signaling

Wingless-related integration site (WNTs) are secreted glycoproteins with an unusual post-translation modification - palmitoylation at a conserved cysteine - essential for their function (Willert et al., 2003). WNTs signal through Frizzled receptors (FZ), seven-pass transmembrane proteins. WNT-FZ complex activates Dishevelled (DVL), a cytoplasmic scaffold protein that brings together components of the pathway for an efficient transduction. In the canonical pathway, DVL induces the disassembly of a complex consisting of Axin, adenomatosis polysis coli (APC) glycogen synthase kinase 3β (GSK3β) and β-catenin. In normal conditions, GSK3β phosphorylates β-catenin, thereby triggering its degradation. Activation of the pathway results in the inhibition of GSK3β, leading to an increase of cytoplasmatic free β-catenin, which translocates into the nucleus and forms, together with β-catenin-T-cell specific transcription factor (TCF), a transcriptional activator complex (**Fig. 1.2C**).

Several lines of evidence indicate that WNT signaling plays a posteriorizing role during antero-posterior specification of the neural tube. Ectopic expression of WNTs or components of the WNT pathway leads to the suppression of anterior fates and induction of posterior markers (Darken and Wilson, 2001; Kiecker and Niehrs, 2001). Conversely, inhibition of WNT signaling leads to the expansion of forebrain markers (Lekven et al., 2001). Studies have been shown that anterior tissues release WNT antagonists crucial for the specification of the anterior neural tube. For instance, the WNT antagonist DKK1 is expressed by the organizer at the onset of gastrulation (Hashimoto et al., 2000); other antagonists, such as Cerberus and Frizzled-related protein (FRZB1) have been implicated in neural tube formation (Leyns et al., 1997).

A non-canonical pathway has been described in *D.melanogaster* and mammals: the polarity cell plan (PCP) pathway controls the orthogonal polarity of the cell within the epithelium (Huelsken and Birchmeier, 2001), the convergent extension movements during gastrulation (Strutt et al., 1997) and the orientation of cochlear cells in the inner ear (Heisenberg et al., 2000). Along this pathway, DVL activates small GTPases RhoA and Rac1, which modulate cytoskeleton reorganization. Another non-canonical pathway, called WNT/calcium pathway, has been described in *X.laevis*: binding of specific WNT to FZ receptors leads to signaling through DVL to induce calcium influx, and activation of protein kinase C (PKC) and calcium/calmodulin dependent protein kinase II (CAMKII): this causes induction of ventral and repression of dorsal cell fates in early *X.laevis* embryos.

During neural tube development, two major non-neuronal signaling centers are formed: at the bottom, the floor plate secretes the ventralizing factor Sonic Hedgehog (SHH), while, at the top, the roof plate secretes Bone Morphogenesis Proteins (BMP). The gradient formed by these secreted factors along the dorso-ventral axis affects the gene expression of individual group of cells, which, ultimately, determines their cell fate.

Shh pathway

Sonic Hedgehog (SHH) starts to be expressed in the notochord as soon as cells have left the regressing node. SHH is a member of the hedgehog family of secreted signaling molecules identified by homology to the *D.melanogaster* hedgehog (HH). Once synthesized, SHH is proteolytically cleaved to produce two secreted proteins, a 19kDa N-terminal protein (N-SHH) that mediates the signaling, and a 25kDA C-terminal protein (C-SHH) that possesses a protease activity (Porter et al., 1995). To signal, N-SHH needs to be modified by addition of a cholesterol moiety, introduced by C-SHH (Porter et al., 1996), and a palmitoyl group (Pepinsky et al., 1998), which facilitates the regulated secretion and its long-range activity.

At the cell surface, SHH binds with high affinity to Patched (PTC), a 12-transmembrane protein, which, bound to Smoothened (SMO), a seven-transmembrane protein with a topology reminiscent of G-protein-coupled receptors, inhibits its activity. Binding of SHH to PTC frees SMO to activate GLI proteins, the intracellular effectors of the pathway (**Fig.**

1.2D). GLI proteins – mammalian homologues of *Drosophila* Cubitus interruptus (Ci) – are Zinc-finger transcription factors capable of binding Ci-related consensus sequences present in several Shh-responsive genes (Sasaki et al., 1997; Sasaki et al., 1999; Yoon et al., 2002). To date, three GLI genes have been found in mammals - *Gli1*, *Gli2* and *Gli3* - each expressed in the neural tube in overlapping territories (Bai et al., 2002). In general, GLI1 acts primarily as an activator, GLI2 as both activator and repressor and GLI3 mostly as repressor, although their activity is context-dependent (Bai et al., 2004; Nguyen et al., 2005).

Downstream of GLI proteins, hedgehog signaling mediates cell specification through simultaneous repression of Class I homeobox transcription factors - for instance Pax6, *Pax7*, *Irx3* and *Dbx1/2* - and the induction of Class II homeobox transcription factors - for instance *Nkx2.2*, *Nkx6.1* - in the ventral spinal cord progenitors (Briscoe et al., 2000; Briscoe et al., 1999; Ericson et al., 1997; Litingtung and Chiang, 2000). Cross-repressive interactions between these homeodomain transcription factors act to sharpen the expression boundaries and direct the cells to differentiate into specific subtypes.

BMP pathway

Bone Morphogenic proteins (BMPs) are members of the transforming growth factor-β (TGF-β) protein family of extracellular ligands. These proteins act as morphogens for the development of various embryonic tissues, from the oocytes to the heart, lung, kidney and neural tube. BMP ligands form a homomeric or heteromeric complex that binds avidly to two types of transmembrane serine-threonine kinase receptor, the type I (BMPRIA or BMPRIB) and type II (BMPRII, ACTRIIA and ACTRIIB) receptors. Once in close proximity to the type I receptor, the type II receptor complex phosphorylates it, activating the BMP signaling cascade through the phosphorylation of members of the Small/male tail abnormal/ Mothers Against Decapentaplegic homologs (SMAD) protein family. SMADs fall into three subfamilies: receptor-activated SMADS (R-Smad: SMAD1, SMAD5 and SMAD8, activated by the BMP family; SMAD2 and SMAD3, activated by the receptors binding activin, Nodal and the TGF-β family); common mediator (Co-Smads: SMAD4); inhibitory Smads (I-Smads: SMAD6 and SMAD7). Upon activation and multimerization (Inman and Hill, 2002), the R-Smad-Smad4 complex translocates to the nucleus and regulates gene

expression (Fig. 1.2E).

SMAD proteins bind to Smad-binding element (SBE) sequences, with the minimal motif 5'-CAGAC-3', via the MH1 domain of the R-Smads, although with low affinity (Shi et al., 1998); almost universally, in fact, the complex has to interact with other DNA-binding cofactors to achieve high affinity and selectivity for specific subsets of target genes. SMAD3, for instance, requires the cooperation of forkhead family members, such as FoxO1, FoxO3 and FoxO4, to activate the transcription of cyclin-dependent kinase inhibitor *p21Cip1* or *CDKN1A* (Seoane et al., 2004); moreover, activation of *Vent2* during ventral mesoderm differentiation in *X. laevis* is mediated by a ZFP423-Smad1-Smad4 complex in response to BMP (Hata et al., 2000).

BMP signaling is modulated in various ways, from preventing receptor activation to degrading the intracellular effectors. During neurulation, for instance, secreted BMP antagonists, such as *Noggin, Chordin* and *Follistatin*, bind the ligand avidly in the extracellular space, block its interaction with their receptors, thus preventing the activation of the signaling cascade and triggering neural induction. In the cytoplasm, BMP pathway can be modulated by additional antagonists, such as the I-Smads: SMAD6 competes with SMAD4 for the binding with the activated SMAD1, such that non-functional SMAD 1-SMAD 6 complexes are formed (Hata et al., 1998); SMAD7 binds to activated receptors in competition with R-Smads (Hayashi et al., 1997; Nakao et al., 1997). Interestingly, both *Smad6* and *Smad7* are transcriptional targets of the TGF-β/BMP signaling cascade (Afrakhte et al., 1998; Brodin et al., 2000; Ishida et al., 2000; Nakao et al., 1997; Stopa et al., 2000), indicating the existence of a negative feedback loop in the pathway.

In the developing spinal cord, the roof plate secretes BMP ligands, such as BMP2, BMP4 and BMP7, as well as other TGF-β molecules, such as GDF7, establishing a concentration gradient that, together with the opposite gradient formed by floor-plate-secreted SHH, is essential for the dorso-ventral patterning. Perturbation of the gradient, through forced expression of Noggin, or inactivation of SMAD4, causes the loss of dorsalmost dI1 interneurons and the expansion towards the roof plate of dI2-dI4 neurons, which are normally located more ventrally (Chesnutt et al., 2004).
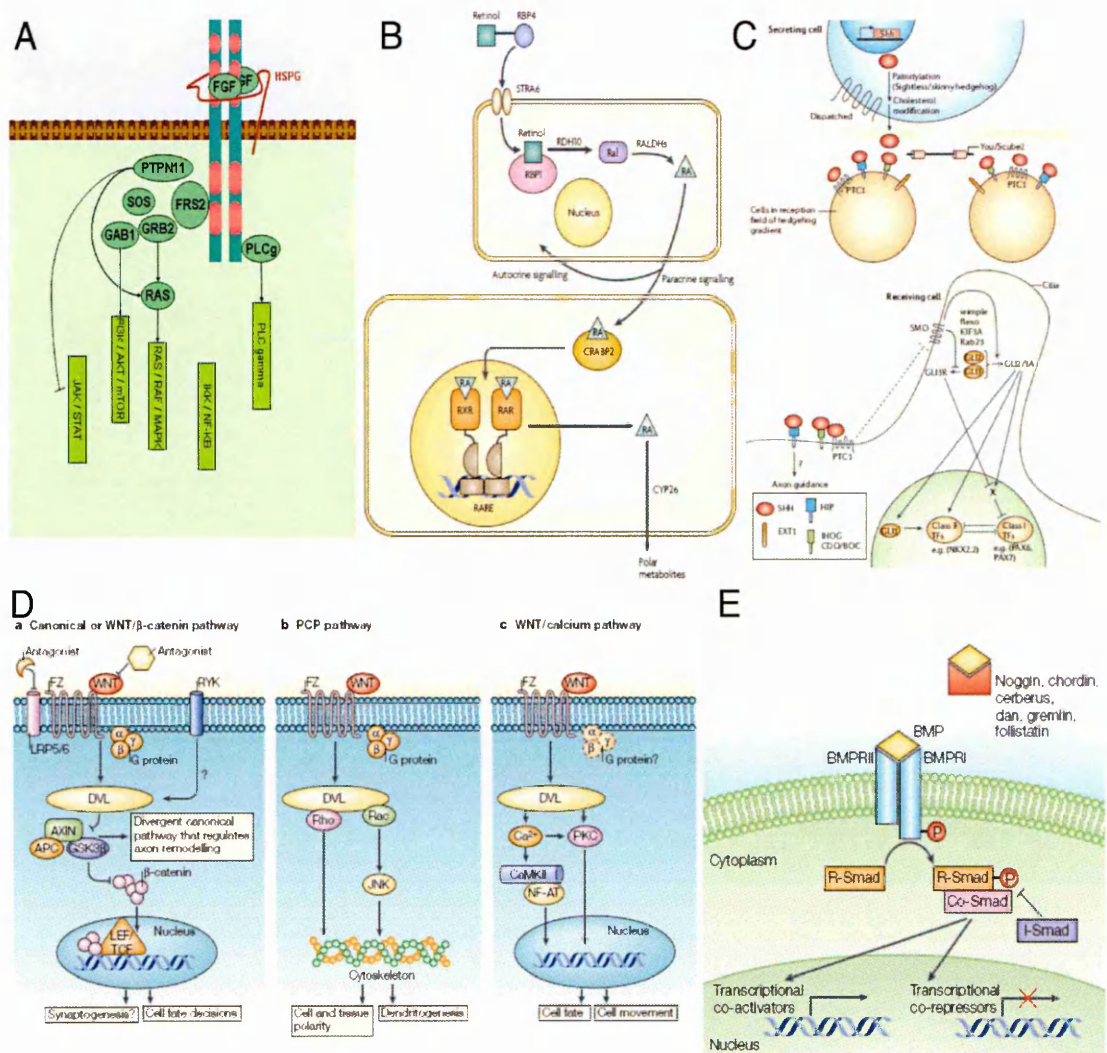
Figure 1.2 – Schematic pictures of major extrinsic signaling pathways important during development. A) Fibroblasts growth Factor Pathway. **B)** Retinoic Acid Pathway sketch (adopted from (Maden, 2007)). **C)** Wingless-related intergration site (WNT) pictures (adopted from (Ciani and Salinas, 2005)). **D)** Sonic Hedgehog (SHH) signaling cascade (Fuccillo et al., 2006). **E)** Bone Morphogenic Protein (BMP) pathway (from (Liu and Niswander, 2005)).

Intrinsic factors: structure and function of proneural basic helix-loop-helix proteins

Genetic studies in *D.melanogaster* and vertebrate models have provided evidence that a small number of genes, which encode transcription factors of the basic-helix-loop-helix (bHLH) class, are both necessary and sufficient, in the context of the ectoderm, to initiate the development of neuronal lineages and promote the generation of progenitors committed to neuronal differentiation. Therefore, these genes have been called "proneural genes" (**Fig. 1.3A**). In *D.melanogaster*, five genes have been found to regulate the early steps of neural development: *achaete* (ac), *scute* (sc), *lethal of scute* (lsc), *asense* (ase), which form a

complex, termed as *achaete-scute* (asc) , and *atonal* (ato) (Garcia-Bellido, 1979; Gonzalez et al., 1989; Villares and Cabrera, 1987). Many genes related to asc and ato have been found in vertebrates. The vertebrate asc family includes *ash1*, present in every species (*Mash1/Ascl1* in mouse, *Cash1* in chick, *Zash1*, in zebrafish and *Xash1* in *X.laevis*) and three other genes specific for one class of vertebrates (*Mash2* in mouse, *Cash4* in chick, and *Xash3* in *X.laevis*). The number of vertebrate genes related to ato is larger, but only two of them (*Math1/Atoh1* and *Math5/Atoh5* in mouse) can be considered orthologues to the founding member. Other vertebrate ato-related genes can be grouped into distinct families – the Neurogenin (Neurog) family, the NeuroD family and the Olig family – characterized by the presence of family-specific residues in their bHLH domain.

Like other bHLH proteins, proneural proteins bind DNA as heterodimeric complex formed with the ubiquitously expressed E proteins, namely E12 and E47, encoded by the gene *E2A* – orthologue of the *D.melanogaster* gene *daughterless* (*da*) –, or with the proteins HEB and E2-2 (Cabrera and Alonso, 1991; Massari and Murre, 2000). Because heterodimerization is a prerequisite for DNA binding, molecules that interfere with dimerization act as passive repressors of proneural proteins activity. Inhibitor of differentiation (*Id*) genes, for instance, encode HLH proteins lacking the basic domain, which is responsible for DNA binding: these molecules have a high affinity for the E proteins such that they can compete with proneural proteins, forming complexes unable to bind DNA (Massari and Murre, 2000; Yokota, 2001). Other bHLH proteins, such as those of the Hes/Her/Esr family, can bind E proteins, thus interfering with the formation of functional proneural complexes (see later, (Davis and Turner, 2001)).

Like other bHLH, proneural proteins specifically bind DNA sequences that contain a core motif, CANNTG, known as E-box, although each proneural gene family has a preferential consensus site (**Fig. 1.3B**).

Genetic analyses have revealed that vertebrate bHLH genes are functionally highly heterogeneous. Genes of the *ash* and Neurogenin families, and members of the *ato* homologues families, have similar proneural function to that of their *D.melanogaster* counterparts, while others do not have a proneural role, although they contribute to neuronal differentiation or subtype specification. In most cases, the proneural activity of such proteins has been demonstrated through loss and gain of function experiments. For instance, mice carrying

a null mutation in *Mash1* have severe defects in neurogenesis in the ventral telencephalon, whereas *Neurog1* or *Neurog2* single mutant mice lack complementary sets of cranial sensory ganglia, and *Neurog1/Neurog2* double mutants lack also spinal sensory ganglia and a large fraction of ventral spinal cord neurons (Fode et al., 1998; Ma et al., 1998; Ma et al., 1999; Scardigli et al., 2001). These defects are associated with a loss of progenitor populations and a premature generation of astrocytic precursors: independently of its proneural activity, Neurog1 also inhibits glial differentiation by sequestering CBP/p300/SMAD1 complex away from glial promoters and by repressing the JAK/STAT signaling pathway (Sun et al., 2001b). Conversely, when Neurog1 is ectopically expressed, it promotes the generation of supranumerary neural progenitors, drives progenitor cell out of cell division, and promotes neuronal differentiation by activating the transcription of differentiation genes such as *NeuroD* (Ma et al., 1998; Mizuguchi et al., 2001).

Loss of function experiments have suggested that other bHLH genes act as proneural factors: mouse mutants for *Math1* and *Math5* demonstrated that they are essential for the development of a small number of neuronal lineages in the CNS, such as cerebellar granule cells and hair cells in the inner ear – *Math1* (Ben-Arie et al., 1997; Bermingham et al., 1999) – or the loss of most retinal ganglion cells (RGCs) and the concomitant increase in other retinal cell types – *Math5* (Brown et al., 2001; Wang et al., 2001).

Notch Pathway and the control of neurogenesis

One of the most relevant questions in developmental neurobiology concerns the regulation of neurogenesis: how are progenitor cells committed toward a neuronal lineage over time, generating successive waves of committed post-mitotic cells? Which mechanisms control proneural gene expression?

In the animal kingdom, the Notch pathway plays a very important role in controlling cell fate decision. Cell-cell signaling through Notch pathway is involved in many and diverse processes, such as proliferation, axis formation, hematopoiesis, angiogenesis, morphogenesis and neurogenesis. Notch pathway is both "simple" and "complex": simple in that it does not require secondary messengers, but complex because many proteins contribute to regulate it. Notch signaling is initiated when one of the ligands binds its receptor. Subsequently,
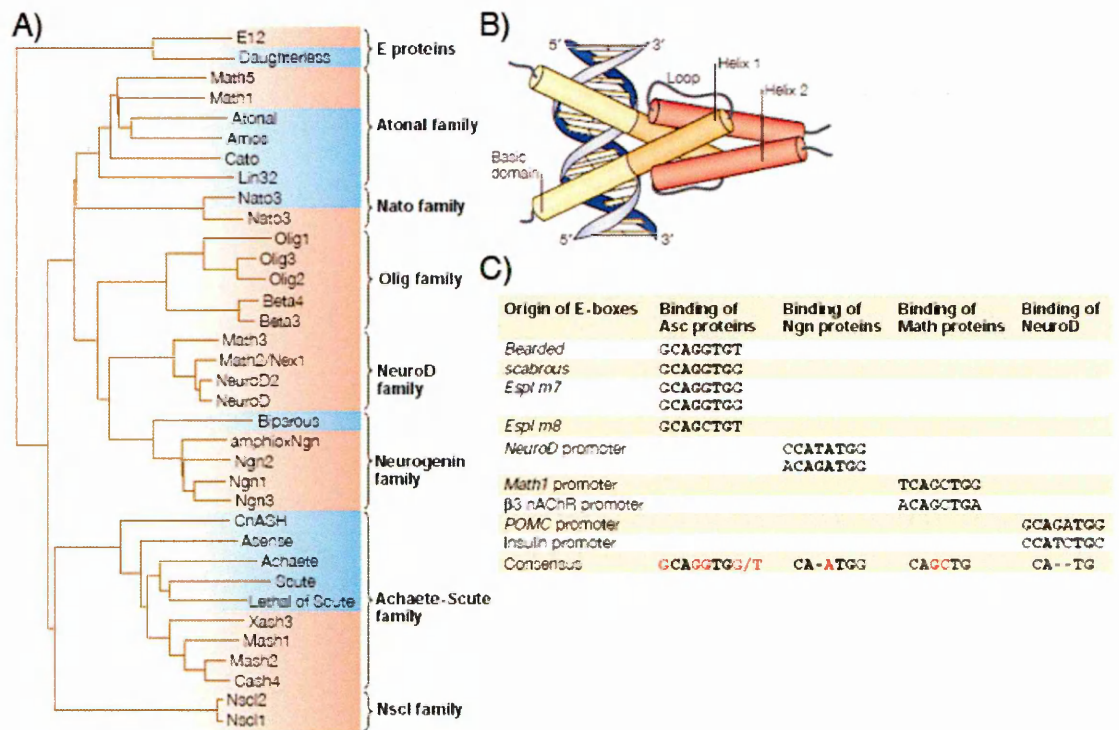
Figure 1.3 – Proneural genes: clustering, structure and binding site specificity. A) Proneural proteins have been grouped in distinct families on the basis of closer sequence similarities in the bHLH domain. In blue, invertebrate neural bHLH proteins, in red, vertebrate proneural proteins **B)** Schematic representation of the structure of a bHLH dimer that is complexed with DNA. **C)** Although neural bHLH proteins from different families recognize the common hexamer CANNTG, named E-Box, they must recognize different bases in the two central positions, as well as adjacent positions. Picture adopted from (Bertrand et al., 2002).

Notch receptor is proteolytically cleaved to release its intracellular domain, named Notch intracellular domain (NICD). NICD translocates into the nucleus where activates target genes by binding to a DNA-bound transcription factor, CBF1 **(Fig. 1.4A)**. In the following sections, I will describe the biochemical properties of the Notch pathway, how it is regulated, the known targets, then I will focus my attention on the role of this pathway during mammalian neurogenesis, with particular interest on what is known about Notch and cerebellar neurogenesis.

Structure of Notch ligands and receptors

Notch signaling occurs predominantly via cell-cell contact: this allows the extracellular domain of a ligand in a signal-producing cell to interact directly with the extracellular domain of Notch on an adjacent signal-receiving cell (Fehon et al., 1990; Rebay et al., 1991).

Notch ligands, collectively named DSL ligands, are transmembrane proteins that are characterized by a N-terminal DSL (Delta, Serrate and LAG-2) domain, essential for the interaction with the Notch receptors. The extracellular domain of the ligands contains varying numbers of epidermal growth factor (EGF) repeats. In mammals, ligands are subdivided into two classes, Delta-like (Dll1-4) - orthologues of *D. melanogaster Delta* gene - and Jagged (Jag1, Jag2) - similar to the *Serrate* gene in *D. melanogaster*. Jagged ligands contain almost twice the number of EGF repeats as Delta-like ligands, and have also a cysteine rich (CR) domain (**Fig. 1.4B**). The intracellular regions of ligands contain multiple lysine residues and a C-terminal PDZ motif, required for the ligand signaling activity and the interactions with the cytoskeleton.

The *Notch* gene, firstly identified in *D. melanogaster*, encodes a 300-KD single pass transmembrane receptor, composed by an extracellular subunit, responsible for the interaction with the ligands, and an intracellular domain. To date, four Notch receptors have been identified in mammals (NOTCH1-4, **Fig. 1.4C**).
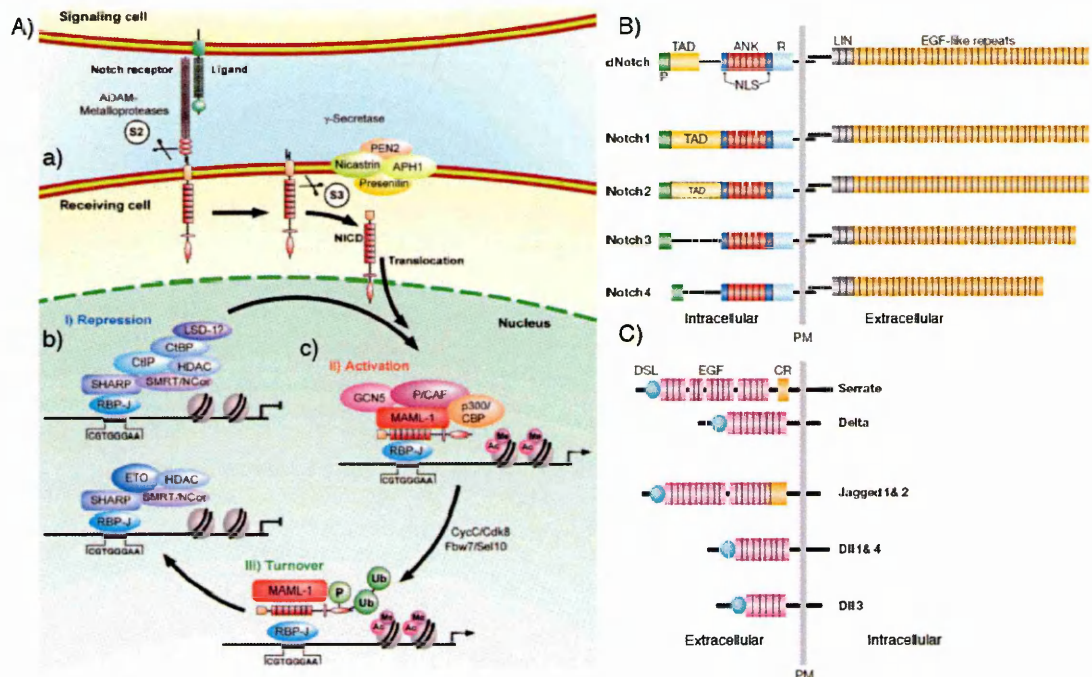
Figure 1.4 – Notch pathway: a simple and complex signaling cascade. A) Sketch of Notch pathway. See text for details. Adopted from (Borggrefe and Oswald, 2009). **B)** Schematic representation of the structure of Notch receptors. Adopted from (Radtke et al., 2005). **C)** Schematic representation of the structure of Notch ligands. Adopted from (Radtke et al., 2005).

The mature receptor requires the synthesis of a 300-KD polypeptide: in the Golgi vesicles, the polypeptide is cleaved in two fragments – 180kDa and 120kDa - that are assembled to form the working receptor (Fig. 1.4B) (Blaumueller et al., 1997). Specific vesicles carry the receptor to the cellular membrane, where they fuse allowing the exposure of the extracellular subunit to the external environment. This part of the protein contains both domains involved in the ligand interaction and stabilization, EGF-like repeats, and three Lin/Notch repeats (LNR), required for the activation of the intracellular subunit. Adjacent to the LNR, there are cysteine residues, necessary for the formation of disulphide bonds between the two subunits of the receptor. The intracellular fragment is composed of a transmembrane region, several domains involved in protein-protein interaction, a PEST sequence - proline, glutamate, serine and threonine - important for the turnover of the protein (Fig. 1.4B).

When a DSL ligand binds to the extracellular portion of the Notch receptor, two proteolytic events occur, resulting in the release of the intracellular domain of Notch, NICD. The first cleavage, called S2 cleavage, causes the release of the extracellular domain, and is due to the activity of two metallo-proteases of the ADAM family, ADAM17, also known as TNFα-converting enzyme (TACE, (Mumm et al., 2000)) and ADAM10, also called Kuzbanian (Jarriault and Greenwald, 2005); the second cleavage event, named S3 cleavage, determines the release of the intracellular domain from the membrane, and depends on the presenilin-γ-secretase complex (Selkoe and Kopan, 2003). NICD carries nuclear translocation signals (Stifani et al., 1992) and can therefore translocate into the nucleus. Here, it activates transcription after the recruitment of a complex composed of the Notch signaling effectors CBF1, or RBPjκ (Suppressor of hairless, SuH in *D.melanogaster*) (Fortini and Artavanis-Tsakonas, 1994) and MAML, mastermind-like (Mastermind in *D.melanogaster*) (Smoller et al., 1990).

CBF1 is a nuclear protein usually bound to the DNA sequence 5'-CGTGGGAA-3': in its "switched off" state, it interacts with co-repressor proteins, such as HDAC/SMRT complex (Kao et al., 1998), SHARP (Oswald et al., 2002), and CIR (Hsieh et al., 1999). In the presence of NICD, CBF1 is "switched on", so that the co-repressor complex is displaced by NICD, and MAML is recruited.

Firstly identified in *D. melanogaster* as one of the neurogenic loci along with Notch (Yedvobnick et al., 1988), *Mastermind* genes encode nuclear proteins that have limited

sequence homology with their orthologues, yet are highly conserved in their structure. The MAML co-activators contain a highly conserved N-terminal basic domain (BD) and two transcriptional activation domains (TAD) each containing one acidic motif. Biochemically, all MAML proteins do not bind directly DNA, but rather they form stable DNA-binding complexes with NICD and CBF1 upon Notch activation (Lin et al., 2002; Wu et al., 2002) and potentiate the transcription of target genes. A domain in MAML, TAD1, has been shown to interact with p300/CBP (Fryer et al., 2002), but the recruitment of these chromatin modifiers is not sufficient to potentiate Notch activity, as mutants retaining only this domain fail to enhance Notch target gene expression. On the contrary, TAD2 is required for transcription *in vivo*, but to date no proteins have been found to interact with TAD2 domain.

The final outcome of Notch signaling is the transcription of target genes, which, in turn, are the "true" effector of the signaling.

Tuning Notch signaling

The apparent simplicity of Notch pathway raised the question how a single pathway can be used by many different processes. Part of the diversity comes from the multiplicity of receptors and ligands, at least in mammals, and part from the identification of post-translational modification affecting the signaling cascade. For instance, glycosylation of the receptors changes ligand-binding properties, by increasing the interaction affinity between Notch and Delta and by inhibiting the interaction between Notch and Serrate (Bruckner et al., 2000; Panin et al., 1997). In *D. melanogaster* two gycosyl-transferases are able to modify the Notch receptor, OTUF1 and Fringe. In vertebrates, the situation is more complicated, as three Fringe homologs have been identified, *Radical Fringe, Manic Fringe* and *Lunatic Fringe*, which may regulate Notch interaction in a specific way.

A second level of regulation of Notch signaling has been revealed in the last years, and involves the cleavage and internalization of both ligands and receptor.

Biochemical studies in *D. melanogaster* and mammals have indicated that, similar to Notch receptor, ligands are sequentially cleaved to release extracellular and intracellular fragments (Bland et al., 2003; Sapir et al., 2005). It has been suggested that the intracellular domain of Delta and Jagged may be involved in bidirectional signaling, although studies on

purified Delta suggest that the cleavage is associated with its degradation (Mishra-Gorur et al., 2002).

Irrespectively of the role of the intracellular domain of Delta, recent genetic studies, mostly conducted in *D.melanogaster*, have shown that endocytosis is important in both signal-receiving cells in signal-sending cells to promote Dll-dependent Notch activation. For instance, genetic screens in *D.melanogaster* and zebrafish identified epsin, Neuralized (Neur) and Mind Bomb (Mib in zebrafish; Dmib in *D.melanogaster*) as regulators of ligand signaling activity. Mutants in one of these genes causes an accumulation of Delta at the cell surface, resulting in phenotypes that are associated with the loss of Notch signaling (Overstreet et al., 2004; Tian et al., 2004; Wang and Struhl, 2004).

On the signal-receiving cell side, endocytosis seems to be involved in regulating Notch S3 cleavage: in fact, inhibiting endocytosis, through dominant negative forms of Eps15 or Dynamin2, uncoupled the formation of the S2-cleaved Notch – N1ΔE, a form of the Notch receptor that lacks most of its extracellular domain, constitutively cleaved by γ-secretase (Gupta-Rossi et al., 2004) – with its subsequent proteolityc cleavage mediated by the γ-secretase. As a large pool of active γ-secretase complexes is known to reside in lipid rafts within the endosomal compartment (Vetrivel et al., 2004), it has been suggested that γ-secretase is prevented from contacting its substrate at the plasma membrane, such that endocytosis is required to bring S2-cleaved Notch from the plasma membrane, to an intracellular compartment containing biologically active γ-secretase. Nevertheless, further studies are required to exclude the presence of a minor pool γ-secretase at the cell surface that would be specifically involved in Notch S3 cleavage (Tarassishin et al., 2004).

Another molecule involved in regulating Notch is Numb, firstly isolated in a screen to identify genes affecting neuronal development in *D.melanogaster* (Uemura et al., 1989). Numb is asymmetrically segregated during cell division in several lineages, and mice null for Numb display profound CNS defects; recently, it has been demonstrated that mammalian Numb promotes the ubiquitination of membrane-tethered Notch1 and the degradation of the intracellular domain following receptor activation (McGill and McGlade, 2003). Numb interacts with E3 ubiquitin-ligase Itch to enhance Notch1 ubiquitination, and down-regulates Notch1-dependent signal transduction (McGill and McGlade, 2003).

Once in the nucleus, NICD binds to the activator complex and activates the transcription of

target genes: in order to prevent hyper-activation, Notch seems to act at very low concentration (Schroeter et al., 1998); moreover, Mastermind and a protein named Ski-interacting protein (SKIP) are able to recruit kinases that specifically phosphorylate NICD in the TAD and PEST domain, leading to NICD degradation and stopping the signaling process in the absence of new NICD entering the nucleus (Fryer et al., 2004).

Notch targets

Only a fairly limited set of Notch targets have been identified in various cellular and developmental contexts. The capability to elicit different responses might partly arise from crosstalk with other pathways.

The NICD activator complex up-regulates the expression of primary target genes such as *HES* in mammals, (E/(spl) (for *Enhancer of Split*) in *Drosophila*) (Egan et al., 1998; Greenwald, 1998) and *HEY* (*Hairy/E(spl)-related YRPW*, known also as HERP/Hesr/ gridlock, (Leimeister et al., 1999)). Both HES and HEY families are basic helix-loop-helix (bHLH) type transcriptional repressors and act as Notch effectors by negatively regulating the expression of downstream targets such as tissue-specific transcription factors (Ohsako et al., 1994; Van Doren et al., 1994).

To date, seven members of HES family have been identified (*Hes1-7*) (Akazawa et al., 1992; Bae et al., 2000; Bessho et al., 2001b; Hirata et al., 2000; Ishibashi et al., 1993; Koyano-Nakagawa et al., 2000; Sasai et al., 1992) and three members of HEY family (*He1, 2, HeyL*) (Kokubo et al., 1999; Nakagawa et al., 1999) have been isolated in mammals (**Fig. 1.5A**). Of these, *Hes1, Hes5* and *Hes7* genes are regulated by the Notch pathway, while *Hes2, Hes3* (Nishimura et al., 1998), *Hes6* (Koyano-Nakagawa et al., 2000) appear to be independent of Notch signaling, and further analysis on *Hes4* are lacking. All members of HEY family can be induced by Notch (Iso et al., 2002; Leimeister et al., 2000; Maier and Gessler, 2000).

The two families share several common features: they contain two well conserved domains, a basic-helix-loop-helix domain (bHLH domain), required for DNA binding and dimerization, and a second one called Orange domain, in the corresponding regions carboxy-terminus to bHLH region, whose function diverges between HES and HEY families (**Fig.

1.5B). The amino sequences of these domains are highly conserved within the respective family, but less so between the two different families. The most remarkable difference between HES and HERP in the basic region is a proline residue; moreover, all HES members share the C-terminal tetrapeptide WRPW motif, whereas the HEY family has YRPW, and an additional conserved region close to the tetrapeptide motif, TE(V/I)GAF, which is absent in HES.

Both HES and HEY families have been reported to act as transcriptional repressors, except HES6, which antagonizes the function of HES1, resulting in de-repression (Bae et al., 2000; Koyano-Nakagawa et al., 2000).

Recently, another Notch target gene has been described: Brain lipid-binding protein (*Blbp*, or *Fabp7*, Fatty Acid binding protein 7) (Anthony et al., 2005).

Repression mechanisms of HES and HEY

Mechanisms for transcriptional repression by HES have been studied genetically and biochemically. Three mechanisms have been proposed (**Fig. 1.5C**). The first mechanism is DNA-binding-dependent transcriptional repression, also known as "active repression" (**Fig. 1.5Ca**): HES form homodimers and bind specific consensus DNA sites (namely, class C or N box, see **Table 1**; (Ohsako et al., 1994; Sasai et al., 1992; Van Doren et al., 1994)). They recruit the co-repressor Groucho or its mammalian homologue TLE (TLE1-4) via the C-terminal WRPW motif (Grbavec and Stifani, 1996; Paroush et al., 1994). In turn, Groucho/TLE can recruit the histone deacetylase Rpd3, an orthologue of HDAC (Chen et al., 1999), thus altering local chromatin structure, but TLE retains a repressor activity on its own, as recently shown (Sekiya and Zaret, 2007).

HEY proteins can bind both class B and C sites, while HEY2 can bind also class A sites, raising the possibility that HEY2 may directly compete with tissue-specific bHLH activators for the E boxes (Iso et al., 2001). Regardless HES, HEY repression does not require the Orange domain and does not involves TLE; in fact, bHLH domain directly recruits co-repressor proteins, such as N-Cor and mSin3a, which interact with HDAC1 (Iso et al., 2001). Interestingly, HES and HEY proteins are able to form heterodimers, and such heterodimers bind DNA target sequences with even higher affinity the corresponding homodimers (Iso et

al., 2001). This observation leads the possibility that different combinations of HES/HEY dimers, depending on the abundance of each protein, may contribute to regulate specific subsets of target genes, increasing the complexity of Notch signaling.

The second mechanism through which HES proteins inhibit transcription of downstream targets is called "passive repression" (**Fig. 1.5Cb**). This kind of repression can result from two distinct mechanisms: protein sequestration or site occupancy. In the former situation, HLH domain allows the interaction with other HLH proteins important for transcription activation: for instance, HES1 can form heterodimers with E47, a bHLH protein important in the formation of heterodimer with other bHLH activator factors such as MyoD and Mash1, thereby disrupting the formation of functional heterodimers such as MyoD-E47 (Jogi et al., 2002). In the developing pancreas, HES1 can bind the PTF1-p48 complex (also known as Ptf1a), inhibiting its ability to drive transcription of target genes (Ghosh and Leach, 2006). As regards site occupancy, bHLH may occupy DNA consensus sequences thus disturbing the binding of the activator complex. This is the case of HEY1, which reduces the binding of MyoD-E47 to E-box sites present in the myogenin promoter (Sun et al., 2001a).

The third mechanism of HES/HEY transcriptional inhibition requires the Orange domain (**Fig. 1.5B**): in HES1 protein, this domain is essential to repress transcription of HES1 promoter as well as p21^{WAF} promoter (Castella et al., 2000) (**Fig. 1.5Cc**). The mechanism of repression mediated by Orange domain is still unknown, but it might involve the stabilization of WRPW-mediated repression function through intra- or intermolecular interaction (Castella et al., 2000). Orange domain significantly improves interaction strength between HES and HEY (Leimeister et al., 2000).

In the recent years, dozens of potential target genes of HES and HEY have been described in the literature. The regulation of some genes has been verified through *in vitro* assays on the promoter (luciferase assay, CAT assay, EMSA, ChIP), in other cases the mis-expression has been found in mutants - either Notch, or Hes mutants. For instance, HES1 has been found to regulate, directly or indirectly, genes involved in cell proliferation, such as *E2f1*, *p27*, *p21*, *Mdm2*, *p57* (Georgia et al., 2006; Hartman et al., 2004; Huang et al., 2004; Murata et al., 2005; Ross et al., 2004), and genes involved in differentiation, such as *Mash1*, *Neurogenin3*, *Blbp*, *Ath5*, *Dll1*, *Neurogenin2*, *fatty acid synthase* (Anthony et al., 2005; Baek et al., 2006; Chen et al., 1997; Hatakeyama et al., 2004; Lee et al., 2001; Matter-Sadzinski et al., 2005;

Ross et al., 2006). HES5 binds to the *Mbp* promoter (Liu et al., 2006), and myelin levels are increased in *Hes5* null mutants.

Auto-regulation of Notch target genes

One of the targets repressed by HES1 is *Hes1* itself (Takebayashi et al., 1994): in fact, three N-box sequences are present on the *Hes1* promoter, and the mutation of one of them causes the abrogation of the repression mediated by HES1. A similar negative feedback loop has been observed for *Hes7* (Bessho et al., 2003; Bessho et al., 2001a; Bessho et al., 2001b) while for *Hes5* detailed data are still lacking, although its expression pattern in the presomitic mesoderm seems to be dynamic (Dunwoodie et al., 2002).
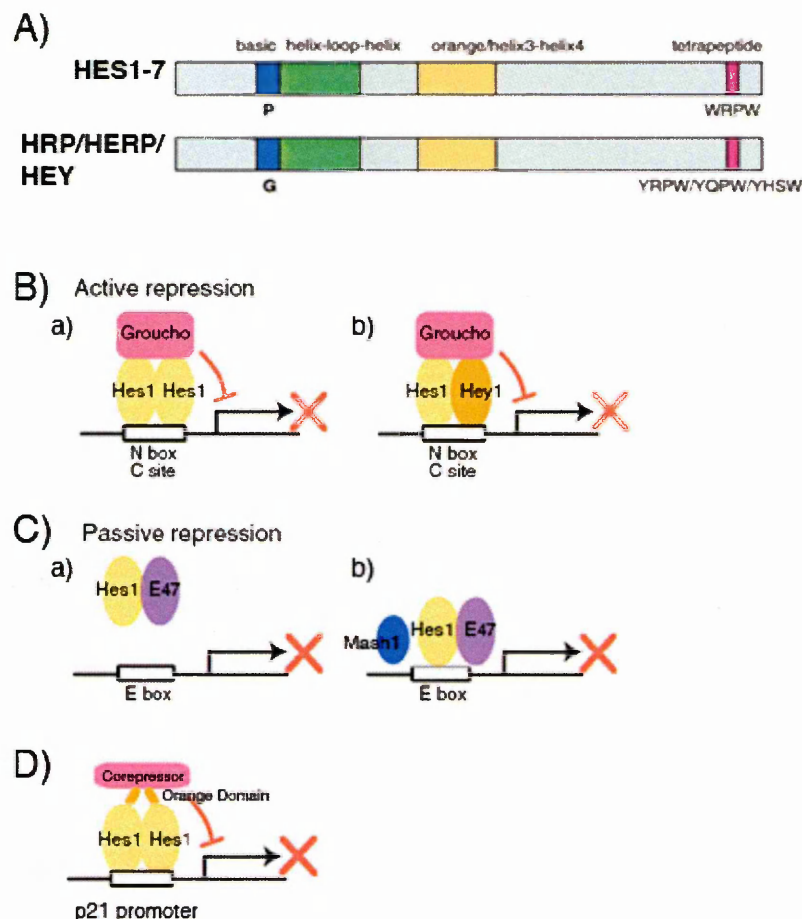
Figure 1.5 – HES and HRP/HERP/HES as transcriptional repressor effector of Notch pathway. A) Schematic representation HES and HRP/HERP/HEY proteins. Adopted from (Iso et al., 2003). **B)** Active transcriptional repression mediated HES-HRP/HERP/HEY proteins: they can bind C- or N-box (see table1) and recruit co-repressors proteins, either as homo- (a) or as hetero-dimer (b). Adopted from (Iso et al., 2003). **C)** Passive repression can occur either by sequestering co-activator (a) or by reducing binding affinity of proneural gene (b). **D)** HES1 requires Orange domain to actively repress p21 promoter.

Classification	Consensus	Examples
Class A	CANCTG	CACCTG, CAGCTG
Class B	CANGTG	CACGTG, CATGTG
Class C	CACGNG	CACGCG, CACGAG
E box	CANNTG	CACCTG, CAGCTG, CACGTG, CATGTG
N box	CACNAG	CACGAG, CACAAG

Class A and B are subtypes of E box. Class C and N box are mutually overlapping.

Table 1 – Classification of consensus sites recognized by HLH transcription factors.

Negative feedback loop *per se* is a mechanism that avoids an hyper-repression of target genes, but, when studies on mRNA and protein turnover were performed (Hirata et al., 2002), it became clear that the negative loop is part of a more complex oscillatory process, through which HES genes control a variety of developmental stages, from cell cycle progression (mainly *Hes1*, (Murata et al., 2005)), to somite segmentation (*Hes7*, (Bessho et al., 2003)) and neural progenitor maintenance (*Hes1* and *Hes5*, (Hatakeyama et al., 2004)).

The first evidence of the oscillatory mechanism came from *in vitro* studies: in 2002 the group of Kageyama showed that *Hes1* mRNA expression oscillates with 2-hour cycle in several cultured cells, such as myoblast (C2C12), fibroblasts (C3H10T1/2), neuroblastoma cells (PC2) and teratocarcinoma (F9), when the serum was added to the culture medium (Hirata et al., 2002). HES1 protein expression follows the same periodicity, but 15 minute delayed relative to *Hes1* mRNA oscillation. This oscillation, which continues for 6 to 12 hours, corresponding to three to six cycles, occurs for two main reasons: the first is the negative feedback loop, the second is the short half-life of both *Hes1* mRNA (about 25minutes) and HES1 (about 25 minutes) (Hirata et al., 2002). Real time studies demonstrated that *Hes1* mRNA expression changes dynamically at the single cell level (Masamizu et al., 2006).

In the mouse presomitic mesoderm (PSM), *Hes1*, *Hes5* and *Hes7* are expressed in a similar fashion to each other, but *Hes7* is the most important in somite segmentation. The relevance of the oscillatory expression of *Hes7* is such that somites fuse as a consequence of Hes7 mis-expression – either knock-down or constitutevely expression (Bessho et al., 2001b; Hirata et al., 2004).

Notch signaling during neuronal development

Notch signaling has been extensively studied first in *D.melanogaster*, where it acts by

restricting cell fate in the neural-epidermal choice, in a process called "lateral inhibition". Strikingly, lateral inhibition occurs during neurogenesis where a group of equipotent cells expressing equal amounts of Notch receptors and ligands begin to gradually express either more Notch receptor or more ligand (**Fig. 1.6A**). Notch-expressing cells (cell "a") up-regulate the expression of *Hes* genes, which, through the suppression of proneural gene expression, maintain the cells in an uncommitted state; ligand-expressing cells (cell "b") express proneural genes, and thus commit themselves to a neuronal fate (**Fig. 1.6B**).

In other situations, such as during sensory organ precursors (SOP) lineage commitment, Notch signaling between two daughter cells is dependent on asymmetrical inheritance of Notch regulators, the best known of which is NUMB. Daughter cell retaining NUMB undergoes differentiation, while the other remains uncommitted.

In mammals, the role of the Notch pathway has been studied mainly by constitutive and inducible knock-out mouse models. The first gene to be disrupted by homologous recombination was *Notch1*: mutant embryos die during embryogenesis (around E11) featuring a severe defect in somitogenesis and a precocious onset of neurogenesis (Barrantes et al., 1999; de la Pompa et al., 1997; Swiatek et al., 1994).
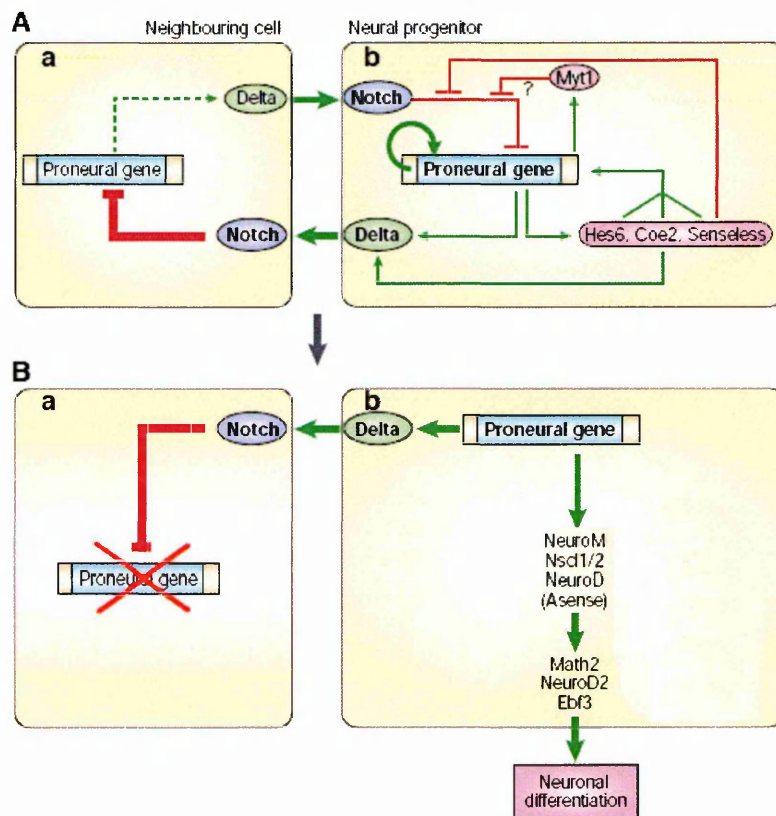
Fig.1.6 - Scheme of "lateral inhibition" model. Picture modified from (Bertrand et. al, 2002) .

To overcome the early developmental lethality in *Notch1* null embryos, an inducible knock-out strategy was developed, based on the Cre-Lox technique. In brief, this technique is based on the ability of an enzyme, the Cre-recombinase, to recognize and recombine specific DNA sequences called LoxP: when Cre-recombinase is active, the DNA sequence flanked by the two LoxP sites is excised and lost. In this way, it is possible to generate knock-out mice, or mutant alleles – if, for instance, LoxP sequences are flanking exons encoding specific domains of a protein – only in the tissue of interest and/or in a specific time window, simply choosing an appropriate promoter to control the expression of *Cre-recombinase* gene, and leaving the other tissues in the native state.

Notch1 conditional knock-out (cKO) mice were crossed with *Engrailed2-Cre-recombinase* mice (Lutolf et al., 2002), so that the ablation of *Notch1* could occur only in *Engrailed2*-expressing tissue, namely the midbrain-hindbrain region of the neural tube, starting from E9 (Zinyk et al., 1998), a stage that sets the onset of cerebellar primordium development.

Notch1 cKO embryos were analyzed at different developmental stages, and found a clear reduction of *Notch1* mRNA expression in the medial portion of the cerebellar primordium at E10.5, coupled to a strong reduction in *Hes5* expression in the same region. In agreement with previous findings, the ablation of *Notch1* causes promiscuous expression of Delta-like ligand and an early onset of neurogenesis in the cerebellum, observed by the premature expression of proneural genes such as *Mash1* and *Math1*, at E10.5. Interestingly, in *Notch1* cKO embryos, the early differentiating neurons – TuJ1-positive cells – fail to undergo a complete maturation, i.e. they do not express Calbindin-28kD, a marker of differentiated Purkinje cells, and likely die, as revealed by TUNEL staining in floxed embryos at E12.5. The final outcome is the formation of a smaller cerebellum, with a reduced number of Purkinje cells and a reduced presence of Bergmann glia fibers (GFAP-positive cells) derived from recombined cells, although the total number and the distribution of Bergmann glial cells do not show significant differences between control and mutant mice.

Another group studied the role of *Notch1* in cerebellar development with a similar approach (Machold et al., 2007). They crossed the same *Notch1* cKO with the *Engrailed-1-Cre-recombinase* transgenic mouse (En1Cre) (Kimmel et al., 2000): *Engrailed-1* directs the expression of the *Cre-recombinase* widely across the mid-hindbrain region by E9.5, so that by E10.5 no *Notch1* mRNA is detectable anymore, with the exception of the most

lateral territory, where recombination is incomplete. As previously reported, Notch1 ablation caused an early up-regulation of the proneural genes *Mash1*, in the VZ, and *Math1* in the rhombic lip (RL). Interestingly, at E12.5 *Mash1* expression is clearly reduced in the mutants, while *Math1* is still highly expressed, not only in the RL, but also in migrating granule cell progenitors and in the caudal-most portion of the VZ, suggesting an increase in rhombic lip (RL) neurogenesis at the expense of maintaining the VZ progenitor pool. Because BMP signaling has been associated with granule cell generation (Alder et al., 1999), and *Msx2,* a BMP-target, is expressed in the RL, they investigated a possible antagonism between Notch and BMP signaling in granule cell development: strictly, in chicken embryos they found that up-regulation of *Msx1/2* and *Cath1* (chicken homolog of the murine *Math1/Atoh1*) in the RL electroporated with a constitutive active form of BMP receptor (caBMP) could be abolished by the co-electroporation of NICD. NICD does not act on the BMP signaling cascade, as shown by the fact that pSMAD is detected in the nucleus, but rather on the expression of BMP target genes.

Consistent with the view of Notch signaling being important for progenitor maintenance, *Notch1* mutant embryos show a down-regulation of *Hes5* and up-regulation of *Neurog2*, *NeuroD*, *Mash1/Ascl1* and *Dll1*. Similar results were obtained in *CBF1–/–* embryos (de la Pompa et al., 1997). Interestingly, although *Hes1* has been shown to be a primary target of Notch signaling (Ishibashi et al., 1995; Ishibashi et al., 1994), its expression does not seem to be affected in both *Notch1–/–* and *CBF1–/–* mutants: together, these data indicate that *Hes1* is a Notch signaling target, although not exclusive. This notion is supported by the findings that *Hes1* expression can be induced in PC12 cells cultured with NGF, FGF2 or EGF (Feder et al., 1993), and in postnatal cerebellar granule cells cultured in SHH (Solecki et al., 2001).

Mutant mice for *Notch2*, *Notch3* and *Notch4* genes have also been generated: of these, only *Notch2–/–* embryos display clear-cut phenotypic abnormalities, resulting in embryonic lethality at around E11 (Hamada et al., 1999). Defects in *Notch2–/–* embryos include widespread cell death, but neither somitogenesis deficits nor changes in *Hes5* expression have been reported (Hamada et al., 1999).

In addition to mutations leading to the loss of receptors, many Notch ligand mutations have been examined, but the effects of such mutations in neural development were only

analyzed in a minority of cases. One such study found a decrease in *Hes5* gene expression in *Dll1–/–* mutant embryos, consistent with the expected reduction in the Notch activation, together with a reduction in RC2 staining and a increase in βIII-tubulin and GABA (Yun et al., 2002).

Another important player in the Notch signaling cascade is the cofactor CBF1: *Cbf1–/–* mutant embryos show altered gene expression, with *Hes5* reduction and up-regulation of *Dll1* and *NeuroD* (de la Pompa et al., 1997), although the phenotype is difficult to analyze because mutant embryos show severe growth retardation by E8.5.

Role of HES genes during neurogenesis

To date, seven *Hes* genes have been found, but only *Hes1, Hes5* and *Hes7* are targets of the Notch signaling cascade. Of these, *Hes7* does not seem to play a major role during neural development, but rather it is important during the somitogenesis: its expression oscillates in 2-hour cycles in the presomitic mesoderm, and *Hes7*-null murin embryos present an uncorrected somite segmentation and the disruption of the anterior-posterior polarity (Bessho et al., 2001a; Bessho et al., 2001b).

In the developing nervous system, *Hes1* starts to be expressed early in the neuroectoderm, before the onset *Notch1* mRNA expression: this initial observation suggested that *Hes1* might play roles unrelated with the Notch signaling, at least at early stages of development. This hypothesis was investigated in Hes1–/– mutant embryos, which show severe defects in neural development, including lack of cranial neural tube closure and anencephaly (Ishibashi et al., 1995), and precocious neurogenesis, demonstrated by the early expression of markers such as *Math1* and *Nscl1*, despite the increased expression of *Hes5* (Ishibashi et al., 1995).

Hes5 mRNA is firstly detected at E8.5-9 in the midbrain/hindbrain region of the neural tube and extends caudally and rostrally as development progresses. The expression of *Hes5* correlates with the expression of *Notch1* in the nervous system and the appearance of radial glial cells in the neuroepithelium. Indeed, *Notch1* null embryos show marked decrease in *Hes5* expression (de la Pompa et al., 1997). Although *Hes5* expression depends upon Notch pathway, thus suggesting a remarkable role in the transduction of the signaling, Hes5–/– mutants are largely normal (Hatakeyama et al., 2004; Ohtsuka et al., 1999), despite a reduced

number of Müller glial cells (about 30-40%) (Hojo et al., 2000). The absence of evident defects in *Hes5* null embryos suggests the existence of compensatory mechanisms, or a redundancy in the pathway. To test whether the disruption of *Hes5* may be compensated by other *Hes* genes, Hatakeyama and colleagues generated *Hes1;Hes5* double mutants, and *Hes1;Hes3;Hes5* triple mutants and compared them with single mutants (Hatakeyama et al., 2004). They found that *Hes5* expression is up-regulated in *Hes1–/–*, as previously demonstrated (Ishibashi et al., 1995), and similarly *Hes1* expression is increased in *Hes5–/–*, indicating a possible compensatory mechanism. *Hes1;Hes5* mutants show neural tube defects closely related to the ones observed in the Notch1–/– embryos, that is a precocious neuronal differentiation and a depletion of the pool of progenitor cells. Although neuronal differentiation is severely accelerated in *Hes1;Hes5* double mutants, neuroepithelial cells are normally formed at E8.5, indicating that *Hes1* and *Hes5* have a role in radial glial cell maintenance during neurogenesis, but not in their generation. *Hes1;Hes3;Hes5* show even more pronounced defects, with the onset of neuronal differentiation as early as E8.5: nevertheless, at this stage many neuroepithelial cells (Nestin+, Ki67+) are still present in the mutant neural tube, suggesting that neuroepithelium is formed without the contribution of *Hes* genes, but become dependent upon *Hes* gene activities by E8.5 (Hatakeyama et al., 2004).

Regulation of *Hes5* expression

To date, *Hes5* is the only gene clearly regulated by Notch signaling and involved in a specific developmental process, the maintenance of a pool of progenitor cells during neuronal commitment. Because of these two peculiar features, *Hes5* promoter has been analyzed *in vitro*, as a promoter capable to respond to Notch pathway, and *in vivo*, to label radial glial cells and study their nature and their potential in the context of neurogenesis.

The research group of Ryoichiro Kageyama cloned a 1Kb fragment of the *Hes5* promoter (-1034 +73 bps) and, through *in vitro* studies, they demonstrated that (I) the promoter is active in the neural precursor cells, (II) a short version of the promoter – -248+73 – maintains the transcriptional regulatory elements for the activation in neural precursors cells (Takebayashi et al., 1994), and (III) promoter activity decreases with cell differentiation.

Some years later, another group showed that *Hes5* expression could be induced in neural precursor cells by BMP2-mediated treatment (Nakashima et al., 2001), and a specific deletion in the *Hes5* promoter abolishes the activation BMP2-mediated. As a further step, they found that BMP signaling is not able *per se* to activate *Hes5* promoter, but rather it potentiates its Notch-mediated activation (Takizawa et al., 2003). They mapped the CBF1-binding site in position -79 relative to the transcription start site (TSS), while the SMAD-binding-site (SBS) at -161 bps with respect to the TSS. They also found that the interaction between SMAD1 and NICD is barely detectable (Takizawa et al., 2003). Interestingly, the linker-MH2 of SMAD1 can co-precipitates with P/CAF (Takizawa et al., 2003), which interacts with p300 and NICD to mediate transcriptional activation (Wallberg et al., 2002). They demonstrated that (I) BMP stimulation boosts the activation of *Hes5* promoter in cells transfected with NICD- and p300-expressing vectors (Takizawa et al., 2003); and (II) p300 co-precipitate with P/CAF and NICD with higher rate when activated SMAD1 is part of the complex (Takizawa et al., 2003).

Because of its specific expression in neural stem cells within the developing CNS, researchers took advantage of the *Hes5* promoter to drive the expression of the Green Fluorescent Protein (*Gfp*) gene, so as to study the timing of Notch activation in the VZ, and to visualize the maintenance of neural stem cells and the cell commitment towards differentiation. To this aim, a transgenic mouse was generated (Ohtsuka et al., 2006) in which 760 bps of the murine *Hes5* promoter directs the expression of destabilized enhanced GFP protein (d2EGFP) whose half-life is about 2 hours. In developing CNS, *Hes5* and *Gfp* expression was largely overlapping, defining a temporal and spatial patterning that allowed the identification of neural stem cells from other progenitors and differentiating cells. They also reported some discrepancies between endogenous expression of *Hes5* and the *Gfp* in the transgenic mice − GFP was expressed in branchial arches, optice placodes and limbs, all regions that lack detectable *Hes5* levels by *in situ* hybridization − possibly indicating the lack of regulatory regions in the promoter used. At 11.5, *Hes5*-driven GFP is expressed in a spotted pattern in the telencephalic VZ, while two days later, at E13.5, GFP labels the dorsal VZ of the midbrain, with the exception of the roof plate, where, conversely, *Hes1* is expressed. Co-localization experiments with Ki67, a known marker of proliferation, and RC2, a general marker of stem cells, together with morphological analyses, demonstrated that GFP-positive

cells resident within the VZ are indeed mitotically active radial glial cells, with radial fibers extending towards the pial surface. GFP-positivity did not co-localize with TuJ1-positive cells. Isolated GFP-positive cells from E11.5 *Hes5*-GFP transgenic dorsal midbrain gave rise to primary and secondary neurospheres, suggesting the self-renewal capability, and a differentiation assay demonstrated the ability of these neurospheres to generate either neurons, astrocytes or oligodendrocytes. Interestingly, time lapse experiments performed on isolated GFP-positive cells revealed that *Hes5*-expressing cells can undergo both symmetrical and asymmetrical divisions: when asymmetrical division occurs, one of the two daughter cells remains GFP-positive, the other one become TuJ1-positive, and inherits NUMB, supporting the notion that NUMB inheritance may favor neuronal commitment (Ohtsuka et al., 2006).

To circumvent the discrepancies between endogenous *Hes5* expression and GFP labeling, a second group generated transgenic mice in which GFP is controlled by regulatory elements of the *Hes5* gene (Basak and Taylor, 2007). They cloned 3 kb of the murine *Hes5*, including 1.6 kb of the 5'-flanking region and 1.4 kb of downstream sequence that includes the three exons and two introns of the *Hes5* gene. In the exon 1 they cloned the *eGfp* gene together with a translational stop codon, in order to maintain every putative regulatory element present in the gene without the synthesis of a GFP-HES5 fusion protein. They generated transgenic mice in which GFP protein recapitulates endogenous *Hes5* expression almost faithfully. To demonstrate that the Hes5-GFP transgene is under the control of Notch signaling, they crossed the transgenic mouse onto a Notch1-deficient background (Lutolf et al., 2002), and found that the reporter expression is almost completely abolished in that background. In keeping with previous work, they found that Hes5-GFP reporter is expressed in the VZ of the neural tube throughout development, it co-localizes with Nestin and not with TuJ1-positive cells. Interestingly, they sorted GFP-positive cells into three groups, depending on the intensity of the fluorescence: they found that only cells with high GFP expression can form neurospheres, and the same cell type expresses a higher level of *Blbp* gene compared to the cells with medium and low levels of *Gfp* expression.

Taken together, these data strongly support the notion that *Hes5* is a major target of Notch signaling, acting mainly in the dorsal part of the developing midbrain/hindbrain, specifically in the germinative area.

Early B-cell Transcription Factors: a class of HLH proteins involved in neuronal differentiation and migration

Early B-Cell Factor (EBF) was isolated as transcriptional regulator of genes specifically expressed in early stages of mouse B-cell differentiation (Travis et al., 1993); Olfactory 1 (Olf-1) was isolated as a rat nuclear factor recognizing cis-regulatory elements of the olfactory marker protein (*OMP*) gene (Kudrycki et al., 1993). Cloning and sequencing of *ebf* and *olf-1* cDNAs revealed that EBF and Olf-1 correspond to orthologous proteins, involved in two separate regulatory networks (Hagman et al., 1993; Wang and Reed, 1993). It was accordingly named Olf-1 or early B-cell factor (EBF), which in turn led to the designation of the factor O/E-1. Later reports showed that mice express at least three more genes closely related with O/E-1, EBF2 (mMot1), EBF3 (O/E-2) (Garel et al., 1997; Malgaretti et al., 1997; Wang et al., 1997), and O/E-4 (Wang et al., 2002), with a high degree of similarity in the DNA binding and dimerization domains. Isolation of the O/E homologue *Collier* (*col*) from *D. melanogaster* (Crozatier et al., 1996) provided a proof of principle for the existence of a new family of conserved proteins. Other family members have been cloned in several species and **Table 2** (Liberg et al., 2002) summarizes the nomenclature for the proteins.

Structure of EBF TFs

The COE protein family represents a novel type of HLH transcription factors, as the dimerization domain contains two helices with homology to the second helix of the classical bHLH protein dimerization domain, but with a different type of DNA binding domain (DBD). COE factors, in fact, bind DNA through a cysteine- and histidine-rich domain of about 250 amino acids located in the amino–terminal part of the proteins (**Fig. 1.7A**). Binding of EBF-1 requires Zn^{2+}, as three of the cysteines together with one of the histidine residues can form a small Zn^{2+}- stabilized loop. Mutation in either of these cysteines or histidine eliminates DNA binding and the requirement of Zn ions for binding (Hagman et al., 1995). The Zn coordinating motif is highly conserved – more than 90% – in all O/E proteins and for that reason has been referred to as COE motif.

| Protein | Vertebrate protein(s) | | | | | | | Invertebrate proteins | |
	Human	Mouse	Rat	X. laevis	Zebra fish	Chicken	Skate	D. melanogaster	C. elegans
COE1	EBF,O/E-1	EBF, O/E-1	Olf-1			EBF	EBF1		
COE2		EBF2, O/E-3, Mmot1		xCOE2	zCOE2				
COE3		EBF3, O/E-2		xCOE3, xEBF3					
COE4		O/E-4							
COE								Collier, Knot	unc-3, CeO/E

Table 2 – Summary of the names used to identity COE proteins in different publications.

Downstream of the DBD is a second conserved region with an apparent similarity to IPT/TIG (immunoglobulin-like, plexins, transcription factors/transcription factor immunoglobulin) domain, present in transcription factors such as NFAT and NF-κB. To date, the role of this region is unclear, although it has been suggested to be involved in the interaction with Zinc finger protein 423 (ZFP423); an interesting hypothesis which comes from the finding that IPT domain-containing plexin proteins are involved in axonal guidance (Tamagnone and Comoglio, 2000).

The mouse COE1-2-3 and 4 bind DNA as homo- or heterodimers, and dimerization is dependent on the region downstream of the DBD containing an atypical HLH motif (**Fig. 1.7A**). The classical helix-loop-helix motif, present in bHLH proteins, contains two different amphipathic helices, helix1 (H1) and helix2 (H1), connected by a loop. Vertebrate COEs contain H1 and a duplication of H2, resulting in a domain capable of mediating dimerization when coupled to heterologous protein (Hagman et al., 1995). The H2 duplication is only present in vertebrate COEs and not in *D.melanogaster* Collier (Crozatier et al., 1996) or *C.elegans* unc-3 (Prasad et al., 1998). However, this region can be deleted without a dramatic effect on EBF-1 DNA binding ability (Hagman et al., 1993). A similar result was obtained with a splice variant of O/E-4, which lacks helix 2' (Wang et al., 2002): this protein can still bind DNA on its own or together with a longer O/E-4 splice variant containing H2'.

A trans-activation domain (TS II) occupies the C-terminal part of EBF-1: this region, rich in serine/threonine/proline residues, can activate transcription when coupled to a GAL4-DBD (Hagman et al., 1995), and also C-terminal part of the other COEs proteins shows the same ability (Hagman et al., 1993; Wang et al., 2002; Wang et al., 1997), although the sequence is poorly conserved among the family members.

In vitro studies showed that COE proteins can bind the palindromic sequence

5'-ATTCCCNNGGGAAT-3' (Pozzoli et al., 2001; Travis et al., 1993), either as hetero- or homodimers (Hagman et al., 1993; Wang et al., 1997); EBF-1 with a disrupted HLH domain can still interact with one perfect consensus half-site, although with a reduced affinity (Hagman et al., 1995; Hagman et al., 1991). Recently, it has been demonstrated that EBF-1 mutants in the "Zn knuckle" motif have a highly reduced ability both to bind and activate the transcription of target genes, suggesting that this motif is important for EBF-1 to exert its function (Fields et al., 2008).

Since their identification, COE transcription factors have been implicated in many developmental processes, from muscle development to neuronal migration. I will briefly cover most of these processes, and then I will focus my attention on central Nervous System development.

COE proteins in development

EBF-1, the founder member of the COE family, was first discovered as factor essential for B-cell development (Hagman et al., 1991): in fact, B-cell development in the bone marrow of EBF1 mutant mice appears arrested at the pro-B-cell stage (Lin and Grosschedl, 1995). Identification of transcriptional targets suggested that EBF-1 regulates a multitude of genes in the B-cell specific program, such as *mb-1* (Ig-α, *CD79a*) (Hagman et al., 1991), *VpreB* surrogate light chain (Sigvardsson et al., 1997), *B29* (Ig-β) (Gisler et al., 1999), *CD19*, $\lambda 5$ and the B lineage commitment factor PAX5, through DNA binding or by acting in synergy with E-proteins (Sigvardsson et al., 1997). In addition, EBF-1 promotes the accessibility of immunoglobulin (Ig) gene segments for generating *V(D)J* gene rearrangement (Romanow et al., 2000). The ability of EBF-1 to activate promoters controlling expression of the surrogate light chains appears to be conserved also in humans although the primary DNA sequence of the promoters is poorly conserved (Gisler et al., 2000; Goebel et al., 2001).

COE proteins in neuronal differentiation and migration

The gene *Col*, identified in *D.melanogaster*, was initially characterized for its requirement at the blastoderm stage for the formation of a specific head segment (Crozatier et al., 1996). Moreover, *col* is expressed in a specific subset of post-mitotic neurons of both central nervous

system (CNS) and peripheral nervous system (PNS) (Crozatier et al., 1996). Further analysis of *col* mutants showed that the gene is required for a number of developmental processes including the formation of distinct embryonic somatic muscle and of adult wing.

Genetic evidence for multiple roles of COEs in neural development came with the identification of *C.elegans unc-3* (Prasad et al., 1998). *unc-3* is expressed in motor neurons which form the ventral nerve cord: *unc-3* mutants move abnormally, and this phenotype is
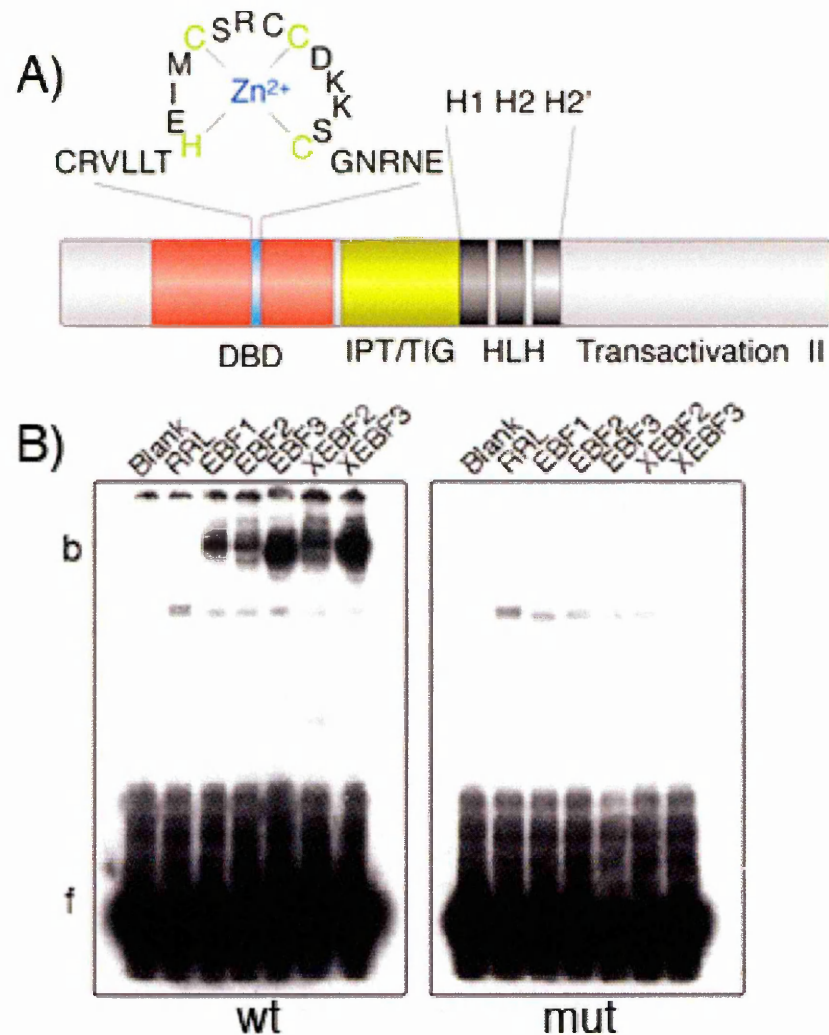

Figure 1.7 – Main features of COE/EBF proteins. A) Schematic primary structure of COE/ EBF proteins: note the presence of a Zn-finger motif in the DNA binding domain (DBD), and the duplication of the helix 2 in the HLH domain (see text). B) COE/EBF TFs bind a palindromic sequence – ATTCCCNNGGGAAT (a) –, but not to a mutated form (b), from (Pozzoli et al., 2001).

reminiscent of motor neuron axonal pathfinding defects (Wightman et al., 1997).

Ebf1, *Ebf2* and *Ebf3* are expressed along the rostro-caudal axis of the developing CNS, with overlapping patterns, except in the forebrain where each of them is restricted to specific regions (Garel et al., 1997; Wang et al., 1997), and in the cerebellum (Croci et al., 2006b). Expression of these genes is observed in differentiating neurons, *Ebf2* being restricted to early post-mitotic neurons whereas *Ebf1* and *Ebf3* expression is maintained in more mature differentiated neurons. The hypothesis that Ebf genes play a role in neuronal differentiation was corroborated by the observation that the over-expression of a dominant negative form of *XEbf2* prevents primary neuronal differentiation in *X.laevis* embryos (Dubois et al., 1998). Both *XEbf2* and *XEbf3* have a neurogenic activity, downstream of *XNeuroD*, during neuronal differentiation in this system (Dubois et al., 1998; Pozzoli et al., 2001). In the mouse, analysis of *Ebf1–/–* mutants revealed neuronal differentiation defects in CNS regions where *Ebf1* is the sole member of the family to be expressed, for instance in the embryonic striatum (Garel et al., 1999).

Studies in *X.laevis* provided insight on the role of Ebf genes in the neurogenic cascade, but in higher vertebrates neurogenesis differs in the respect that newly generated neurons from the VZ migrate to their final destination: analysis of Ebf mutants has revealed that these genes are also involved in neuronal migration. Evidence came from the observation that branchiomotor neurons migrate improperly in *Ebf1* null embryos (Garel et al., 2000) and that a migration defect is present in the gonadotropin-releasing hormone-synthesizing cells in *Ebf2–/–* background, resulting in generation of hypo-fertile mice (Corradi et al., 2003). A detailed set of gain-of-function and loss-of-function experiments conducted in chick embryo neural tube clearly demonstrated that Ebf genes are important for the initial steps of migration towards the mantle layer and neuronal differentiation, but are not required for cell cycle exit (Garcia-Dominguez et al., 2003). EBF1 can trigger *Neurog1* and *Neurog2* expression soon after electroporation (10 hours) (Garcia-Dominguez et al., 2003), while at later stages (20 hours) up-regulation of neuronal markers, such as β3-Tubulin, neurofilament, R-cadherin (Redies and Takeichi, 1996) was found, indicating clearly a neuronal differentiation in the electroporated half chick neural tube, compared to the untreated side. EBF-1 over-expressing cells escape the VZ and migrate towards the mantle layer. Electroporation of plasmids for a dominant negative form of EBF-1 together with wild type EBF-1 prevents precocious

neuronal differentiation and migration (Garcia-Dominguez et al., 2003).

Ebf2–/– mice are viable, but display cerebellar hypoplasia, primarily in the rostralmost part – lobules 2, 3 and fusion of the lobules 4-5 (Croci et al., 2006a). In *Ebf2* null embryos, the number of Purkinje cells is reduced, and this is not due to an alteration in progenitor proliferation, but rather to a migration defect of post-mitotic neurons, which accumulate in the cortical transitory zone during their migration (E14.5-E15.5), and some of them remain in the prospective cerebellar white matter at a stage when they should have already reached the cortex to form the Purkinje cell (PC) layer (P0-P3) (Croci et al., 2006a). An increased cell death is observed in migrating Calbindin-positive cells, which may, at least partially, account for the loss of PCs in the postnatal and adult *Ebf2* null mice (Croci et al., 2006a). Interestingly, a strong reduction in Insulin Growth Factor 1 (IGF1), a known secreted molecule important for cell survival (D'Ercole et al., 1996), has been observed in *Ebf2* null embryos, together with a reduction in the activation of the intracellular effectors such a s phosphorylated AKT (Croci L, Barili V, Chia D, Massimino L, van Vugt R, Masserdotti G, Longhi R, Rotwein P, Consalez GG. submitted. Local Insulin-like Growth Factor I expression is essential for Purkinje neuron survival at birth. Cell Death Differ.).

In summary, these data support the hypothesis that Ebf genes are involved in the neuronal commitment, neuronal differentiation, migration and, survival.

Ebf genes and the Notch Pathway

As the Notch pathway is important in the maintenance of progenitor cells, and Ebf genes trigger cell differentiation and migration, an interesting hypothesis is that the two pathways may be linked, and possibly act antagonistically. To test this hypothesis, two-cell stage *X.laevis* embryos were injected with mRNA for *Xebf2* or *XEbf2*, with or without mRNA for *Nicd* (Pozzoli et al., 2001): interestingly, *Nicd* mRNA co-injection abolishes neuronal differentiation — evaluated by *N-Tubulin* and *XNF-M* expression – triggered by *XEbf2*, while it has no effect on *XEbf3*-induced differentiation. Interestingly, they found that Notch signaling regulates *XEbf2* expression, as injection of Delta[Stu], a dominant negative form of the Delta ligand that inhibits Notch function (Chitnis et al., 1995), up-regulates endogenous *XEbf2* expression, but not X*Ebf3* (Pozzoli et al., 2001).

The Notch-EBF crosstalk was investigated also in a different developkental process, the hematopoiesis (Smith et al., 2005): through luciferase assay, transient transfection in hematopoietic pre-B cells and electromobility shift assay (EMSA), it was shown that NICD can abolish the EBF-mediated activation of known targets such as λ5, *B29*, *mb-1* and *CD19* genes, because of a reduced DNA-binding activity of EBF-1 in Notch-activated condition – either NICD-over-expression or constitutive activation of the endogenous Notch receptor (Smith et al., 2005).

Taken together, these data strongly support the hypothesis of a Notch-EBF crosstalk, but they looked only in one sense, that is the Notch regulation of EBF activity. To date, nothing is known about a possible role of EBF in regulating Notch signaling.

Zn finger proteins

Zn finger domains (ZFs) are small, self-folding protein structures that coordinate the binding of a zinc ion. Although there are 20 different types of ZF domains (Krishna et al., 2003), each categorized by the structure of their zinc stabilizing aminoacids, the most common type is the Cys2-His2 (C2H2) type. This motif, which self-folds to form a $\beta\beta\alpha$ structure, obtains its name from the coordinated binding of a zinc ion by the two conserved cysteine and histidine residues.

Zinc finger proteins (ZFP) may contain between 1 and 40 ZF domains, which are frequently arranged in groups or clusters of tandem repeats. C2H2 ZFs were initially identified in the DNA-binding domain of transcription factor TFIIIaA in *Xenopus laevis*, which has nine fingers (Miller et al., 1985). Since their discovery, the C2H2 ZFP have grown to be recognized as an important class of genomic regulators, because of their broad distribution and their expansion within the genome of eukaryotes. In humans, recent estimates calculate that approximately 3% of genes code for C2H2 proteins (**Table 3**), making them the second most prevalent protein motif.

C2H2 domains have been shown capable of interacting with RNA and proteins (Lee et al., 2006); in multi-zinger proteins, typically only 3-4 ZFs are involved in DNA binding. The remaining fingers are frequently involved in other types of interactions (Lu et al., 2003; Sun et al., 1996). In other cases, the ZFs seem to play a dual role of providing both DNA

and protein-binding functions (Seto et al., 1993). An increasing amount of functional and structural studies of ZF-mediated protein-protein interactions have been published, clearly indicating ZFs as important mediators of diverse functions.

Taxon	Number of proteins with C2H2 domains[a,b]	Ranking within proteome[b]	Coverage (%)[c]
Archaea	68		
Bacteria	153		
Eukaryotes	13,617		
Arabidopsis thaliana	164	50	0.5
Caenorhabditis elegans	216	13	1
Danio rerio	216	9	1.8
Drosophila melanogaster	349	2	2.1
Gallus gallus	74	18	1.4
Homo sapiens	1,055	2	2.8
Mus musculus	837	4	2.5
Rattus norvegicus	183	8	1.5
Saccharomyes cerevisiae	47	19	0.8
Viruses	74		

Table 3 – Summary of the proteins containing C2H2 Zinc finger domain.

Zinc-Finger Protein 423 (ZFP423), known also as O/E-1-associated zinc finger protein (OAZ)

Molecular and biochemical features

In 1997, a yeast-two-hybrid screening, performed by the group of R. Reed, identified a new putative partner for the O/E transcription factor family: the protein, firstly called ROAZ, rat O/E-1 Associated Zinc-finger protein, was then called ZFP423, Zinc-Finger Protein 423 (Tsai and Reed, 1997).

Murine *Zfp423* gene encodes a 148 KDa protein containing 30 Zinc-finger motifs, organized in six clusters (**Fig. 1.8Ab**). Working with the rat ortholog, rOAZ, Tsai and Reed showed that the Zn-finger 1-7 motif (cluster 1) binds DNA through the consensus sequence GCACCC, either direct or inverted (Tsai and Reed, 1997, 1998), while fingers 26-29 (cluster 6) mediate homodimerization as well as interaction with O/E-1 protein. Using "broken finger" mutants,

51

they also showed that Zn-finger 29 is critical for the interaction with O/E-1, but does not affect its homodimerization ability (Tsai and Reed, 1998). O/E-1 interacts with ZFP423 through the HLH domain, which is responsible also for the homo- and hetero-dimerization (Tsai and Reed, 1997).

ZFP423 is thought to modulate the ability of O/E proteins to activate gene transcription: for instance, O/E-1 protein poorly activates the OMP promoter, a known target of O/E-1, when ZFP423 is overexpressed. This effect has been verified also when ZFP423 is expressed together with O/E-2 and O/E-3 (Tsai and Reed, 1997). The functional finding correlates with the observed reduced ability of O/E-1 to bind the consensus sequence on the promoter, likely because ZFP423- O/E-1 heterodimers are unable to bind the specific sequence (Tsai and Reed, 1997). On the other hand, over-expression of ZFP423 and a member of O/E family activates the SV40 early promoter, thanks to the binding of ZFP423 to the promoter.

Some years later, ZFP423 was identified as a putative protein involved in BMP signaling cascade in a yeast-two-hybrid screening performed to identify novel BRE-binding factors (Hata et al., 2000). These authors demonstrated that human ZFP423 cooperates with BMP signaling in the activation of the *Xvent-2* promoter. This occurs because ZFP423 binds the BRE sequence (GCTCCA) on the *Xvent-2* promoter with the fingers 6-13 in a BMP independent manner, and it interacts with MH2 domain of SMAD1 with the Zn-fingers 14-19 (Hata et al., 2000) (**Fig. 1.8Ab**).

Other studies have strengthened the importance of ZFP423 as partner of the BMP cascade. ZFP423 was found to co-operate with the BMP cascade in regulating the expression of *Xretpos,* an integrated LTR-retrotrasposon-like element discovered in *X.laevis* (Shim et al., 2002), previously identified as a transcriptional target of the BMP signaling (Shim et al., 2000). Analyzing the promoter region of the retrotransposon, Shim found three putative Smad Binding Site sequences (SBE), and confirmed that at least SMAD1 binds those sequences *in vitro*. Furthermore, at the 3' of the SBE II, the authors found a sequence very similar to that one bound by ZFP423, namely TGGGGC. They demonstrated that the zinc fingers 9-19 of ZFP423 bind that sequence.

In effort to identify new putative BMP-regulated genes, Von Bubnoff and coworkers combined bioinformatic tools, phylogenetic footprinting and reporter gene assays. They firstly compared the promoter sequences of *Vent2* between *X.laevis* and human and identified

a 21 bp core region both necessary and sufficient for BMP responsiveness (von Bubnoff et al., 2005). This sequence contains both the SBE (CAGACAT) and a direct ZFP423 binding site (ZBS) (GGAGCC). They repeated the analysis with the *XId3* promoter, a novel BMP target identified by the same group (Peiffer et al., 2005) and obtained similar results: in fact, a core sequence of 24 bps contain both an inverted SBE (GTCTG) and a non canonical ZBS (ACGCCA). Despite the fact that most of the genes identified with this approach are induced by BMP treatment *in vivo*, only few of them contain 2 or more BRE sites. Unfortunately, authors did not complete the analysis checking how many promoter regions contain also a putative ZFP423 binding site, but it is likely that only some may require ZFP423. For instance, *Tlx-2*, a known target of BMP (Tang et al., 1998), is not regulated by ZFP423 (Ku et al., 2003). This observation suggests that ZFP423 may be required to regulate a subset of BMP-responsive genes, thus conferring selectivity to that signaling pathway.

Recently, another report showed that *Smad6*, an inhibitor of the SMAD cascade, is transcriptionally regulated by the cooperation between ZFP423 and BMP signaling (Ku et al., 2006). The authors showed that *Smad6* promoter contains a ZBS (GCTCCA), and ZFP423 enhances the BMP-mediated *Smad6* activation. ZFP423 seems to be important but not essential; in fact, luciferase assay on the *Smad6* promoter with mutation on the ZBS did not respond to ZFP423 over-expression and BMP4 treatment, while endogenous *Smad6* gene expression was up-regulated upon BMP4 treatment, even in the absence of ZFP423.

Human ZFP423 was used as model to study the capability of C2H2 zinc-finger proteins to interact with DNA or proteins (Brayer et al., 2008). To this end, all the six clusters were analyzed for DNA or protein-binding capacity by target site selection or yeast two-hybrid screening analysis, respectively. They found that all six clusters are capable of specific protein interactions, but only cluster 1 (zinc finger 1-7) can bind DNA through the GGGTGT consensus site. This site is very similar to that one found by Reed and colleagues (GCACCC) (Tsai and Reed, 1998). Quite surprisingly, neither hOAZ nor EBF were among the positive clones for cluster 6 (zinc fingers 26-30), and cluster 2 (zinc finger 9-13) was not found to be able to bind DNA.

In 2003, a group demonstrated that ZFP423 interacts with Parp1, Poly(ADP-ribose) polymerase 1 (Ku et al., 2003), a DNA-binding protein which modifies target proteins involved in chromatin decondensation, DNA replication and DNA repair.

These results clearly show the potential ability of ZFP423 to interact with many partners, but the major concern about the above mentioned experimental approaches that use part of the protein as bait is the high rate of false positives: this is because a motif may expose certain aminoacid residues that are usually hidden when the motif is placed in a more complex context, such as the tridimensional structure of the ZFP423 protein.

Taken together, these papers suggest that ZFP423 activity strongly depends upon the proteins it interacts with: it may act as co-repressor, co-activator, and it may bind DNA through two distinct clusters of zinc-fingers, which recognize slightly different binding sites.

Expression pattern and putative roles of ZFP423 during development

Zfp423 is expressed early during mouse development. Taking advantage on a gene-trap approach, in which the *β-geo* gene was fused to the *Zfp423* gene, Cheng and Reed analyzed the expression of *Zfp423* through X-gal staining (Cheng et al., 2007) (**Fig. 1.8B**). At embryonic day (E) 8.5, ZFP423$^{LacZ/+}$ displays bilateral expression along the dorsal neural tube, and this expression continues through later embryonic stages (**Fig. 1.8Bb-k**). At E9.5 *Zfp423* is expressed as two narrow continuous bands along the dorsal midline extending from the telencephalon caudally along the entire body axis (**Fig. 1.8Bc-d**). In transverse sections, *Zfp423* is mainly detected in the neuroepithelium, with the most intense staining in the dorsal region flanking the roof plate (**Fig. 1.8Be-g**). Later, X-gal staining is detected in limbs, lung, and in the cranial sensory placodes, including the olfactory and lens. In sagittal sections at E14.5, *Zfp423* expression is found mainly in the olfactory epithelium, thalamus, septum, midbrain ventricular zone and cerebellar primordium (**Fig. 1.8Bh**). In the developing cerebellar primordia, *Zfp423* expression is detected in the Purkinje cell layer (PC) and the external granular layer, (EGL) (**Fig. 1.8Bi-j**). The staining at both PC and EGL decreased postnatally, and is absent in adulthood (**Fig. 1.8Bh**).

A detailed analysis of *Zfp423* expression in developing olfactory epithelium (OE) (Cheng and Reed, 2007) revealed a broad expression of the gene at E18.5, apically to Mash1-expressing cells: interestingly, in Mash1 null mice, ZFP423-expressing cells are absent in the OE, suggesting the in the OE ZFP423 is downstream of Mash1. *Zfp423–/–* mice display

normal organization with slightly smaller nasal cavity and corresponding reduced OE area, but the number of mature olfactory-receptor neurons (ORNs) is reduced of about 30%, and ORN axons fail to innervate the dorsal caudal regione of the olfactory bulb (OB).
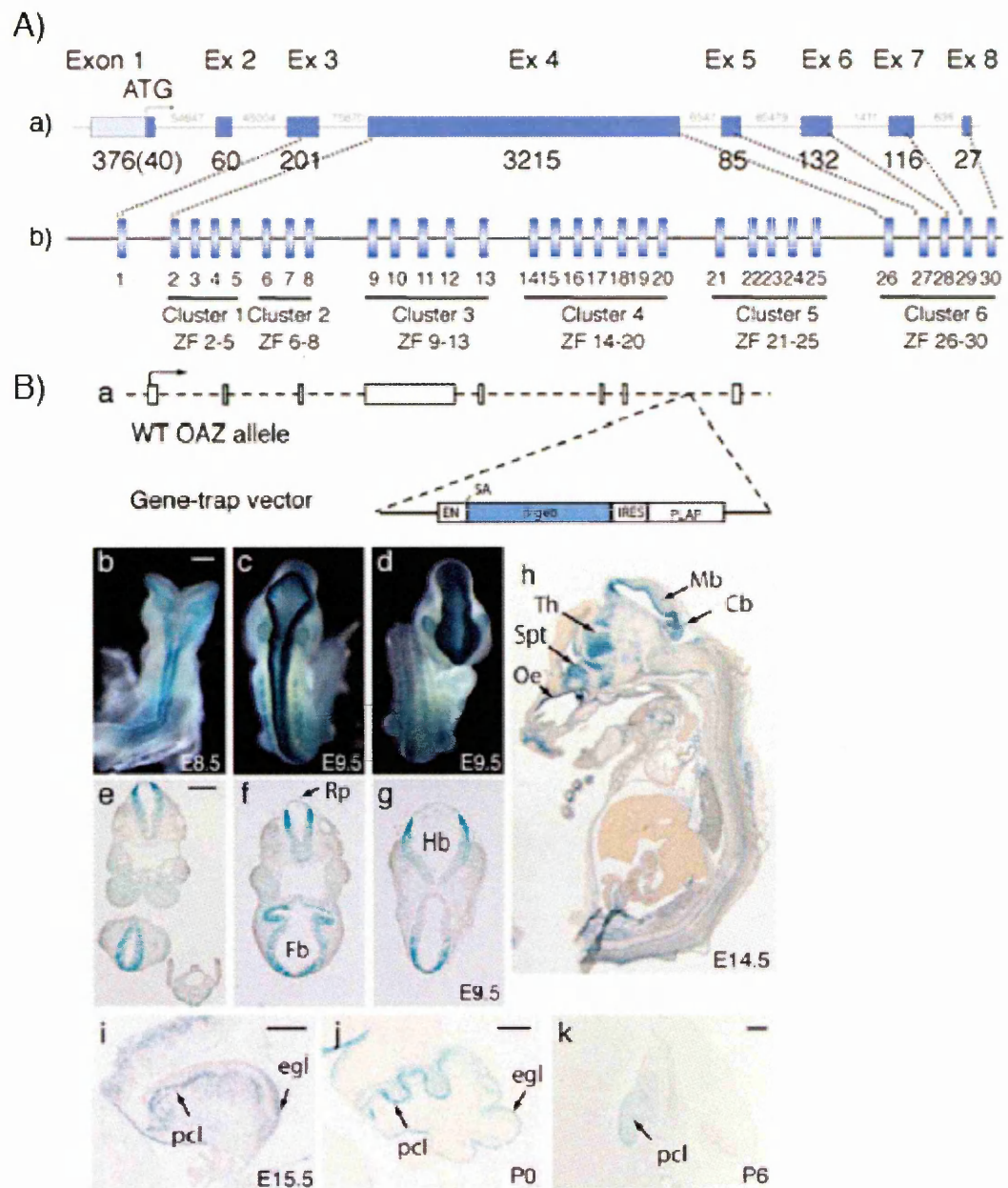
Figure 1.8 - Structure and expression of *Zfp423*. A) Sketch on the gene-protein relationship. **Aa)** Genomic locus of the murine *Zfp423* gene. The genes is composed of 8 exons, separated by small – 631 bp – and very big – up to 86000 bps – introns. **Ab)** ZFP423 contains 30 Zn-finger motifs, organized in 6 clusters (see text for the description). **B)** Analsysis of the expression of a transgene controlled by Zfp423 promoter. **Ba)** Gene trap strategy. **Bb-k)** Analysis of the LacZ expression at different stages of mouse development (see text for description).

To better understand the role of *Zfp423* in the context of olfactory development, the authors generated a knock-in mouse in which a cassette containing the *Zfp423* cDNA, an intra ribosome entry site (IRES) sequence, and a yellow fluorescent protein (*Yfp*) cDNA, was inserted into the *Ebf3* locus. This locus was selected because *Ebf3* is expressed in OE, and YFP was used to visualize ZFP423-expressing cells. In EBF3$^{ZFP423/+}$ mice, there was a dramatic reduction of mature ORNs (positive for OMP, olfactory marker protein), and the majority of the cells in the epithelium were positive for GAP43, a marker of immature state of ORNs. Thus, persistent expression of *Zfp423* seems to block the terminal differentiation of ORNs cells. Activation of *Zfp423* expression in mature ORNs – OMP positive – caused the appearance of a GAP43-expressing population, that is an immature population, in the apical region, where normally only mature ORNs are present. OMP/GAP43 double labeling revealed that OMP expression was suppressed in the reactivated GAP43-positive cells.

Taken together, these experiments indicate that *Zfp423* is involved in the differentiation/ maturation of olfactory-receptor neurons, and it is also sufficient to establish an immature ORN phenotype.

Regardless of its role in OE development, the most striking phenotype observed in *Zfp423* null mice is the cerebellar hypoplasia: *Zfp423–/–* mice show ataxic and uncoordinated movements, and die within 4 weeks after birth (Alcaraz et al., 2006; Cheng et al., 2007; Warming et al., 2006). Morphological examination of *Zfp423-/-* brains revealed severe defects in the forebrain and in the cerebellum. In the *Zfp423-/-* forebrain, the corpus callosum is almost absent, and the hippocampal formations are reduced and disorganized (Alcaraz et al., 2006; Cheng et al., 2007). It is noticeable that, in *Zfp423* null mice, callosal axons project normally along the intermediate zone of the cortical plate, but when they approach the midline, they fail to cross the midline (Cheng et al., 2007). Similar defects are present also in the formation of the septum, which could contribute to the subsequent defects of the commissural axons crossing at the midline (Cheng et al., 2007).

The cerebellum of the *Zfp423-/-* mice is seriously malformed: although cortical foliation is present in young null mice and the laminar arrangement is maintained, the number and size of the lobes are much reduced, lateral cerebellar hemispheres are smaller and the central vermis is severely affected, or, in some cases, fails to form (**Fig. 1.9a, d**) (Cheng et al., 2007). PC are born, but develop more slowly in the mutants, and many are ectopically situated in

the molecular layer of the cerebellar cortex (**Fig. 1.9e**) (Cheng et al., 2007; Warming et al., 2006). IGL is also formed (Cheng et al., 2007), thus indicating that the differentiation and the migration of GC precursors could proceed grossly normally and mature GCs (*Zic1+*) could be detected in the IGL. Nevertheless, a stronger reduction in proliferating (KI67+) and total number of cells (DAPI) in the RL were observed in *nurr12* mutants, a spontaneuous *Zfp423* mutant (Alcaraz et al., 2006); *Math1+* cells, arising from RL and migrating towards the cortex to form the EGL, are reduced at E13.5-E15.5 (Alcaraz et al., 2006), and a delay in the postnatal expansion of GC precursors is observed (Cheng et al., 2007).

As *Zfp423* is expressed early during development and midline fusion initiates at E13.5, Cheng analyzed the proliferation of the precursors and found that at E13.5 the density of proliferating cells (BrdU+/mm) in the cerebellar primordia is comparable between wt and *Zfp423* null embryos, although mutants showed a smaller primordia and the fusion area was limited. At E15.5, the fusion defect was clearly visible, with the two primordia barely attached at the medial region, which failed to further expand. In *nurr12* mutants, Alcaraz et al. counted the total number of cells (DAPI), the number of proliferating cells (KI67+) and the cells in S-phase (or S-G2 phase) (BrdU+) at three stages, E12.5 and E14.5 and E15.5. She found a statistically significant reduction in the total number of cells, in the absolute number of proliferating and S-phase cells in the mutants at every stage, but the ratio between BrdU+ cells and total number is not significantly reduced, except at E15.5 (Alcaraz et al., 2006). This may suggest either fewer initial precursors or cumulative effect of a modest reduction in VZ proliferation.

In *nurr12* mutants, precursor cells from the VZ are capable to start the differentiation program: *in situ* hybridization with an *Ebf1* probe at E14.5 showed a stronger expression in the mutant embryos than in control littermate, and at E15.5 there were many EBF+-TuJ1+ cells, indicating that the cells were differentiating neurons.

As *Zfp423* mutant mice show a clear and severe hypomorphic cerebellum, it is quite surprising that VZ precursors, from which PCs arise from, proliferate and differentiate almost normally: one might expect that either the cells die during differentiation and migration, or, after an initial differentiation, they do not fully differentiate. Alcaraz et al. did not find increased apoptosis in *nurr12* mutants at E14.5, but rather that the expression of *Car8*, a later PC marker that depends on ROR*α*, was reduced both at E15.5 and at P2 (Alcaraz et al.,

57
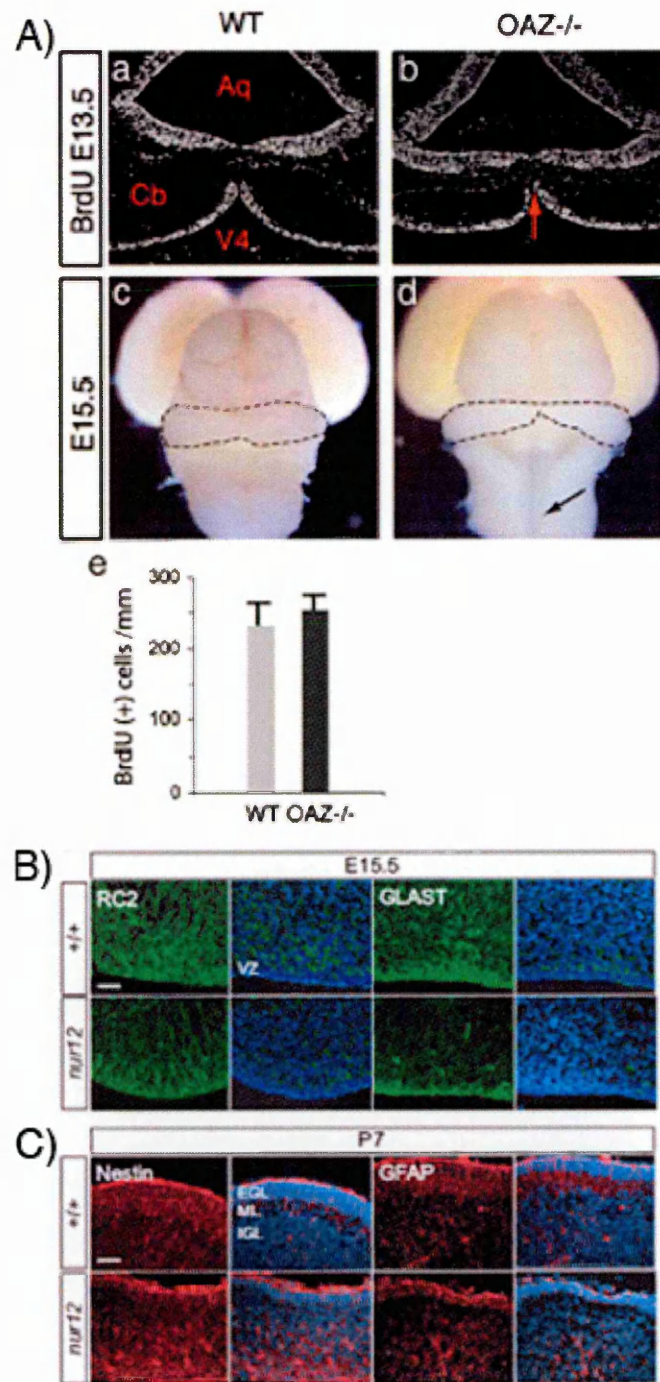
Figure 1.9 – Analysis of developmental defects described in the Zfp423 null mouse. Aa-d) Midline fusion defects present at E13.5 d.p.c. and clearly visible at E15.5. **Ae)** Quantification BrdU positive cells in WT and KO cerebellar primordium at 13.5 d.p.c **B)** Immunostaining for RC2 and GLAST shows the presence of defects in the cerebellar radial glia at 13.5 d.p.c **C)** At P7, Zfp423 null cerebellum shows altered expression of Bergmann glia markers, such as Nestin and GFAP (see text for details).

2006).

Bergmann glia differentiation is also affected in *Zfp423* mutants: in fact, *nurr12* mutant embryos showed a reduction of *Gdf10*, an early lineage-restricted marker of differentiating Bergmann glia, at E13.5-E15.5 (Alcaraz et al., 2006); RC2 and GLAST staining at E15.5 further confirmed the reduction in radial fiber formation; Nestin and GFAP staining at P7 revealed that the paucity and disorganization of glial fibers persist at later stages of development. As Bergmann glia fibers are important for the correct migration of the PC towards the cortex, disorganized glia may account for the ectopic presence of PC in the molecular layer (Cheng et al., 2007; Warming et al., 2006).

Very recently, ZFP423 has been found as a component of the Retinoic Acid signaling pathway, further corroborating its role in neuronal commitment and differentiation (Huang et al., 2009). Through a screen aimed at the identification of genes involved in RA signaling, the authors found that transfection of shRNA against *Zfp423* or *Rxr*α abolished RA-mediated differentiation both in F9 cells – a teratocarcinoma cell line extensively used as a model to investigate RA signaling *in vitro* – and in E14 primary cultures. They found that ZFP423 may interact *in vitro* with both RXRα and RARα, and it is associated with RARE region in the *Rar*β promoter. *Zfp423* knockdown reduced the expression of many R.A. target genes, such as *TrkA, TrkB, Ret, Rar*β in SH-SY5Y human neuroblastoma cell line treated with R.A.. Given this effect on RA responsiveness, they examined whether ZFP423 may be correlated with survival of patients affected by neuroblastoma: although the size of the available cohorts is small (less the 100 patients), high level of ZFP423 are associated to a better survival rate, while patients with low level of ZFP423 have a worse prognosis. These data suggest ZFP423 as a *bona fide* tumor suppressor in tumors of neural origin.

NOTCH, BMP, ZFP423 and EBF: four players and a model system

The development of the CNS is a complex, continuous and tightly regulated process: the neural plate forms from the embryonic ectoderm, and closes giving rise to the neural tube. As development proceeds, cells located close to the ventricle proliferate and differentiate in a space- and time- dependent fashion, determining the generation of different cell types and their migration towards their final destination. There, they establish contacts and form the

neuro-glia network named as Central Nervous System.

In the previous paragraphs, I have described the onset of the neurogenetic program from ventricular radial glial cells, with a particular interest for the *extrinsic* and *intrinsic* cues responsible for such process. I have focused my attention on some molecular mechanisms involved in the regulation of neurogenesis, namely instructive morphogens – BMP signaling –, cell-cell interaction regulation – Notch pathway –, maintenance of uncommitted progenitors and their differentiation – Hes and proneural genes –, migration and differentiation – EBF transcription factors. I have also introduced ZFP423, a molecule capable of regulating some of the signaling cascades.

While BMP and Notch-Hes are pathways used in many different systems to regulate differentiation of uncommitted progenitors, the role of the others is more confined, as in the case of ZFP423, whose deletion in mice causes a dorsal midline fusion defects. Interestingly, these molecules are expressed and play important roles during the development of the cerebellum, as emerged from the description of mutant mice.

Cerebellum: structure, function, neurogenesis

Cerebellar genesis

The *Cerebellum* (from latin: "little brain") is an anatomical part of the CNS located in the hindbrain (the posterior-inferior part of the brain), directly dorsal to the pons; it occupies most of the posterior cranial fossa. It constitutes 1/10th of the total brain volume. However, the cerebellum contains 50% of the total number of neurons in the brain.

The cerebellum plays a very important role in the integration of sensory perception and – above all – motor coordination. In order to coordinate motor control, the cerebellum is connected to the cerebral motor cortex, the primary source of inputs for the voluntary muscular system, by a large number of neural pathways and to the spinal cord through the spinocerebellar tract, which provides proprioceptive feedback on the position of the body in space. The cerebellum integrates these pathways exerting a constant regulatory feedback on body position by fine-tuning motor movements.

The cerebellum is formed by cells deriving from the metencephalon and mesencephalon:

for its correct patterning, the cerebellar primordium requires regulatory factors produced by Isthmic Organizer (IsO), a structure positioned exactly at the boundary between mesencephalon and metencephalon. The IsO is necessary and sufficient to pattern the mid-/hindbrain region of the neural tube.

The formation of the IsO requires complex interactions between genes specifically expressed in defined areas. In particular, *Otx2* (one of the murine homologues of the *Drosophila* gene *orthodenticle*) and *Gbx2*, (homologue of the *Drosophila* gene *unplugged*) are central to the development of the mid-hindbrain boundary.

At E7.5, *Otx2* is expressed in the mouse mesencephalon, with a posterior boundary at the rostral metencephalon, whereas *Gbx2* transcript occupies the metencephalon is delimited anteriorly by the caudal mesencephalon. At E7.5, *Otx2* is expressed in the mouse mesencephalon, with a posterior boundary at the rostral metencephalon, whereas *Gbx2* transcript occupies the metencephalon is delimited anteriorly by the caudal mesencephalon (Ang et al., 1996; Wassarman et al., 1997).

Apart from the determination of IsO position, *Gbx2* and *Otx2* also regulate the expression of *Fgf8*, with OTX2 negatively inhibiting the expression and *Gbx2* maintaining it (Martinez et al., 1999; Millet et al., 1999). *Fgf8* is involved in regulating the various genes expressed in the caudal midbrain and anterior hindbrain: reduced level of *Fgf8* expression results in severe patterning defects of these regions, usually affecting the cerebellum (Meyers et al., 1998). In addition, *Fgf8* induces the expression of *Wnt1* through Lim homeobox 1b (*Lmx1b*) (Reifers et al., 1998), which – in turn – maintains the expression of Engrailed 1 (*En1*): this acts as a positive regulator of *Fgf8* expression. This network of gene expression creates a positive regulatory loop that sustains the expression of *Fgf8* at the IsO.

The cerebellum specifically arises from the whole rhombomere 1 and from the most rostral portion of rhombomere 2 (Marin and Puelles, 1995), and FGF8 negatively regulates *Hoxa2*, a homeobox domain gene specifically expressed in rhombomere 2 (Irving and Mason, 2000); this interaction turns out to be very important for cerebellar development, as studies conducted in *Hoxa2* mutant mice have demonstrated that *Hoxa2* prevents the extension of the cerebellar anlage into rhombomere 2 (Gavalas et al., 1997). Thus, the IsO, and in particular its main secreted factor FGF8, delimits the rostro-caudal extension of the cerebellar primordium.

Concerning the extension of the cerebellar territory along the dorso-ventral axis, several transplantation studies have clearly demonstrated that the cerebellum arises from the dorso-lateral domain of rhombomere 1 (Hallonet et al., 1990; Wingate and Hatten, 1999). Members of the TGF-β super-family, in particular BMP4, as well as members of the Growth Differentiation Factors family, like GDF7 (Chizhikov and Millen, 2003), secreted by the roof plate, have been implicated in the specification of cerebellar boundaries. Taken together, the spatial and temporal combination of all these regulatory factors is sufficient to pattern and establish the cerebellar primordium by E9, concluding the first step in the cerebellar development.

The second phase of development begins between E9 and E11: during this period the two different germinative zones of the cerebellum arise from the cerebellar primordium, that will lead to the specification of the different types of cerebellar neurons. At this time, the cerebellar anlage is composed by two dorso-lateral symmetric structures on each side of the rhombencephalic midline; these protrusions will eventually fuse and form the primitive cerebellar plate. The more ventral germinal layer is called Ventricular Zone (VZ), whereas the more dorsal one is dubbed Rhombic Lip (RL).

Cerebellar neurogenesis

All cerebellar neurons derive from two germinative neuroepithelia with distinct developmental potential. Glutamatergic lineages – projection neurons of the deep nuclei (DCN), unipolar brush cells and granule cells – derive from progenitors expressing *Math1*, that emigrate from the rostral RL and undergo subsequent waves of differentiation (Alder et al., 1996; Fink et al., 2006; Hevner et al., 2006; Machold and Fishell, 2005). GABAergic neurons – PCs, Nucleo-Olivary Neurons, Deep Nuclear Interneurons and the different classes of inhibitory interneurons – are produced by pancreas transcription factor1-a (Ptf1-a)-positive precursors of the VZ (Hoshino, 2006; Hoshino et al., 2005).

Neurogenesis from the Rhombic Lip: The Glutamatergic cerebellar component

The RL is located between the IV ventricle and the roof plate and is characterized at the

level of rhombomere 1-8 by the rhombic shaped opening of the neural tube that delimits the rhombencephalon dorsally. *Math1* starts to be expressed in the RL germinative zone at E13, and plays a key role for granule cell neurogenesis. Many neuronal cell types originate from these cells: granule cells, glutamatergic deep nuclear projection neurons and unipolar brush cells (UBCs) (Englund et al., 2006; Fink et al., 2006; Machold and Fishell, 2005).

Postmitotic neuronal precursors of deep nuclei start moving from the RL at E11.5 and reach the NTZ via a subpial migratory pathway. During their migration, they express *Pax6*, *Tbr1*, and *Tbr2* (Fink et al., 2006). Progenitors of UBCs express *Tbr2* and have a unique migratory behavior: they leave the RL during late stages of embryonic life (E13-E17), they veer deep into the cortex, ventral to PCs, and settle in the prospective internal granular layer (IGL), which is their final destination.

Granule cell progenitors leave the RL at E13, while expressing *Math1*, *Zic1* and *Zic3*, and *RU49*, migrate tangentially along the cerebellar surface and between E15 and P15 generate the External Granule Layer (EGL), a second germinative neuroepithelium that covers the whole cerebellar surface. This zone can be also divided into an inner and outer EGL, considering that the massive proliferation occurs in the external half of this area, deeper to which accumulate post mitotic granules ready to migrate radially into the cortex. The EGL undergoes a progressive expansion, as the granule cell precursors strongly proliferate after birth, but it gradually disappears after P15 as mitotic activity ceases. All postmitotic granule cells migrate inwards, forming the Internal Granule Layer (IGL) after cell-cycle exit. The proliferation of Granule Cell Precursors in the EGL is regulated by the production of SHH by Purkinje cells (Wallace, 1999). SHH is expressed by Purkinje cells during postnatal life, whereas molecules involved in the SHH-signaling pathway, such as patched and Gli1/Gli2, are expressed by granule cell precursors.

Neurogenesis from the Ventricular Zone: The GABAergic cerebellar component

The generation of VZ-derived neurons follows a specific sequence, as clearly demonstrated by various fate mapping studies (Morales and Hatten, 2006). Firstly, Deep Nucleo-Olivary Projection Neurons (*DNOPN*) are generated between E10.5 and E12.5 in the mouse embryo.

63

These cells express several distinctive transcription factors (IRX3, MEIS2, LHX2/9) and migrate deeply into the primordium to a territory called *Nuclear Transitory Zone* (NTZ). Then, PC arise from VZ: they become post-mitotic between E12 and E13 and migrate just below the NTZ. At this stage, PCs express transcription factors *Lhx1* and *Lhx5,* and are positive for *RGS8,* a GTPase-activating protein (Morales and Hatten, 2006) and for RORα, an orphan nuclear receptor specifically expressed in PCs (Boukhtouche et al., 2006) and, later on, in molecular layer interneurons.

Between E14 and E17, in the mouse embryo, the development of these two populations proceeds, and the DNOPNs reach their final position beneath the PCs in the NTZ, while PCs start to express − from E14 − the calcium-binding protein Calbindin (*CaBP*), and migrate radially, guided by clues produced by the developing granule cells, which in turn are migrating to form the EGL, and by the cerebellar nuclei neurons.

All the GABAergic neurons in the cerebellum express the bHLH transcription factor *Ptf1α (Pancreatic Transcription Factor 1α),* which is necessary for the correct development of these neurons, as demonstrated by studies on the mutant mouse named *cerebelless,* deficient for *Ptf1α* (Hoshino et al., 2005; Morales and Hatten, 2006; Pascual et al., 2007). While it has been established that Ptf1a is necessary for VZ progenitors to generate GABAergic cerebellar neurons, less in known about the molecular interactions that further specify the different GABAergic subtypes, but several indications suggest that the germinative neuroepithelium of the VZ is composed of different subsets of progenitors, defined by the expression of specific combinations of transcription factors (Maricich, 1999; Zordan et al., 2008).

From E13 on, the VZ starts to give rise to interneuron progenitors, a process that will continue during late embryonic and postnatal development. The cerebellar inhibitory interneurons arise from Pax2-positive precursors (Weisheit et al., 2006) that can be found in the medial region of the VZ at that time, and continue to proliferate while migrating through the white matter until they reach their final destination in the cerebellar nuclei or cortex. This process, that will give rise to nucleo-olivary neurons, and Golgi, Lugaro, Basket and Stellate inteneurons, concludes the neurogenesis from the VZ.

As stated before, VZ neurogenesis generates different cell types over time: this implies that VZ-radial glial cells must differentiate and maintain themselves. When the equilibrium between neurogenesis and progenitor maintenance is lost, as in the case of Notch1–/– embryos (Lutolf et al., 2002; Machold et al., 2007), premature neuronal differentiation occurs, with the depletion of the progenitor pool and a loss of late-born neurons.

BMP signaling exerts both neurogenic and antineurogenic functions depending on the context in which it acts: during cerebellar development, roof plate secretes BMP molecules, mainly acting on the proliferation and specification of RL-derived neurons. Alder and colleagues showed that BMPs are important regulators of cerebellar granule neuron fate determination (Alder et al., 1999); recently, Notch pathway has been shown to antagonize BMP-induced granule cell development, as over-expression of NICD is sufficient to reduce expression of granule cell fate determinant *Cath1* (Machold et al., 2007). Nevertheless, Notch and BMP signaling can cooperate in activating the *Hes5* promoter (Takizawa et al., 2003), and pull down assays suggest that effector molecules of the two pathways – NICD and SMAD1-SMAD4 – may be part of the same complex (Takizawa et al., 2003).

Early-B cell transcription factors play important roles in neuronal differentiation and migration (Garcia-Dominguez et al., 2003) and, during cerebellar development, EBF2 triggers the initial steps of PCs migration (Croci et al., 2006b). Interestingly, a functional relationship between Notch pathway and EBF activity has been demonstrated in two developmental processes: in *X. laevis*, EBF-driven neuronal differentiation is abrogated when Notch pathway is activated (Pozzoli et al., 2001). Likewise, during hematopoiesis, the activation of EBF1 target genes is reduced upon Notch activation, possibly because of a reduced DNA-binding capability of EBF (Smith et al., 2005).

Recently, the analysis of *nurr12* mutant mice (Alcaraz et al., 2006) or knock-out mice for the *Zfp423* gene (Cheng et al., 2007; Warming et al., 2006) revealed severe cerebellar defects along the dorsal midline in these animals: these findings are even more important when associated with previous works showing that ZFP423 interact with BMP-intracellular effectors SMAD1-SMAD4 triggering transcription of specific target genes (*Xvent2, Xretrop2, Smad6*) and it interacts with EBF TFs. The finding that, in *Zfp423–/–* mice, the number of

Bergmann glia is reduced (Alcaraz et al., 2006), and ZFP423 may revert differentiated cells to a neuronal progenitor fate (Cheng and Reed, 2007), raised the question of whether ZFP423 may contribute to balance the mentioned pathways in regulating progenitor maintenance and early differentiation steps.

Aim of the project

As *Zfp423* interacts with BMP signaling and EBF TFs, *Zfp423* mutants display developmental defects possibly associated with radial glia maintenance, and Notch pathway has been linked with BMP and EBF TFs, we examined whether ZFP423 may have any role in Notch signaling. Firstly, we analyzed in detail the expression of *Zfp423* and the Notch targets *Hes5* and *Hes1* during cerebellar development; then, we moved to an *in vitro* system to test whether a functional and physical connection existed between Notch and ZFP423. We used two *in vitro* models, such as neuralized P19 cells and myoblastic C2C12 cells, to analyze endogenous Notch target activation and *Hes5* promoter responsiveness. We also collaborated with Prof. Monica Vetter, University of Utah, to verify our observations *in vivo*, in *Xenopus laevis* embryos. Taking advantage of established *in vitro* essays, we also tested whether BMP and EBF TFs may regulate Notch targets in a ZFP423-dependent fashion. Finally, we investigated the direct interaction between ZFP423 and NICD.

Taken together, the results presented in this PhD thesis indicate ZPF423 as an important partner for Notch signaling for two main reasons: among the possible Notch targets, only a subset of them is activated in a given context, and ZFP423 may help define contextual activation of specific targets; secondly, as ZFP423 interacts with important pathways, it may contribute to determine a cooperation between them – for instance, Notch and BMP signaling on *Hes5* – or, alternatively, an antagonism – as in the case of Notch and BMP signaling in granule cell differentiation. Alternatively, it could affect the ability of EBF to promote neuronal commitment in progenitor cells.

Results

Expression of *Hes5*, *Hes1* and *Zfp423* in developing cerebellar primordium

During cerebellar development, *Zfp423* labels the rhomboencephalon and mesencephalon at E8.5 and E9.5, and the hindbrain and the cerebellum thereafter. We examined the expression of *Zfp423* at the onset of cerebellar neurogenesis using a transgenic line (Id: W008G09, (Skarnes et al., 2004)), which carries a *LacZ* gene inserted by gene trapping within the *Zfp423* gene. X-GAL staining of whole mount transgenic embryos revealed the expression of *Zfp423* in the neural tube, in the hindbrain and in the cerebellar primordium at E10.5 (**Fig. 2.1A**). To characterize in detail the expression of *Zfp423*, we performed *in situ* hybridization on embryonic cerebellar tissue sections at E10.5 and E11.5 (**Fig. 2.1B-E**). The analysis showed that *Zfp423* is expressed in both the germinative epithelia of the cerebellar primordium – the RL (arrow) and the VZ (solid arrowhead) – both in medial and lateral sections at the stages analyzed. Interestingly, its expression seems to be reduced, or absent, in the Isthmic Organizer (IsO) region (empty arrowhead) (**Fig. 2.1B-E**). As Notch signaling is known to play important roles both in VZ (Lutolf et al., 2002), RL (Machold et al., 2007) and IsO development (Hirata et al., 2001; Lobe, 1997), we analyzed the expression of *Hes5* and *Hes1* in the context of cerebellar development via *in situ* hybridization. Whole mount *in situ* hybridization revealed that *Hes5* mRNA is expressed in the cerebellar primordium and the hindbrain at E10.5 (**Fig. 2.1A'**); at E11.5 and E12.5, *in situ* hybridization on sections showed that *Hes5* is highly expressed in the VZ (arrowhead) and RL (arrow) and absent in the IsO (**Fig. 2.1B'-E'**), a pattern of expression overlapping the expression of *Zfp423*. The expression pattern of *Hes1* differs from *Hes5*: in fact, at E10.5 *Hes1* is expressed in a thinner region of the cerebellar primordium compared to *Hes5* (**Fig. 2.1A"**), while at later stages – E11.5 and E12.5 – *Hes1* domain labels mainly the IsO (empty arrowhead) and the RL (arrow), adjacent to the cerebellar roof plate, and a very weak signal is detected in the VZ (**Fig.2.1B"-E"**). Interestingly, in the cerebellar primordium at E12.5, *Zfp423* is expressed at high levels flanking the midline, where it co-localizes with *Hes5* (**Fig. 2.1D-D'; E-E'**).

Since *Zfp423* precedes the expression of *Hes5* and seems to overlap with it, at least in the cerebellar VZ, we sought to know whether ZFP423 might act in the context of Notch signaling pathway.
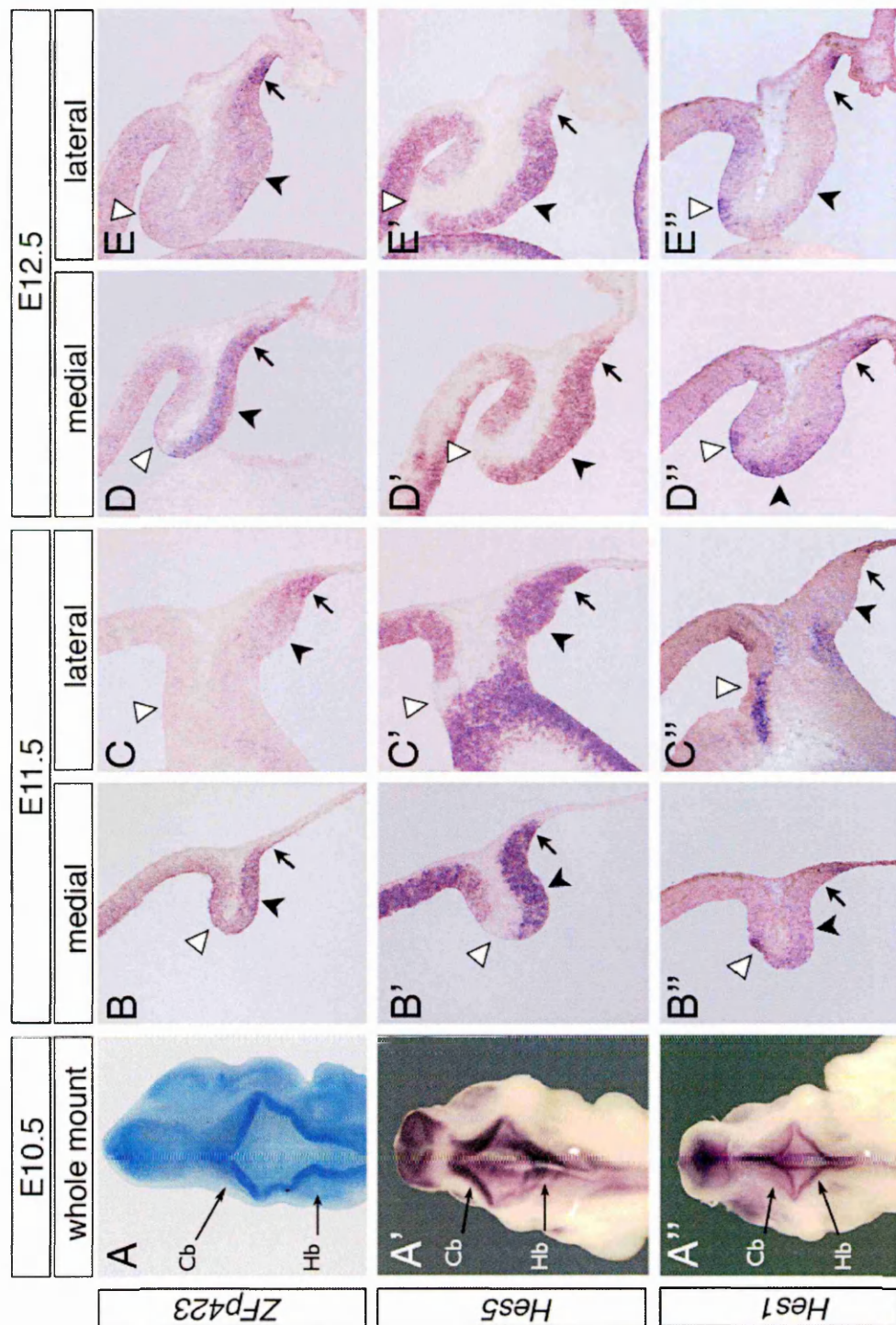
Figure 2.1 – Colocalization of *Zfp423* and *Hes5* in the prospective cerebellar vermis. A) Whole mount LacZ staining of an E10.5 embryo carrying a gene trap insertion in the *Zfp423* locus. **A', A")** Whole mount E10.5 embryos hybridized with *Hes5* and *Hes1*, respectively. Cb, cerebellar primordium; Hb, hindbrain. Note *Zfp423* expression at the border with the roof plate. **B-E)** E11.5 and E12.5 sagittal sections from medial and lateral territories of the cerebellar primordium, hybridized with *Zfp423*. Solid arrowhead: ventricular zone (VZ); arrow: rhombic lip (RL). **B'-E' and B"-E")** As above, hybridized with *Hes5* and *Hes1*, respectively. Empty arrowhead in B" indicates the isthmic organizer (IO). Notably, *Hes5* is expressed in VZ and RL and sharply silenced in the IO, whereas *Hes1* is transcribed in the RL and IO, and silenced in the VZ

ZFP423 cooperates with NICD in activating *Hes5* expression in P19 cell line

To test the hypothesis of a possible link between Notch pathway and ZFP423, we chose P19 cell line as an *in vitro* model system. P19 cell line was derived from a teratocarcinoma induced in C3H/HC mice (McBurney et al., 1982). These pluripotent embryonal stem cells can be maintained in culture in an undifferentiated state, or treated to differentiate into specific cell types. When injected into early mouse embryos, P19 cells are capable of contributing to a variety of apparently normal tissue, suggesting that the mechanisms of their differentiation are similar to those of normal embryonic cells (McBurney et al., 1982). P19 cells can also be induced to differentiate *in vitro* into multiple cell types, including beating cardiac myocytes, skeletal myocytes, as well as neurons (Ding et al., 2006; Jones-Villeneuve et al., 1982; McBurney and Rogers, 1982). Retinoic acid (R.A.) treatment can trigger P19 cells to differentiate into neurons *in vitro*: R.A. treatment for 2 days is sufficient to commit P19 towards a neuronal fate (Jones-Villeneuve et al., 1982).
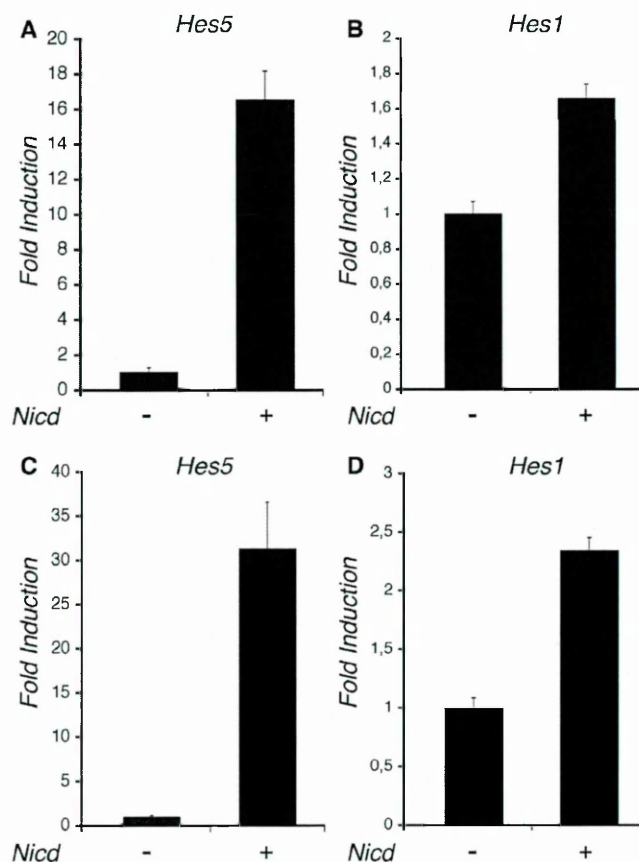
Figure 2.2 – Activation of *Hes5* and *Hes1* gene expression by NICD in P19 cell line in absence and presence of Retinoic Acid. A-D) Real-time RT-PCR analysis of P19 treated as below. **A,C)** Over-expression of *Nicd* induces *Hes5* mRNA upregulation, both in absence (**A**) or in presence (**C**) of Retionic Acid (10⁻⁶M) in the medium for 24 hours. **B,D)** Over-expression of *Nicd* induces *Hes1* mRNA upregulation, both in absence (**B**) or in presence (**B**) of Retionic Acid (10⁻⁶M).

As a first step, we verified the responsiveness of P19 cells to Notch signaling activation, as previously shown (Takizawa et al., 2003), both in presence or absence of R.A. treatment. To this end, we transfected P19 cells with a plasmid encoding the Notch Intracellular Domain (NICD), and 24 hours after the transfection, we collected the cells, extracted the RNA, retro-transcribed it to cDNA and performed a real time q-PCR to evaluate the activation of two known Notch targets, *Hes5* (**Fig. 2.2A, C**) and *Hes1* (**Fig. 2.2B, D**). P19 cells responded to NICD over-expression by up-regulating both Notch targets, both in absence or presence of R.A., at a similar magnitude. In agreement with our first observation and the literature (Takizawa et al., 2003), we chose to evaluate the role of ZFP423 in the context of Notch signaling 24 hours after the transfection.

We repeated the experiment in neuralized – treated with R.A. – P19 cells, transfecting a constant amount of the plasmid for NICD and increasing amount of a plasmid encoding *Zfp423* cDNA. We verified the expression of both constructs through semi-quantitative PCR (**Fig. 2.3A**) and then, analyzed the expression of the endogenous *Hes1* and *Hes5* in each sample via real time q-PCR. The expression of *Hes5* (**Fig. 2.3B**) was unaltered in presence of ZFP423 alone, but increased in a dose dependent fashion when ZFP423 is co-expressed with NICD. *Hes1* expression was up-regulated by NICD, but not enhanced by the co-expression of ZFP423 (**Fig. 2.3C**). To test whether the cooperative effect was specific for *Hes5*, we evaluated the expression of other Notch targets, such as *Blbp* and *Nrarp*, in presence or absence of ZFP423: we found that *Blbp* mRNA was increased in NICD-ZFP423 co-transfected cells (**Fig. 2.3D**), compared to NICD transfected cells, while *Nrarp* expression was not enhanced by ZFP423 over-expression (**Fig. 2.3E**) in presence of NICD.

These experiments suggested that ZFP423 alone does not have a direct effect on the activation of Notch downstream targets, but rather cooperates with NICD to sustain or increase their expression, and possibly, select specific targets among the putative ones.
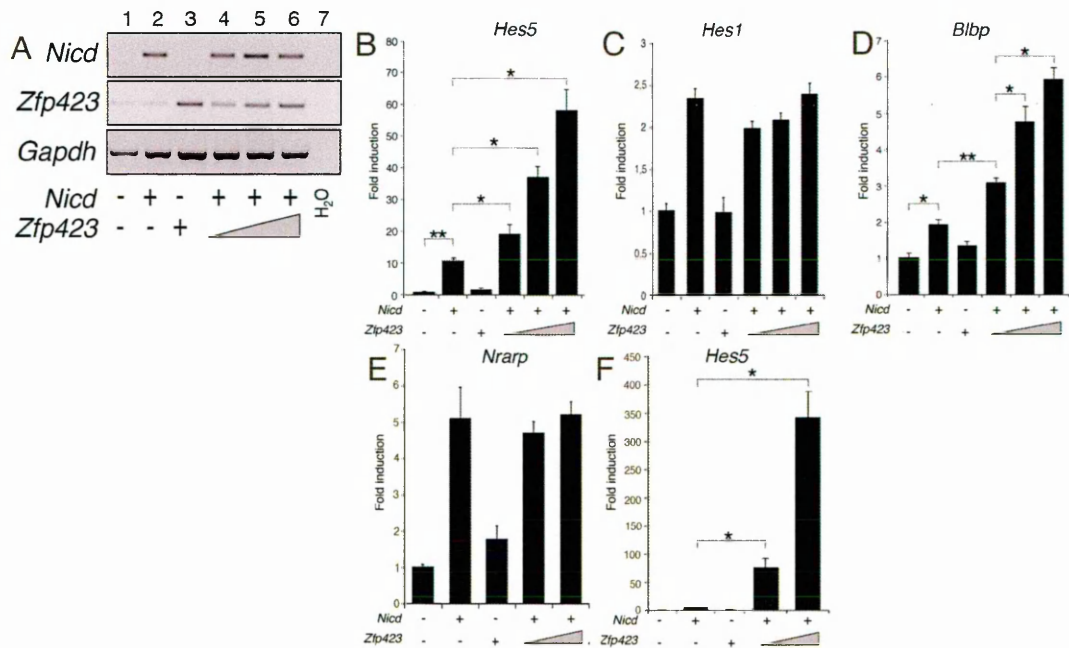
Figure 2.3 – Cooperative activation of *Hes5* **and** *Blbp* **gene expression by NICD and ZFP423 in cell lines. A)** Semiquantitative RT-PCR analysis of exogenous *Nicd* and *Zfp423* levels in transfected P19 cells. Note increasing *Zfp423* levels in lanes 4-6. This is representative of the amounts of *Nicd* and *Zfp423* cDNAs used in B-F. **B-E)** Real-time RT-PCR analysis of P19 cells treated as indicated below. **B, D)** *Nicd* and *Zfp423* co-expression in neuralized P19 cells upregulates endogenous *Hes5* and *Blbp* expression, respectively, to a level greater than cells transfected with *Nicd* alone. Induction of *Hes5* and *Blbp* transcription is dependent on *Zfp423* dosage. **C. E)** Co-transfection of P19 cells with *Nicd* and *Zfp423* fails to activate *Hes1* and *Nrarp* gene expression to a level greater than *Nicd* alone. **F)** Transfection of C2C12 cells with *Nicd* and *Zfp423* induces *Hes5* gene expression in a *Zfp423* dose-dependent fashion. In this line, *Hes5* expression is strictly dependent on the addition of exogenous *Zfp423*. *, $p<0.05$; **, $p<0.01$

ZFP423 cooperates with NICD in activating endogenous *Hes5* expression in C2C12 cell line

As previously shown (Hata et al., 2000) and confirmed by our RT-PCR (**Fig. 2.3A**, *Zfp423* expression in control), P19 cells express endogenous *Notch1* and *Zfp423*, and this may confound or interfere with the results found in this cell line. To overcome this problem, we decided to repeat the gain-of-function experiment in a different cell line, namely the C2C12 myoblastic cell line. C2C12 cells can differentiate in muscle cells upon DMSO treatment or starvation, and important for our experiments, they do not express endogenous *Zfp423* (Hata et al., 2000), they can respond to NICD expression up-regulating target genes (*Hes1* and *Hey1*, (Dahlqvist et al., 2003)), while *Hes5* mRNA is almost undetectable in growing

condition (our observations, in real time q-PCR experiments, Ct values for *Hes5* in mock sample were always higher than 40). In this system, over-expression of NICD alone produced a poor increase in *Hes5* mRNA expression (**Fig. 2.3F**, second bar), while co-expression of ZFP423 and NICD caused a strong up-regulation of *Hes5* transcript expression (**Fig. 2.3F**, fourth bar).

ZFP423 knock-down reduces NICD-dependent *Hes5* activation

Gain-of-function experiments, both in P19 and C2C12, suggested that ZFP423 could cooperate with NICD in regulating the expression of *Hes5*: this led us to hypothesize that perturbation of ZFP423-NICD cooperation would cause a reduction in *Hes5* gene expression. To test this hypothesis, we decided to knock-down ZFP423 in P19 cells through specific small interfering RNA (in our system, miRNA) against *Zfp423* mRNA, and then evaluate the expression of *Hes5*. We designed miRNA against *Zfp423* transcript (**Fig. 2.4A**) and cloned them downstream to *eGfp* gene: when *eGfp* mRNA is processed, miRNA is released and can trigger both double strand mRNA degradation and mRNA translation inhibition, while *eGfp* is translated into a Green Fluorescent Protein (GFP). In this way, transfected cells can be identified through GFP expression.

We tested the ability of the *Zfp423*-specific miRNA to interfere with the expression of ZFP423: we transfected HEK cells with a vector encoding 6myc-ZFP423, alone or in combination either with a scramble miRNA, or with the ZFP423-specific miRNA. Cells were harvested and lysed in RIPA buffer 48 hours after transfection, and a Western blot was performed to evaluate the efficacy of the specific miRNA (**Fig. 2.4B**). As shown, *Zfp423*-specific miRNA abolished ZFP423 expression, while scramble miRNA did not affect ZFP423 over-expression.

To test whether *Zfp423* knockdown might affect *Hes5* transcript level, we moved to our established *in vitro* model system (**Fig. 2.4C-F**): we transfected P19 cells with either a scramble miRNA or *Zfp423*-specific miRNA and, 48 hours after the transfection, GFP-positive cells were sorted, RNA extracted and retro-transcribed. We evaluated the expression of endogenous *Zfp423* and *Hes5* mRNA via real-time q-PCR. *Zfp423* knockdown was analyzed with primers designed specifically to span the sequence recognized and annealed by

the miRNA (**Fig. 2.4A**). As shown in **Fig. 2.4C**, *Zfp423*-specific miRNA reduced the *Zfp423* expression of about 25-30% compared to the scramble miRNA, while *Hes5* expression was reduced by 50% (**Fig. 2.4D**). As we expected a greater *Zfp423* transcript reduction, we repeated the loss-of-function assay in P19: we carried out a time course experiment, collecting scramble-miRNA and *Zfp423*-miRNA transfected cells at various time points (24, 36, 48, 60, 72 hours).
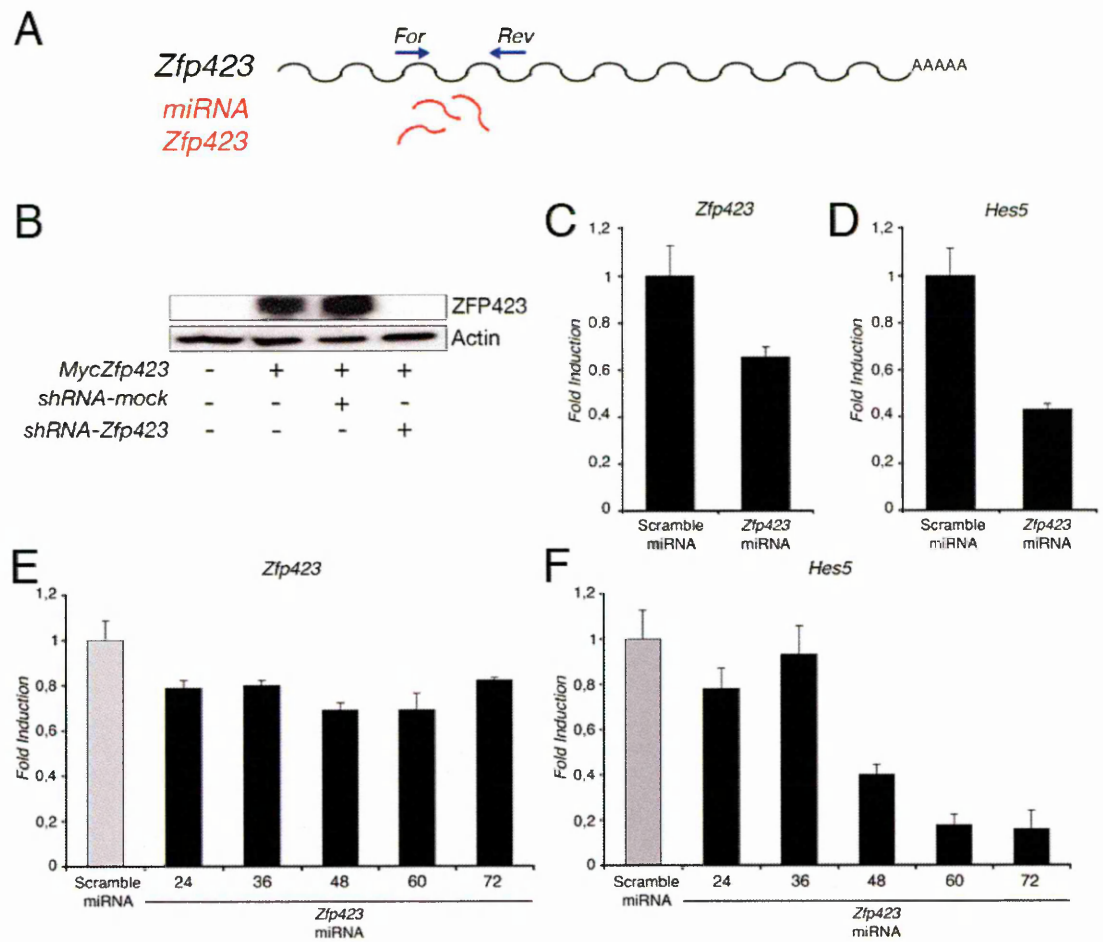
Figure 2.4 – *Zfp423* knock-down causes a reduction of *Hes5* expression *in vitro* A) Specific *Zfp423*-miRNA (red lines) recognizes and binds *Zfp423* mRNA (black line). Specific primers (in blue) have been used to measure the degradation of *Zfp423* transcript upon treatment with *Zfp423* miRNA. **B)** HEK293 cells transfected with the indicated constructs were lysed and equal amounts of protein lysate from each sample were loaded. Anti-myc antibody was used to evaluate ZFP423 protein expression. *Zfp423*-specific miRNA almost completely abolished the over-expression of 6mycZFP423. **C-D)** P19 cells transfected with either scramble-miRNA or *Zfp423*-specific miRNA. GFP+ cells were sorted and endogenous levels of *Zfp423* and *Hes5* analyzed by real-time PCR. **C)** *Zfp423* mRNA expression level in control and knockdown. **D)** *Hes5* expression in control and *Zfp423* knock-down. **E-F)** P19 cells transfected with either scramble-miRNa or *Zfp423*-specific mRNA. Samples were collected at the indicated time points. GFP+ cells were sorted, and endogenous *Zfp423* and *Hes5* transcript levels were evaluated by real time PCR. **(E)** *Zp423* expression during the time course. **F)** *Hes5* mRNA level during the knock-down experiment.

74

We analyzed the expression of *Zfp423* and *Hes5* via real-time q-PCR, and, again, we found that endogenous *Zfp423* mRNA knockdown was poor (20-25% reduction, **Fig. 2.4E**). Nevertheless, we could observe that *Hes5* mRNA expression was clearly and constantly reduced from 48 hours on after the transfection in the cells transfected with the *Zfp423*-specific miRNA, compared with the cells transfected with scramble miRNA (**Fig. 2.4F**). This data confirmed and supported the initial knockdown experiment. To date, we could not find an anti-ZFP423 antibody for testing the down-regulation of the endogenous protein, but the high efficacy of the *Zfp423*-specific miRNA in the knock-down experiment on the over-expressed ZFP423 (HEK cells, **Fig. 2.4B**) suggests that miRNA may act mainly in inhibiting mRNA translation rather than triggering RNA degradation. Taken together, loss-of-function experiments support the hypothesis that ZFP423 cooperate with Notch signaling in activating *Hes5 in vitro*.

ZFP423 and NICD cooperate *in vivo*

In vitro experiments showed that ZFP423 can functionally cooperate with Notch signaling to activate a subset of Notch target genes, and we focused our attention on *Hes5*. To test whether this cooperation also occurs *in vivo*, we moved to *Xenopus laevis* model system. *X.laevis* embryos are widely used to study developmental processes, share many pathways with higher species, and can be easily manipulated, for both gain-of-function and loss-of-function. To this aim, we collaborated with Prof. Monica Vetter, from University of Utah. As a first step, we analyzed the expression of *Zfp423* in *X.laevis* embryos at various developmental stages by whole mount *in situ* hybridization (**Fig. 2.5A-D**). The staining revealed that *Zfp423* mRNA is widely expressed starting in the neural plate/tube first (front view), and then, extending to the cranial neural crest both at stage 17, 22, 28 and 34 (**Fig. 2.5A-D**). In the lateral view (**Fig. 2.5B-D**), *Zfp423* is expressed along the dorsal midline of *X.laevis* embryos.

To study the cooperation between Notch signaling and ZFP423 *in vivo*, two-cell stage *X.laevis* embryos were injected unilaterally with a *Xenopus* mRNA *Notch* ΔE mRNA (N^{act}) and/or mouse *Zfp423*, and *beta galactosidase* mRNA was added as an injection tracer. N^{act} encodes an N-terminally deleted, constitutively active *Xenopus* NOTCH protein, devoid of

the extracellular and transmembrane domain (Coffman et al., 1993). Both N^{act} and *Zfp423* mRNA concentration were titrated so that either construct would produce a moderate change in target gene expression when over-expressed alone. The first target tested was *ESR1* (Davis and Turner, 2001; Lamar and Kintner, 2005), the *Xenopus* homolog of *Hes5*. Whole mount *in situ* hybridization revealed that the side of the embryos (bracket) injected with *Zfp423* mRNA (600 pg) has a moderate activation of *ESR1* expression (**Fig. 2.5E**) compared with the un-injected side; likewise, injection of low amounts of N^{act} alone (100 pg) promoted a low-level expansion of the *ESR1* domain (**Fig. 2.5F**); conversely, the simultaneous injection of N^{act} and *Zfp423* sharply increased *ESR1* expression on the injected side (**Fig. 2.5G**). Because increasing amount of *Zfp423* mRNA injection produced a moderate (Fig. 2.5E, 600 pg) or robust (**Fig. 2.5H**, 1 ng) expression of *ESR1*, we tested whether *Zfp423*-induced *ESR1* expression was *Notch*-dependent: to this end, we injected 1 pg of *Zfp423* mRNA together with a dominant negative Delta ligand (DeltaStu, (Chitnis et al., 1995)). *Delta^{Stu}* co-injection ablated the expansion of *ESR1* consequent to *Zfp423* over-expression (**Fig. 2.5I**), indicating that this response is strictly dependent upon endogenous Notch signaling activation. Finally, we injected two-cell stage embryos with a morpholino antisense oligonucleotide against endogenous *Zfp423* mRNA, and we found a decrease in *ESR1* expression (**Fig. 2.5J**) in the injected side; on the contrary, injection of a scramble morpholino did not alter endogenous *ESR1* expression (**Fig. 2.5K**), thus indicating the *Zfp423* knockdown is responsible for the observed *ESR1* reduction.

Because a previous report had shown that ZFP423 may act as SMAD cofactor in the context of mesodermal patterning (Hata et al., 2000), and BMP signaling plays an important role during the early stages of *X.laevis* development, we wanted to exclude that the up-regulation of *ESR1* upon *Zfp423* over-expression was due to an alteration in BMP signaling rather than an effect of *Zfp423* on Notch signaling. Thus, the over-expression experiments were repeated by injecting *Zfp423* mRNA unilaterally in dorsal blastomeres at 16-cell stage to prevent a possible interaction between exogenous ZFP423 and the BMP effector complex SMAD1-SMAD4 during gastrulation. The result of this experiment (**Fig. 2.5L**, arrow) confirmed the functional cooperation between ZFP423 and the Notch signaling in regulating *ESR1* expression. In similar experiments, *Hes1* orthologue *Hairy1* (Dawson et al., 1995; Jennings et al., 1994) was slightly down-regulated on the injected side (**Fig. 2.5M**, arrow)
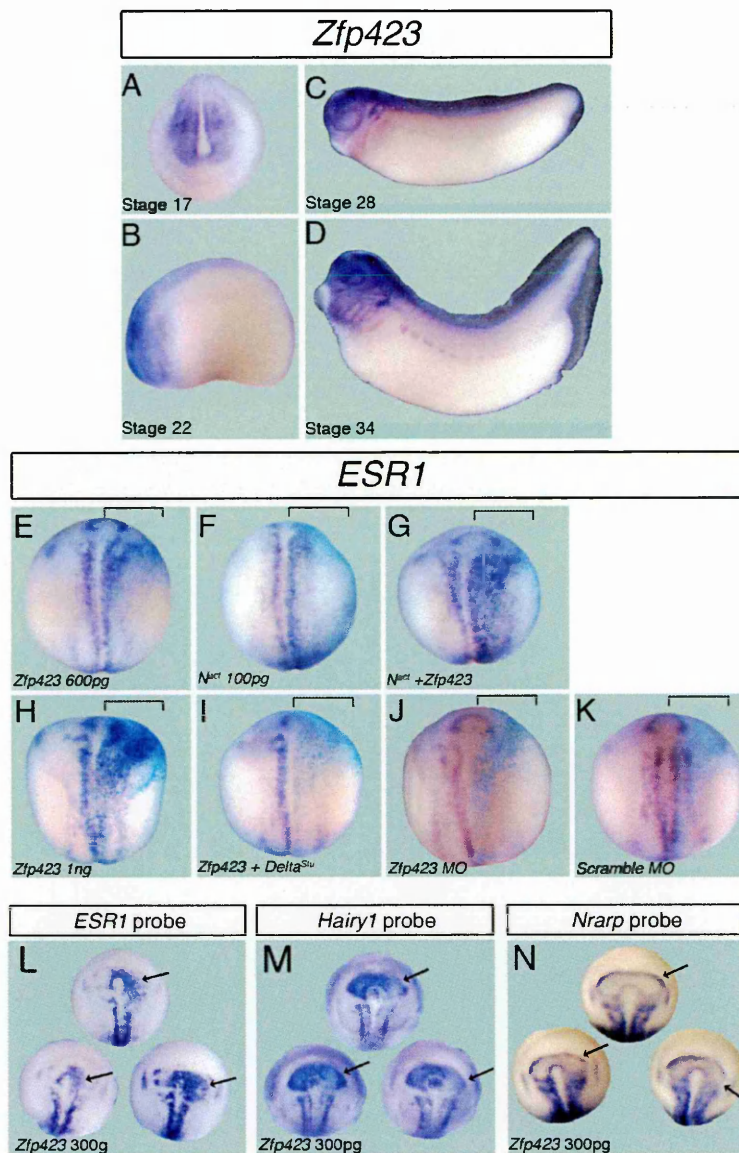
Figure 2.5 - Cooperative activation of *ESR1* gene expression by N^act and ZFP423 in *Xenopus* embryos. A,D) Whole mount *in situ* hybridization analysis of *Xenopus Zfp423* gene expression in stage 17 **(A)** and stage 22 **(B)** (frontal view), stage 28 **(C)** and stage 34 **(D)** (lateral view, head to the left) embryos: the gene is widely expressed starting in the neural plate/tube first, and then moving to the cranial neural crest. **E-G)** Whole mount *in situ* hybridization analysis of *ESR1* gene expression in embryos injected unilaterally (bracket) with *Zfp423* (600 pg) and/or *N^act* (100 pg), as indicated. *LacZ* (blue stain) serves as an indicator of the injected side. Note strong *ESR1* expression after coinjection of *N^act* and Zfp423. **H)** Embryo injected unilaterally (bracket) with 1 ng of *Zfp423*. **I)** Embryo injected unilaterally (bracket) with 1 ng *Zfp423* and 400 pg *Delta^Stu*, encoding a dominant negative Notch ligand. Note disappearance of *ESR1* signal on the co-injected side. **J-K)** Unilateral injection (bracket) of a *Zfp423* morpholino **(J)** or scramble morpholino **(K)**. Note disappearance of *ESR1* signal on the injected side in **(J)**, while no alteration in *ESR1* signal can be detected in the scramble morpholino injected side **(K)**. **L-N)** Whole mount *in situ* hybridization analysis of *ESR1, Hairy1, and Nrarp* gene expression in embryos injected unilaterally with *Zfp423* (300pg, arrow) in a dorsal blastomere. Note expanded *ESR1* expression domain **(L)**, but reduced/unaffected expression of *Hairy1* **(M)** and *Nrarp* **(N)** on the injected side. GFP was coinjected with *Zfp423* as a lineage tracer (not shown).

and *Nrarp* (Krebs et al., 2001; Lamar and Kintner, 2005) mRNA levels were also slightly reduced, or not altered, (**Fig. 2.5N**, arrow) in response to *Zfp423* over-expression. These results indicated that ZFP423 may promote a dissociation in the response to NICD *in vivo*, favouring the expression of *Hes5* over *Hes1* and other targets.

Taken together, *in vivo* results further corroborated our previous results obtained in different cell lines, and clearly indicated ZFP423 as a cell-autonomous modifier of Notch signaling to activate the *Hes5* promoter..

ZFP423 and NICD cooperate to activate *Hes5* promoter *in vitro*

ZFP423 is a multi zinc-finger protein capable of binding DNA *in vitro* (Brayer et al., 2008; Ku et al., 2006). To investigate the molecular mechanisms underlying the functional cooperation between Notch signaling and ZFP423, we compared the *Hes5* promoter of different species – mouse, rat and human – to identify putative conserved ZFP423-binding sites (herein referred to as ZBS) present in the promoter (**Fig. 2.6A**). We analyzed 1Kb fragment of the promoter, and found several putative ZBS, some of which are of particular interest because they are in close proximity with known binding sites, such as the BMP Responsive Element (BRE) and the CBF1-binding site (CBF1) (**Fig. 2.6A**).

We cloned 1 Kb fragment of the murine *Hes5* promoter in the pGL3 vector, so that *Zfp423* promoter could control the expression of the *Luciferase* gene (**Fig. 2.6B1**). Using this type of construct, the activation state of the promoter can be indirectly evaluated by analyzing the enzymatic activity of the luciferase protein, as it is dependent on the amount of the luciferase present in the cell, which, in turn, depends on the level of activation of the promoter that controls the gene expression. Firstly, we tested in C2C12 cells whether the cloned promoter fragment was sufficient to recapitulate the cooperation between ZFP423 and NICD observed in the endogenous *Hes5* promoter, and we found that it was the case (**Fig. 2.6C**). ZFP423-NICD co-expression doubled the activation of the *Hes5* promoter compared to the activation observed with the expression of NICD alone (**Fig. 2.6C**).
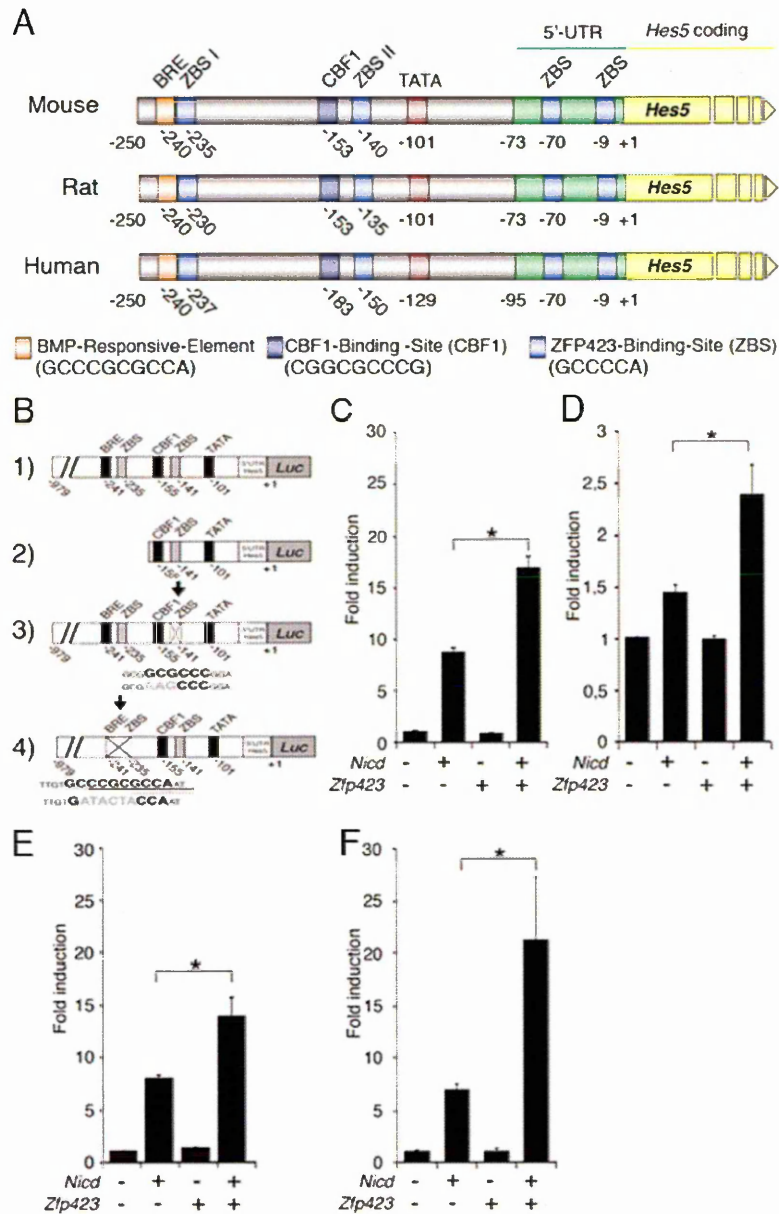
Figure 2.6 – *Hes5* promoter presents putative conserved ZFP423-binding sites but its activation is independent of canonical Zfp423 binding domains. A) *In silico* analysis of murine *Hes5* promoter revealed the presence of several putative ZFP423-binding sites (ZBS) in the promoter (canonical sequence: GCNNCA). Comparison of mouse, rat and human *Hes5* promoter confirmed that some of them (blue squares) are conserved among species. In the sketch, BRE (BMP-responsive Element) (orange square), CBF1 (purple square), TATA box (red square), 5'UTR of *Hes5* (green) gene are indicated. B) A 1kb wt 5' sequence of *Hes5* promoter was cloned in pGL3 vector (1). Subsequently, a shorter version (2), a mutated form in ZBS II (3) or in ZBS I (4) were generated. C-F) Promoter-reporter assays performed in C2C12 cells using wt, deleted and point-mutated stretches of the *Hes5* gene promoter fused to luciferase. C) A 1kb wt 5' sequence responds to co-transfection with ZFP423 by upregulating luc compared to levels reached with NICD alone. D) Likewise, a 200 bp proximal element is cooperatively activated by NICD and ZFP423, albeit to a lower level with respect to the experiment in C. E, F) Site-directed mutagenesis of two of the numerous canonical ZFP423 binding sites found in the *Hes5* promoter does not abolish the cooperative interaction occurring between ZFP423 and NICD. *$p<0.05$.

We generated a shorter version of the *Hes5* promoter: the resulting promoter (**Fig. 2.6B2**) contains the CBF1 binding site and three putative ZBS (-160 +1). We performed the luciferase assay in C2C12 cells and found that ZFP423 and NICD can cooperate in activating the *Hes5* short promoter (**Fig. 2.6D**). Notably, we could observe a decrease in the activation of the short promoter both in NICD and NICD-ZFP423 transfected cells, suggesting that the deleted part contains regulatory elements important, but not essential, for the activation of the promoter mediated by NICD and ZFP423.

As shown in **Fig. 2.6A**, many putative ZBS are present in the *Hes5* promoter, but two of them of particular interest: the first one – at -235 bps – overlaps with the BRE, the second one – at -140 bps – is very close to the CBF1 binding site. We mutated each site (**Fig. 2.6B3, B4**), and performed luciferase assays in C2C12 cells to assess whether they are important in mediating ZFP423 activity. The results (**Fig. 2.6E, F**) showed that none of these sites is essential for the ZFP423, although we observed a slight decrease in the *Hes5* promoter activation in the case of the site mutated in position -140 bps.

Molecular interaction between ZFP423 and NICD

In vitro data indicated the existence of a functional cooperation between ZFP423 and NICD, and *in vivo* assay strongly supported the hypothesis. The next question to address was whether this cooperation occurs via the ZFP423-NICD interaction, or by other mechanisms. To answer this question, we performed an experiment of co-immunoprecipitation. As first attempt, we tested several commercially available antibodies raised against ZFP423, but none of them recognized the endogenous ZFP423 via Western Blot in P19 cells, and very weakly the over-expressed form in HEK cells. To overcome this problem, we tagged ZFP423 with 6-Myc epitopes, and then performed immunoprecipitation (IP) experiments.

To setup the conditions for the IP, we took advantage on previous published results, showing that ZFP423 can interact with EBF transcription factors (Tsai and Reed, 1998). We transfected HEK cells with a construct encoding 6Myc-ZFP423 and EBF3, and 48 hours after the transfection, cells were collected and subjected to immunoprecipitation with an anti-myc antibody. The same anti-myc antibody was used to hybridize the membrane: the antibody recognized a specific band at around 150 KDa in the input lane (**Fig. 2.7A**), and a band of the

same size was revealed in the lane where we loaded the immunoprecipitated proteins. This result showed that the anti-myc antibody efficiently immunoprecipitated ZFP423, as almost no ZFP423 was found in the immunodepleted sample (ID1, lane 1) and the strengthen of the binding was good, as no ZFP423 was released by the antibody during the washing step (ID2). An anti-EBF antibody was used to reveal EBF3: the result demonstrated that EBF3 co-precipitates (IP anti-myc, row 2) with ZFP423, although a fraction of EBF3 was found in the immunodepleted sample (ID1, row 2), most likely because EBF3 was produced at higher rate compared to ZFP423, as suggested by the input lane (Lys, rows 1 and 2, **Fig. 2.7A**).

Next, HEK cells were co-transfected with 6Myc-ZFP423 and Flag-NICD encoding vectors. Protein lysate was subjected to immunoprecipitation with the anti-myc, and then, we loaded on a 8% acrylamide gel a fraction of the total lysate (10%, input sample), a fraction of the immunodepleted sample (10%), the first washing (ID2) and the IP sample. The hybridization of the nitrocellulose filter with the anti-myc antibody revealed that ZFP423 was immunoprecipitated quite efficiently (**Fig. 2.7B**); the filter was then hybridized with an anti-Notch antibody, revealing a specific doublet at around 110KDa in the IP lane (**Fig. 2.7B**). This suggested that over-expressed NICD and ZFP423 may interact *in vitro*.

We examined whether the interaction was direct or mediated by P/CAF , a known member of NICD-containing transcriptional complexes (Kurooka and Honjo, 2000). To address this point, we transfected COS7 cells with 6Myc-ZFP423, Flag-NICD, CBF1 and Flag-PCAF (Yang et al., 1996). Lysates were immunoprecipitated with an unrelated monoclonal antibody (anti-GFP) or with anti-myc. IP samples were analyzed by WB using antibodies for Notch, CBF1, Myc, Flag, and ACTIN, as negative control (**Fig. 2.7C**): NICD co-precipitated with ZFP423, but PCAF was not found to co-precipitate with them. As expected, we did not find ACTIN in the IP lane. CBF1 is present in the lysate, and it seemed to be present also in the IP lane, although the blot was not clear enough to confirm that observation.
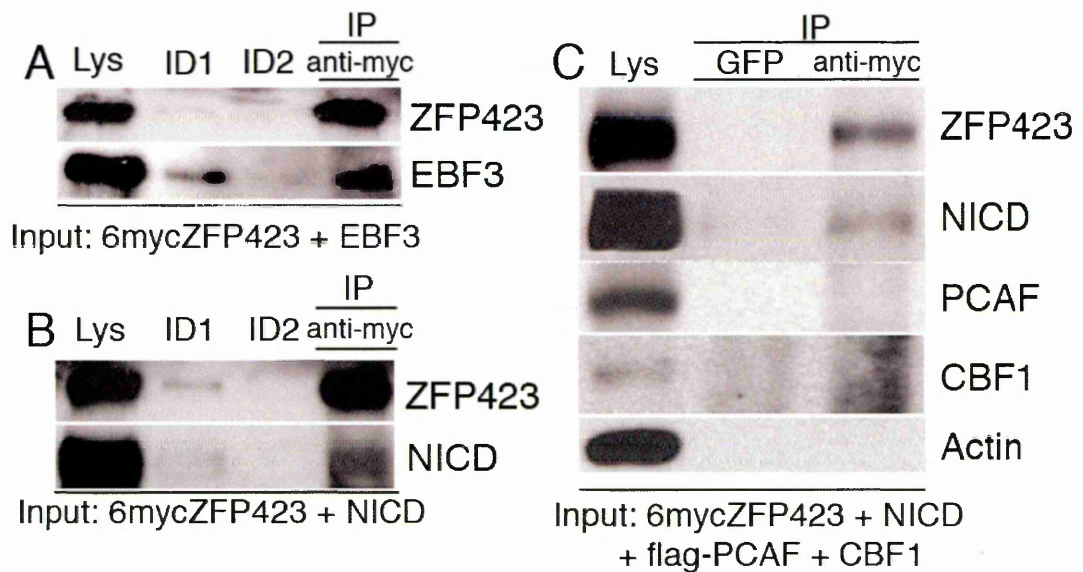
Figure 2.7 – Molecular interaction between ZFP423 and NICD. A, B) HEK293 cells transfected with the indicated constructs were used for immunoprecipitation. Filters were cut and incubated for immunoblotting. Anti-myc Ab was used to immunoprecipitate tagged ZFP423. In **A**, EBF3 co-precipitated, as previously reported (Tsai and Reed, 1997). In **B)** an NICD-specific doublet co-precipitated with ZFP423. Lys, lysates; ID1, immunodepleted fraction; ID2, first wash. **C)** COS7 cells transfected with the indicated constructs, were subjected to immunoprecipitation with anti-GFP as an unrelated antibody, or with anti-myc. Filters were cut and stained for ZFP423, NICD, CBF1, PCAF and actin (unrelated protein). Only NICD co-precipitated in the fraction immunoprecipitated with anti-myc.

EBF TFs interfere with the ZFP423-NICD cooperation

ZFP423 was firstly identified as partner of the EBF transcription factors (Tsai and Reed, 1998); interestingly, several lines of evidence suggest a possible link between EBF TFs and Notch signaling. For instance, over-expression of N^{act} reduced or abolished the ability of $XEbf2$ to induce Nfm gene expression in $Xenopus$ neurulas (Pozzoli et al., 2001); during hematopoiesis, activation of EBF1 target genes was reduced upon Notch activation, possibly because of a reduced DNA-binding capability of EBF (Smith et al., 2005); in addition, EBF TFs are expressed in the SVZ and are important to trigger neuronal commitment and differentiation (Croci et al., 2006a; Garcia-Dominguez et al., 2003) while Notch pathway plays an important role in maintaining radial glial progenitors (Lutolf et al., 2002; Machold et al., 2007). Thus, we hypothesized that ZFP423 might be the link between Notch pathway and EBF activity.

Firstly, we tested this hypothesis *in vitro*: we transfected P19 cells with EBF1, EBF2

or EBF3 alone or in combination with NICD and ZFP423: then, via real-time q-PCR we analyzed the expression level of *Hes5* mRNA. EBF1, EBF2 or EBF3 single over-expression did not change the expression of *Hes5* (**Fig. 2.8A**, bars 4, 5 and 6) similarly to ZFP423 single over-expression (**Fig. 2.8A**, bar 3). Interestingly, co-expression of NICD, ZFP423 and one EBF member clearly reduced the *Hes5* activation, when compared with the expression of the Notch target in presence of NICD and ZFP423 (**Fig. 2.8A**, bars 8, 9 and 10 compared with bar 7).

The experiment was repeated *in vivo*, by injecting two-cell stage *Xenopus* embryos unilaterally with the same combination of mRNAs. Again, over-expression of either *XEbf2* (**Fig. 2.8C**) or *XEbf3* (**Fig. 2.8D**) reduced *ESR1* activation induced by exogenous *Zfp423* and N^{act} (control, **Fig. 2.8B**). *XEbf2* or *XEbf3* injection led to ectopic *ESR1* expression (**Fig. 2.8E-F**): this might be due either to an increase of X-Delta-1 expression, driven by XEBF2 (Dubois et al., 1998), or to a direct effect of EBF TFs as activators of neuronal migration upon cell cycle exit (Garcia-Dominguez et al., 2003).
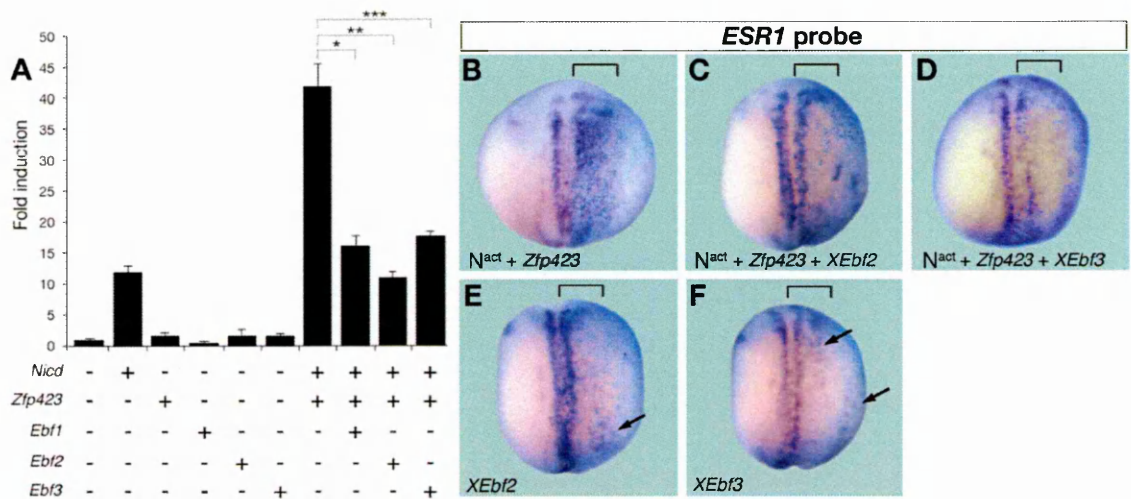
Figure 2.8 – EBF TFs reduce ZFP423-NICD-mediated *Hes5* gene expression *in vitro* and *in vivo*. A) Real time PCR analysis of *Hes5* gene expression in P19 cells transfected with the indicated constructs. Note that *Ebf1*, *Ebf2* or *Ebf3* alone does not affect basal *Hes5* expression. **B-D)** Whole mount *in situ* hybridization analysis of *ESR1* gene expression in embryos injected unilaterally (bracket) with N^{act} (100 pg) and *Zfp423* (600 pg) and/or *XEbf2* (100 pg) or *XEbf3* (100 pg). **E, F)** Whole mount *in situ* hybridization analysis of *ESR1* gene expression in embryos injected unilaterally with *XEbf2* (100 pg) or *XEbf3* (100 pg), as indicated. Note slightly-increased ESR1 positive cells in *XEbf2* and *XEbf3* injected embryos (arrow).**B-F)** *LacZ* (blue stain) serves as an indicator of the injected side.

Is ZFP423 a putative mediator between Notch pathway and BMP/SMAD signaling?

Previous studies showed that ZFP423 interacts with SMAD1-SMAD4 complex to activate *Xvent2* (Hata et al., 2000) and *Smad6* (Ku et al., 2006) promoter in response to BMP signaling activation. Other authors have described the existence of interaction between BMP signaling and Notch pathway in the context of neurogenesis (Takizawa et al., 2003) and myogenesis (Dahlqvist et al., 2003), while others have proposed BMP as a pro-differentiation factor in the cerebellar primordium (Machold et al., 2007). Interestingly, ZFP423 was found to interact with SMAD1-SMAD4 thanks to a domain constituted by Zn fingers 9-20, encoded by exon 4 (see **Fig. 1.7A**, and (Hata et al., 2000)). We asked whether ZFP423 uses the same domain to interact with NICD. To address this question, we generated a deleted form of ZFP423 missing the Zn fingers 9-20, and so far called Δ9-20-ZFP423 (**Fig. 2.9A**). We over-expressed the protein in COS7 cells to test the stability and the localization of the Δ9-20-ZFP423: the protein is produced and localized mainly in the nucleus, although not completely, in contrast to ZFP423 full length (**Fig. 2.9B**). Subsequently, we tested the ability of Δ9-20-ZFP423 to cooperate with NICD to activating *Hes5* promoter (**Fig. 2.9C**): luciferase assay indicated that Δ9-20-ZFP423 failed to contribute in activating *Hes5* promoter, while full length ZFP423 did, as usual. As the deletion introduced in ZFP423 is quite big, one might hypothesize that, although produced, Δ9-20-ZFP423 is not properly folded, and so it cannot interact anymore with NICD, thus resulting in the inability to enhance *Hes5* expression; another possibility is that the Zn finger 9-20 of ZFP423 are important for the interaction with NICD.
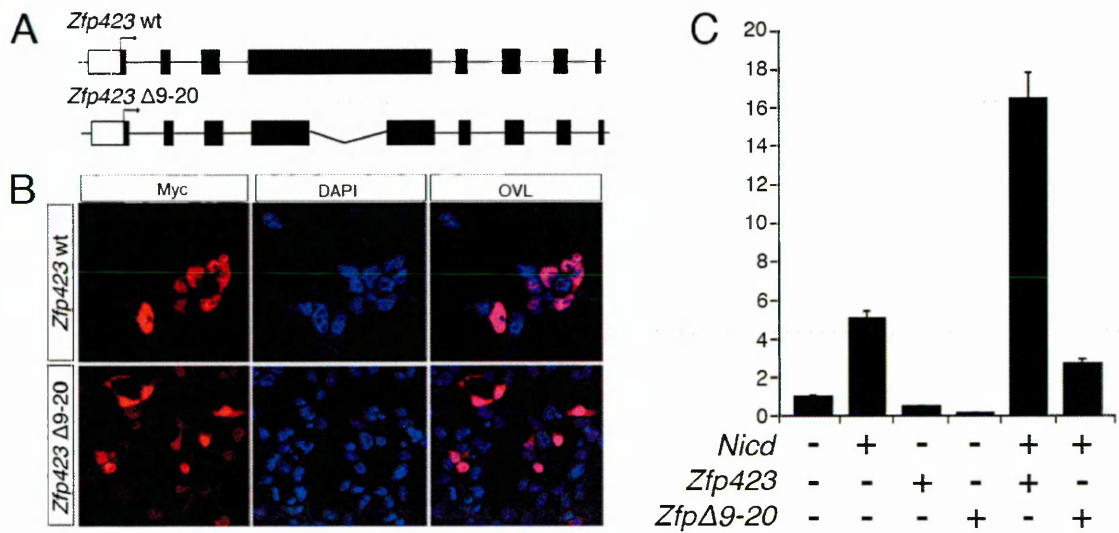
Figure 2.9 – ZFP423Δ9-20 fails to cooperate with NICD in *Hes5* promoter activation. A) Scheme of the generation of cDNA encoding ZFP423Δ9-20 protein, a mutant ZFP423 that lacks the Zn-finger 9-20, responsible for the interaction with SMAD1-SMAD4 complex (Hata et al., 2000). **B)** Immunostaining with anti-myc revealed that both wt ZFP423 and ZFP423Δ9-20 localized in the nucleus, although ZFP423Δ9-20 signal is present also in the cytoplasm. **C)** C2C12 were transfected with 1kb wt promoter (fig.2.4B1) and the indicated constructs, and luciferase assay was performed 24 hours after the transfection. Note that ZFP423Δ9-20 fails to cooperate with NICD in activating *Hes5* promoter.

We hypothesized that the observed functional interaction between Notch pathway and BMP signaling cascade (Takizawa et al., 2003) could be mediated by ZFP423. To address this issue, we transfected C2C12 cells with a combination of vectors – pBlueskript as control, NICD alone, ZFP423 alone, or NICD and ZFP423 – and treated the transfected cells for 2 hours or 16 hours with BMP4 before collecting the cells and extracting the RNA. We analyzed the expression of *Hes5* transcript in each condition, and we found that the cooperation between NICD and ZFP423 in activating *Hes5* is further enhanced by BMP4 treatment, both after 2 hours and 16 hours of treatment (**Fig. 2.10A**). We could observe a slight increase of *Hes5* in the samples transfected with the sole vector for NICD and treated BMP for 2 hours (**Fig. 2.10A**, grey bar), in agreement with previous reports (Takizawa et al., 2003), suggesting that the pathways may cooperate to some extent without the presence of ZFP423. The addition of ZFP423 to the system clearly boosted the expression of *Hes5* (**Fig. 2.10A**, three bars at the rightmost part of the graph), both in the absence and in the presence of BMP4. To exclude that the observed up-regulation in presence of BMP4 could have been due to a stochastically higher expression of NICD, we evaluated the expression of *Nicd* in each sample via real time q-PCR (**Fig. 2.10B**). As we used specific primers to

reveal exogenous *Nicd*, in control experiment *Nicd* level was zero. Samples transfected with *Nicd*-encoding vector showed different levels of *Nicd* expression, but samples that had to be compared (white bars together, or grey bar together) showed similar level of expression. Interestingly, *Nicd* was expressed at similar level in the sample co-transfected with *Zfp423*-encoding vector and treated with BMP4 for 16 hours: this observation clearly excluded the possibility that the higher up-regulation of *Hes5* could be dependent on *Nicd*. Moreover, to confirm that BMP4 treatment was successful, we analyzed the expression of *Smad6* mRNA: *Smad6* is induced by BMP4 treatment, and its expression is reinforced by the presence of ZFP423 (Ku et al., 2006).
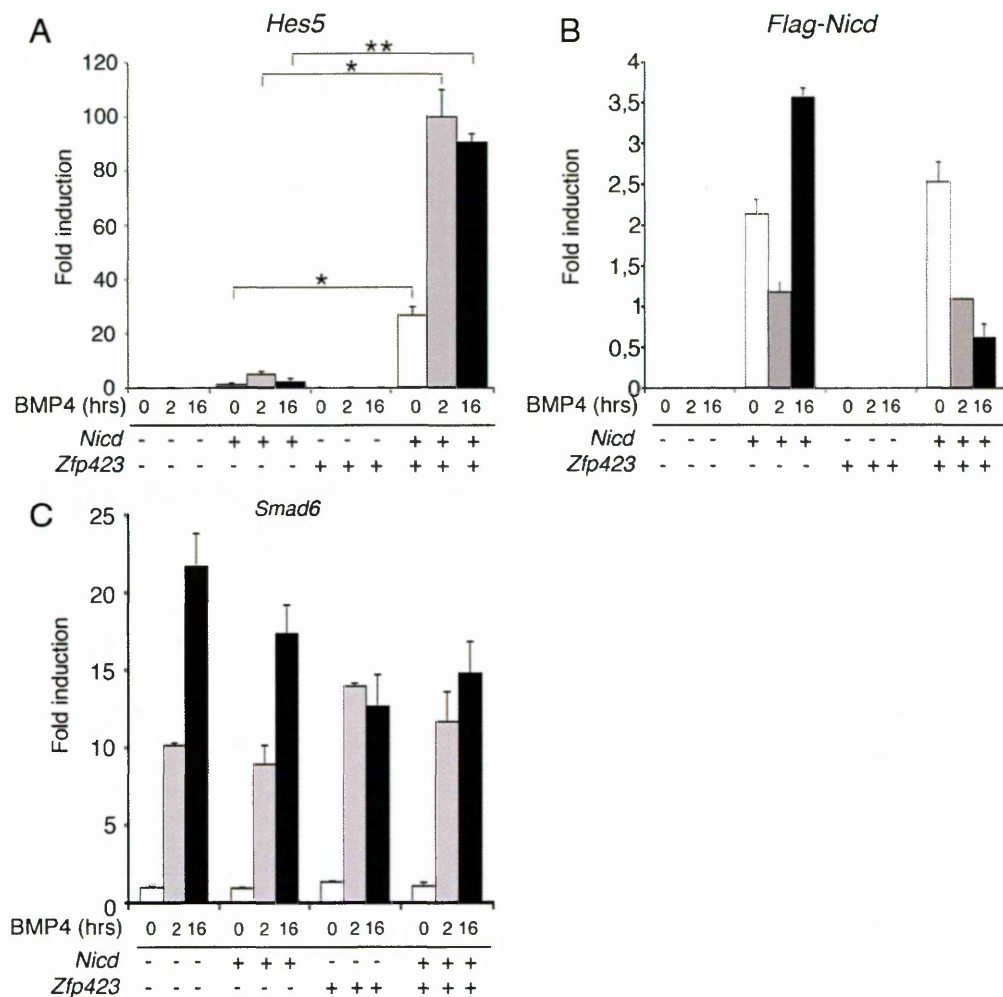
Figure 2.10 - ZFP423 cooperates with NICD and BMP signaling activation to prmote *Hes5* gene expression. A) Cooperative activation of *Hes5* gene expression by NICD, ZFP423 and BMP4 in C2C12 cell line. Real-time RT-PCR analysis of RNA extracted from mock transfected or transfected with either *Nicd, Zfp423*, or both. Cells were either left untreated or treated with BMP4 for 2 or 16 hours. Transfection with *Zfp423* strongly enhances the cooperative effect of NICD and BMP signaling on *Hes5* gene expression. *, $p<0.05$; **, $p<0.005$. **B)** Expression of *Flag-Nicd* cDNA weas evaluated to exclude that hyper-activation of *Hes5* was due to a difference in *Nicd* expression. **C)** To confirm the efficacy of BMP4 treatment we evaluated the induction of *Smad6* gene, and confirmed previous finding (Ku et al., 2006).

Our results (Fig. 2.10C) are in agreement with previous publications: in fact, BMP treatment activates *Smad6* expression, both in control samples and in single- and double-transfected samples, and more interestingly, ZFP423-transfected samples showed higher *Smad6* level in presence of BMP4 (about 1.5 fold, 15 fold compared to control) than in absence of BMP4 (about 10 fold compared to control) (Fig. 2.10C).

To investigate the cooperative effect of NICD, ZFP423 and BMP signaling in activating the *Hes5* promoter, we transfected C2C12 with the sam combination of vectors and the Hes5-luciferase reporter, in the presence or the absence of BMP4 in the culture media for 6 hours, and then performed the luciferase assay (Fig. 2.11A). NICD-ZFP423 co-transfected C2C12 showed a level of *Hes5* promoter activation higher when treated with BMP4 in comparison to the untreated samples, although the fold change was lower than what we observed for the endogenous *Hes5*.

To further assess the role of BMP signaling in ZFP423-mediated activation of *Hes5* in response to NICD, we perturbed BMP signaling cascade in two ways – mutating the BRE present in the *Hes5* promoter , or adding Noggin to the culture medium – and then performed the luciferase assays.

In the first experiment, we assessed the responsiveness of *Hes5* promoter to BMP treatment when the BRE is mutated so to abolish the binding of SMAD1-SMAD4 complex (Fig. 2.6B4): the mutation we introduced is similar to the one (Takizawa et al., 2003) that abrogates the BMP-NICD cooperation. We transfected C2C12 with various combinations of vectors (Fig. 2.11B), we treated the cells for 6 hours with BMP4, and then performed the luciferase assay: BRE-mutated promoter did respond to NICD-ZFP423 co-expression similarly to the wild type (compared to Fig. 2.11A), while BMP4 treatment did not induce any further enhancement of the activation of the mutated promoter, as it did when the wild type promoter was used (Fig. 2.11B compared to Fig. 2.11A).

The second experiment took advantage of Noggin, a BMP antagonist: we tested whether in our culture conditions – 1% FBS during the experiment – even a small amount of BMP could contribute to the cooperative effect observed between ZFP423 and NICD of *Hes5* promoter activation (Fig. 2.11A). Firstly, we checked whether Noggin treatment could reduce the expression of known BMP targets, such as *Id1* and *Msx1* (Hollnagel et al., 1999; Machold et al., 2007). To this end, we cultured C2C12 cells in 1% FBS, with or without Noggin (100ng/

ml) for 24 hours, then we collected the cells and evaluated the expression of those genes via real time q-PCR: both *Id1* and *Msx1* (**Fig. 2.11C**, black bars) showed a reduced expression when compared with the control (**Fig. 2.11C**, white bars). This preliminary experiment confirmed that traces of BMP are present even in 1% FBS, and that Noggin treatment was
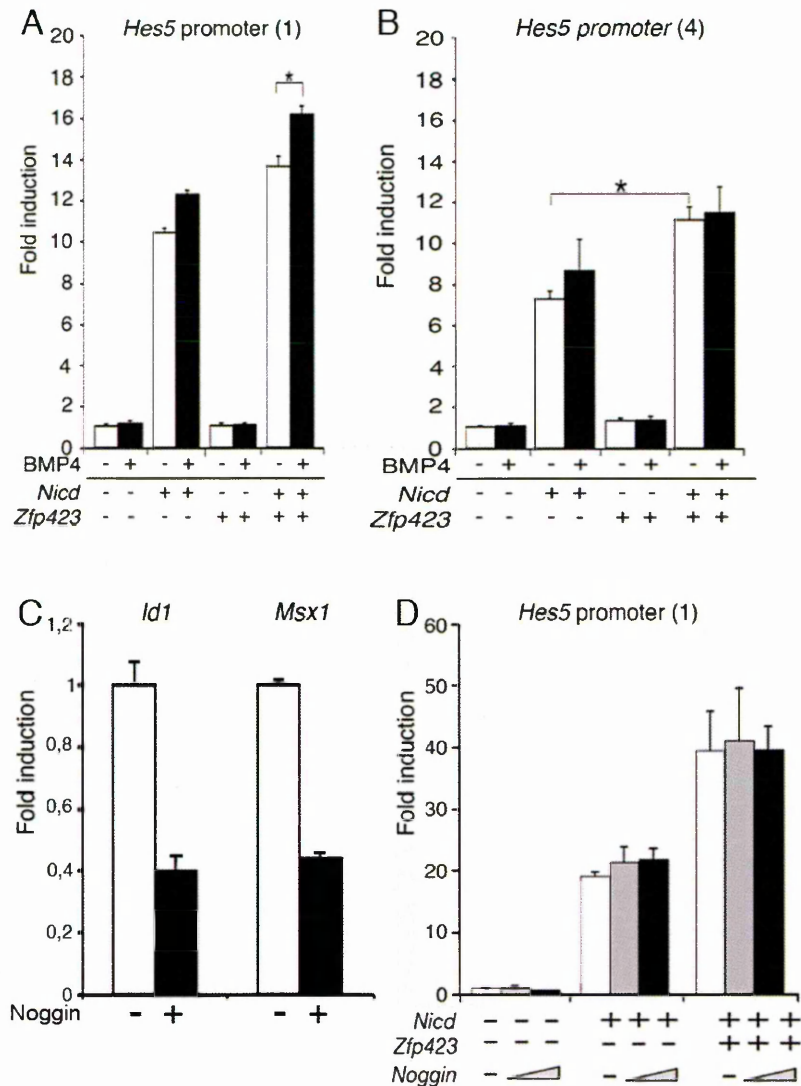
Figure 2.11 - Perturbation of BMP signaling does not impair ZFP423 cooperation with NICD on activating *Hes5* promoter. A) Luciferase assay on 1Kb wild-type promoter (fig.2.4B1) confirmed cooperation between NICD, ZFP423 and BMP4, although to a less extend to what observed for the endogenous *Hes5*. **B)** Luciferase assay after the transfection of C2C12 with 1Kb promoter mutated in the BRE sequence (fig.2.4B4) and the indicated constructs. NICD-ZFP423 cooperation is still present, despite BMP effector molecules are unable to bind the promoter. **C)** Noggin treatment (100ng/ml) reduces expression of BMP targets, such as *Id1* and *Msx1*. **D)** Luciferase assay after the transfection of C2C12 with1Kb wild-type promoter (fig.2.4B1), the indicated constructs, and treatment with increasing amount of Noggin. Treatment, also at high doses of Noggin, does not alter the cooperation of NICD and ZFP423 in activating *Hes5* promoter.

sufficient to abolish BMP activity.

To test the role of BMP traces in the context of ZFP423-NICD cooperation, we kept the C2C12 cells under Noggin treatment during the experiment. Cells were cultured in 10% FBS with Noggin (100ng/ml) for 24 hours before the transfection, and after the transfection, were cultured in 1% FBS. C2C12 were transfected with 1Kb wild type promoter (see **Fig. 2.6B1**), with a control vector, NICD alone, ZFP423 alone or NICD and ZFP423, and treated with increasing amount of Noggin (0, 100, 200 and 400ng/ml). Twenty four hours after the transfection, the luciferase assay was performed. Our results (**Fig. 2.11D**) showed that the activation of *Hes5* promoter was not reduced in presence of Noggin, at any concentration tested, suggesting that the cooperation between NICD and ZFP423 could occur independently of the BMP signaling activity.

To assess the relevance of ZFP423 in BMP-NICD-mediated activation of endogenous *Hes5*, we transfected C2C12 with NICD and ZFP423, together with the scramble miRNA or *Zfp423*-specific miRNA; 46 hours after the transfection, we treated the cells with BMP4 for 2 hours, then we collected the samples, sorted the GFP-positive cells, extracted RNA and performed real time q-PCR to evaluate the level of *Zfp423* and *Hes5* in each sample (**Fig. 2.12A, B**). We setup to 1 the level of *Zfp423* (**Fig. 2.12A**) and *Hes5* (**Fig. 2.12B**) in NICD-ZFP423-scramble miRNA triple-transfected C2C12: *Zfp423*-specific miRNA reduced by about 90% the expression of *Zfp423*, both in absence and in presence of BMP4 (**Fig. 2.12A**); *Hes5* level was reduced by half in the sample transfected with *Zfp423*-specific miRNA in the absence of BMP treatment (**Fig. 2.12B**); *Hes5* mRNA was induced by 4,5 fold in NICD-ZFP423-scramble miRNA after BMP4 treatment, while *Hes5* mRNA level was induced 2,5 fold in *Zfp423*-specific miRNA transfected C2C12 (**Fig. 2.12B**). Thus, *Zfp423*-specific miRNA reduced of about half the induction of *Hes5* in BMP4-treated sample.

Taken together, these data indicated that the cooperation between ZFP423 and Notch signaling in activating *Hes5* is enhanced by the presence of active BMP signaling, which, nevertheless, is not necessary for the cooperation to take place; on the other hand, ZFP423 plays an important role in mediating the effect of BMP in NICD-mediated activation of *Hes5*, although we cannot exclude that BMP can cooperate with NICD via direct interaction or via molecules other than ZFP423.
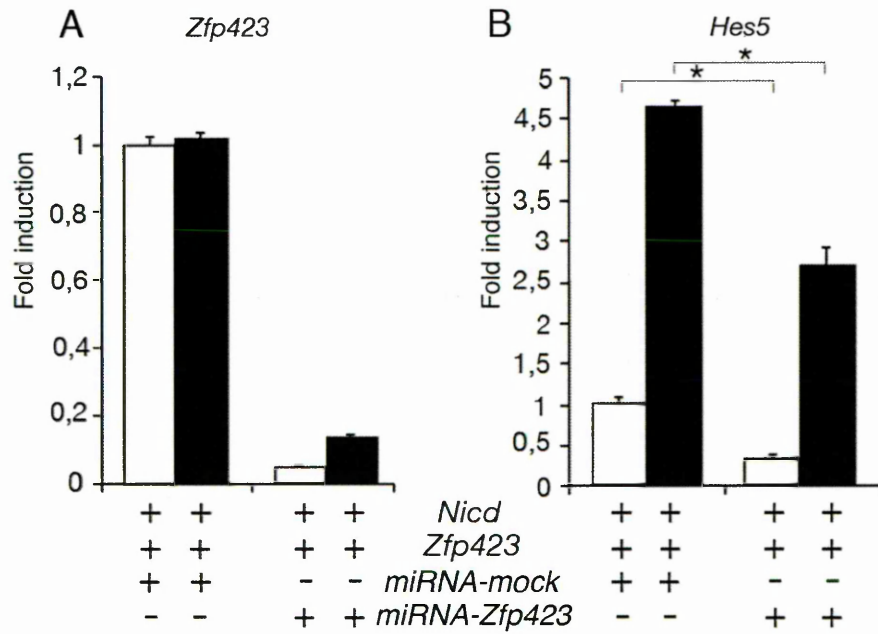
Figure 2.12 - ZFP423 cooperates with NICD and BMP signaling activation to promote *Hes5* gene expression. C2C12 cells were transfected with the indicated constructs, and 48 hours later GFP+ cells were sorted and analyzed by real time PCR. **A)** *Zfp423* mRNA level is reduced by about 90% in *Zfp423*-specific miRNA treated cells, both in the absence and in the presence of BMP4, compared to scramble-miRNA. **B)** *Hes5* expression in is reduced by half, both in absence or in presence of BMP4 treatment.

Discussion

The establishment of the Central Nervous System is a complex process that starts soon after fertilization and lasts throughout life. During embryonic development, neural stem cells proliferate and divide along the ventricular zones, thus expanding the pool of progenitors that will give rise to neurons first, and glial cells – astrocytes and oligodendrocytes – later. In the adult brain, stem cells are confined in two main specialized niches, the subependymal zone (SEZ) of the lateral ventricular wall, from which immature neurons migrate towards the olfactory bulb, and the subgranular zone (SGZ) of the hippocampal dentate gyrus, whose newborn neurons provide a substrate for additional brain plasticity and are crucial for spatial learning and memory (Imayoshi et al., 2008).

Decades of research on CNS development have shed light on extrinsic and intrinsic signals responsible for the generation and the expansion of progenitor cells, their commitment towards different lineages and their migration to a final destination: Notch pathway is one of the most studied, because it has been implicated in a variety of processes, from stem cell maintenance to glial fate commitment. In essence, Notch signaling is a simple pathway: upon binding to a ligand, Notch receptor is cleaved and the intracellular domain (NICD) translocates into the nucleus. Here, it activates the transcription of a subset of B-HLH coding genes, namely HES and HEY genes, which, in turn, repress the activation of downstream target such as proneural genes. Interestingly, despite the common molecular mechanism of transcription activation, Notch specific targets are differently expressed in time and in space in developing brain, and play also some non-overlapping roles, as suggested by the analysis of *Hes1* and *Hes5* single mutants.

Studies conducted in different species – *D. melanogaster*, *C. elegans*, *M. musculus* – have revealed the complexity of Notch signaling and raised many questions about the ability of a "simple" pathway to exert composite and diverse functions. Among them, two major questions are the object of ongoing investigation:

What is the role of Notch signaling in controlling the balance between proliferation and cell commitment in the ventricular zone?

How does the Notch pathway activate specific targets genes among the putative ones?

The simple answer to the first question is summarized by the model called "lateral inhibition" (see Introduction, and **Fig. 1.6**): through a cell-cell interaction, ligand-expressing

cells stimulate Notch-receptor-expressing neighboring cells to maintain their undifferentiated state.

Recent works suggest that the molecular mechanisms of neuronal commitment in mammalian CNS are more complex than the lateral inhibition model found in *D. melanogaster*: strikingly, Kageyama and co-workers showed that Notch signaling drives the activation of Hairy-related genes, whose corresponding proteins have a short half-life and a negative feedback loop on their own promoter. The outcome of those features is the oscillation in the expression/activity of those proteins, and the accumulation of proneural proteins, whose half-life is longer than their repressors. When the proneural protein level is above a given threshold, a cell starts the process of commitment (see for instance, (Kageyama et al., 2007, 2008)).

The second question is still unsolved: many molecules have been identified that modulate Notch activation and function, but to date the mechanism of target selection remains obscure. For instance, in developing cerebellum, *Hes5* is highly expressed in the VZ, from where all glutamatergic neurons arise, while *Hes1* levels are lower (**Fig. 2.1**); on the other hand, *Hes1* is highly expressed in the IsO, where *Hes5* transcript is absent (**Fig. 2.1**).

Recent reports indicated ZFP423 as an important player in the context of cerebellar development: ZFP423 null mice, in fact, are ataxic, show a clear cerebellar hypoplasia, a reduced number of Purkinje cells, and a deficit in the generation of Bergmann glia (Alcaraz et al., 2006; Warming et al., 2006).

Given the above mentioned defects in ZFP423 knock-out mice, most likely due to problems in radial glia development, we wanted to know whether ZFP423 may play a role in this context, and the first signaling pathway candidate to examine was Notch signaling.

The results presented in this thesis indicate that ZFP423 interacts functionally and molecularly with Notch Intracellular Domain to cooperatively activate the expression of some Notch targets both *in vitro* and *in vivo*. Interestingly, we found that ZFP423-NICD cooperation is selective, as only some of the putative Notch targets, namely *Hes5* and *Blbp*, are further up-regulated when ZFP423 is expressed.

ZFP423 is a multifunctional protein firstly identified as transcriptional partner of COE/ EBF transcription factors in olfactory epithelium (Tsai and Reed, 1997); later, the protein was described as cofactor interacting with SMAD1/SMAD4 complex along the BMP signaling

cascade (Hata et al., 2000). Interestingly, ZFP423, Notch, BMP and EBF TFs play important roles during cerebellar development, as *Zfp423* null mice show hypoplastic cerebellum, Notch targets *Hes5* and *Hes1* are highly expressed in cerebellar germinative zones, BMP is secreted by the roof plate, COE/EBF TFs are involved in the differentiation, migration and survival of Purkinje cells (Croci et al., 2006a), (Croci L, Barili V, Chia D, Massimino L, van Vugt R, Masserdotti G, Longhi R, Rotwein P, Consalez GG. submitted. Local Insulin-like Growth Factor I expression is essential for Purkinje neuron survival at birth. Cell Death Differ.). We examined whether ZFP423 could play a role in coordinating different pathways in the context of Notch activity: our results clearly point out that ZFP423 is important in establishing a functional relationship between the above mentioned pathways.

Zfp423 expression in developing cerebellum overlaps with *Hes5*

Zfp423 null embryos show a reduced number of PCs and defects in Bergmann glia genesis: firstly, we performed *in situ* hybridization on wt embryos at different developmental stages (E10.5, E11.5, E12.5, **Fig. 2.1**) to analyze in detail *Zfp423* expression, and found that *Zfp423* is highly expressed in both germinative zones of the cerebellar primordium, the VZ and the RL. Remarkably, *Zfp423* expression is higher in medial sections, where *Zfp423* null embryos show the most prominent defect, and it is almost absent in the IsO (**Fig. 2.1**). This expression pattern largely overlaps with *Hes5* transcript expression: this observation, together with the hypothesis of an involvement of *Zfp423* in the regulation of radial glia development, prompted us to analyze in detail the possible relationship between ZFP423 and Notch signaling.

ZFP423 cooperates with NICD in activating *Hes5 in vitro* and *in vivo*

To test whether ZFP423 may interact with Notch signaling, we moved to different *in vitro* model systems. Firstly, we took advantage of a well-established neural system, namely P19 teratoma cell line, because of its responsiveness to Notch activation (Takizawa et al., 2003) and **Fig. 2.2**). Both Gain-of-function (**Fig. 2.3**) and loss-of-function (**Fig. 2.4**) experiments indicated that ZFP423 could cooperate with NICD in enhancing selectively *Hes5* mRNA

transcription, while the expression of other Notch targets was unchanged (Fig. 2.3D-E). To test whether the cooperative effect between NICD and ZFP423 on *Hes5* activation was a general mechanism of *Hes5* regulation rather than a specific feature of neural cells, we repeated GOF experiment in a myoblastic cell line, namely C2C12, that are negative for both *Zfp423* and *Hes5*. We found that, in this cell line, *Hes5* was clearly dependent upon the addition of exogenous *Zfp423*, as *Nicd* over-expression alone was not sufficient to activate the target significantly (Fig. 2.3E).

The results obtained *in vitro* were sustained and corroborated by the cooperative effect observed *in vivo* (Fig. 2.5): again, *Zfp423* clearly enhanced *ESR1* expression in the injected side of *X. laevis* embryos, while other Notch targets were unaltered, or slightly down-regulated. Nevertheless, the effect of ZFP423 was strictly dependent upon Notch signaling, as depletion of Notch signaling abrogated the up-regulation of *ESR1* in *Zfp423* injected side of *X. laevis* embryos.

Taken together, these results support the notion that ZFP423 acts selectively to recruit NICD onto *Hes5* promoter: as a consequence, ZFP423 could reduce the amount of nuclear NICD available to activate other targets, thus acting as an indirect and passive repressor of NICD non-specific transcription activity. For instance, the slight down-regulation of *Hairy1* in *X. laevis* embryos upon injection of *Zfp423* mRNA could be explained as a "negative" consequence of the specific recruitment of NICD on *ESR1* promoter.

ZFP423 interacts with NICD to activate *Hes5* promoter

In vitro and *in vivo* data indicated that ZFP423 potentiates the activity of NICD in activating some targets, and we focused our attention on *Hes5* transcription regulation. As ZFP423 is capable of binding DNA (Brayer et al., 2008; Tsai and Reed, 1998), we hypothesized that the functional cooperation observed could require binding to DNA or protein-protein interaction, or both.

To test the first hypothesis, we analyzed the *Hes5* promoter from different species – mouse, rat and human – and found several conserved putative ZFP423 binding sites (Fig. 2.6A). Subsequently, we confirmed that the fragment of *Hes5* promoter analyzed *in silico* could respond to NICD-ZFP423 cooperation in luciferase assays (Fig. 2.6C); then, we repeated

the luciferase assay on deleted (**Fig. 2.6B2, D**) or point-mutated (**Fig.2.6 B3, B4, E, F**) form of *Hes5* promoter. In each promoter tested, ZFP423 co-expression doubled the activation of *Hes5* promoter mediated by NICD alone, suggesting that either the sites we mutated are not essential, or the cooperation between NICD and ZFP423 occurs mainly via protein-protein interaction.

We tested the possibility that ZFP423 and NICD interacts with each other by over-expressing them in two different cell lines, HEK and COS7: in both cases, NICD co-precipitated with ZFP423. Although at the moment we cannot determine whether the interaction is direct or mediated by other cofactors, immunoprecipitation experiments suggest that ZFP423 and NICD can, at least, be part of a transcriptional activation complex.

Taken together, the mentioned data suggest that ZFP423 cooperates in regulating gene expression through the interaction with NICD, but this observation is not sufficient to explain the specificity in target selection. One possibility is that ZFP423 recruits, or interacts, with another molecules responsible for the target selection. A second possibility comes from the complex structure of ZFP423: to date, two domains of ZFP423 have been found to bind DNA (Brayer et al., 2008; Tsai and Reed, 1998), and we based our mutagenesis strategy on the DNA sequences recognized by these two domains. However, we cannot exclude that ZFP423 can recognize and bind other unknown DNA sequences. A third possible explanation is that the specific ZFP423 binding site, present on the endogenous *Hes5* promoter, is not included in the *Hes5* promoter fragment we cloned: if so, the NICD-ZFP423 cooperation observed in the luciferase assays could be the result of the physical interaction between the two proteins, devoid of any specificity.

EBF TFs interfere with ZFP423-NICD cooperation *in vitro* and *in vivo*

ZFP423 is an antagonist partner of the COE/EBF transcription factors (Tsai and Reed, 1997). COE/EBF are atypical B-HLH TFs involved in important developmental processes, such as neuronal differentiation, neuronal migration and survival (Corradi et al., 2003; Garcia-Dominguez et al., 2003) (Croci L, Barili V, Chia D, Massimino L, van Vugt R, Masserdotti G, Longhi R, Rotwein P, Consalez GG. submitted. Local Insulin-like Growth Factor I expression is essential for Purkinje neuron survival at birth. Cell Death Differ.). In systems

other than CNS, such as the bone marrow, the Notch pathway interferes with the activity of EBF1 (Smith et al., 2005). During cerebellar development, EBF2 is expressed in the SVZ at the time of neuronal commitment (E11.5 L. Croci, personal communication, and E12.5, see (Croci et al., 2006b), figure 2A). *Zfp423* mRNA is widely expressed in the VZ (**Fig. 2.1**), and possibly in the emerging SVZ. As EBF TFs trigger neuronal differentiation, while the Notch pathway maintains progenitor cells in an uncommitted state, we hypothesized that EBF TFs could interfere with the Notch pathway, and that this could be mediated by ZFP423. We tested this hypothesis and found that EBF TFs can quench the cooperation between ZFP423 and NICD on *Hes5* activation both *in vitro* and *in vivo* (**Fig. 2.8**). As EBFs do not have any direct effect on *Hes5* expression, we could argue that EBFs and NICD may compete for ZFP423 in differentiating progenitors, and recruit ZFP423 in neuronal differentiation process. Recently, Reed and co-workers showed (Cheng and Reed, 2007) that over-expression of ZFP423 in post-mitotic precursors revert them into an undifferentiated state. Our finding suggests a possible interpretation of such a result at the molecular level: in fact, over-expressed ZFP423 could interact with EBFs, interfering with their role during neuronal differentiation, and help the reactivation of *Hes5* expression, leading to the repression of proneural gene. This, in turn, could cause the repression of differentiation markers, and the activation of markers of the undifferentiated state. Along the same line, the reduction in the PCs number observed in the ZFP423 null cerebellum could be the result of the reduced *Hes5* expression, and the subsequent premature neuronal differentiation of progenitors, no longer available to give rise to successive waves of PCs and other neuronal/glial types at later stages.

Based on the expression data and our observations, one may hypothesize that a similar mechanism to that just described for the olfactory neurons may occur during cerebellar development: EBF2, expressed from E11.5 on, could sequester ZFP423 from its interaction with NICD, thus causing a drop of *Hes5* and the subsequent activation of genes important for neuronal differentiation.

ZFP423 as mediator of NICD-BMP cooperation

The cross-talk between Notch pathway and BMP signaling cascade has been studied, and either cooperative or competitive relationship has been found, depending on the system

analyzed (Machold et al., 2007; Takizawa et al., 2003). For instance, Takizawa showed that BMP2 can cooperate with NICD in activating *Hes5* promoter, and SMAD1/SMAD4 can be part of a big complex that includes NICD, CBP/P300 and PCAF. We wondered whether ZFP423 could mediate this cross-talk, and our GOF and LOF *in vitro* experiments suggest that ZFP423 can contribute to mediate the cooperation between BMP and NICD. In fact, ZFP423 over-expression clearly enhances the activation of *Hes5* in NICD-transfected samples treated with BMP (**Fig. 2.10**). Complementary to that, knock-down experiments indicated that ZFP423 depletion reduces the ability of BMP to functionally cooperate with NICD, but to date we cannot exclude that BMP signaling can interact with the Notch pathway independently of ZFP423 (**Fig. 2.12**).

If we consider the role of active BMP signaling in helping ZFP423 to exert its function, our results indicate that NICD-ZFP423 cooperation does not require active BMP to take place (**Fig. 2.11**). This leads us to hypothesize that ZFP423 could function independently of BMP, as well as contributing to couple the Notch pathway and BMP cascade. For instance, in dorsal territories of the cerebellar primordium the interaction between Notch and BMP signaling, promoted by ZFP423, could maintain a pool of *Hes5* positive radial glia progenitors supporting several rounds of asymmetric, neurogenic cell division and preventing premature occurrence of terminal differentiation. An indirect effect of such cooperation could be the recruitment of the BMP effector SMAD1-SMAD4 complexes from their targets onto others, such as *Smad6*, which inhibits BMP signaling, or other unknown targets, which may contribute to maintain undifferentiated progenitors in their proliferative state.

In summary, the results presented in this thesis contribute to reveal new features of the multifunctional protein ZFP423, but, at the same time, they provide a new interpretative key to the findings published so far, and, ultimately, to help the comprehension of the mechanisms regulating the transition between progenitor cells and committed postmitotic cells. Our results, in fact, show that ZFP423 interacts functionally and molecularly with the Notch pathway, that plays a crucial role in radial glial cell maintenance. The working model in **Fig. 3.1** tries to summarize our results and those obtained by others.
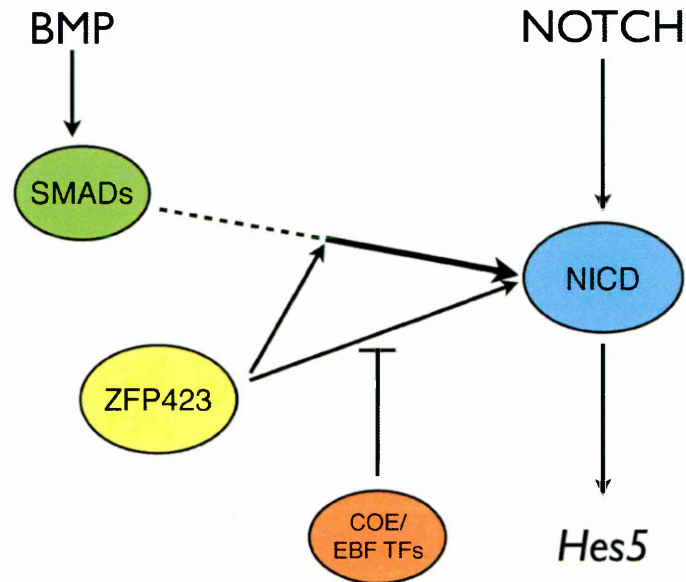
Fig. 3.1 -Working model of the relationship among different pathways based on the literature and the results presented in this thesis work.

It is time to test the role of ZFP423 as mediator and regulator of the three pathways described before in a complex developmental system, such as mouse development. This could clarify the contribution of ZFP423 in maintaining the progenitor pool *in vivo*. To this end, the first step could be to analyze the expression of *Hes* genes and their downstream targets in the cerebellum of *Zfp423* null mice at the onset of Notch activation, to test whether a premature differentiation of progenitor cells occurs. Then, to dissect and understand the role of ZFP423 as balancing molecule of different pathways, one could generate ZFP423 mutants lacking either the domain responsible for the interaction with SMAD1-SMAD4, or with EBF TFs. These mutants would allow us to confirm the importance of ZFP423 in mediating the response to BMP stimuli in developing cerebellum, and to assess its role in neuronal differentiation and migration, in agreement with the model we propose, or providing data that, in contrast to our hypothesis, could help to produce a better model.

Materials
and
Methods

Cell Culture and DNA Transfection

P19 cell line was maintained in MEM-alpha (Invitrogen) supplemented with 10% FBS (Invitrogen). C2C12 myoblastic cell line (American Type Culture Collection), COS7 and HEK293 cell lines were maintained in Dulbecco's Modified Eagle's medium (DMEM) supplemented with 10% fetal bovine serum (FBS, EuroClone). P19, HEK293 and COS7 cells were transfected with Lipofectamine2000 according to the manufacturer's instructions (Invitrogen) (see section *Transfection*). Depending on the experiment, P19 cells were grown in 5% FBS, 2% FBS together with 10^{-6} M retinoic acid for 24 hours or more, or 1% FBS and 10^{-6} M retinoic acid for 24 hours. When specified, BMP4 (R&D Systems) was added to the medium to reach a final concentration of 100 ng/ml BMP4. C2C12 cells were transfected using Lipofectamine2000 and Plus reagent, according to the manufacturer's instructions (Invitrogen), and treated with 100 ng/ml BMP4 (R&D Systems) or increasing amount of Noggin (R&D Systems) when specified.

Plasmids and constructs

To generate pCDNA3-ZFP423, *Zfp423* cDNA was excided from pXY-ZFP423 (RZPD, IRAK MGC full length cDNA, clone 961, Berlin, Germany) with the restriction enzymes SalI and NotI, and the fragment was cloned into pCDNA3. To generate pCDNA3-6Myc-ZFP423, we cloned *Zfp423* cDNA from pXY-ZFP423 in pC2+6Myc. 6Myc-ZFP423 was excised and cloned into pCDNA3 vector (Clontech). pCDNA3-Flag-Notch-Intracellular-Domain (Flag-NICD) was a kind gift from Georg Feger (Serono). pCDNA3-Flag-PCAF and pCDNA3-RBPJ-k were a kind gift from R. Mantovani (University of Milan, Italy).

The fragments of the murine *Hes5* promoter were generated by PCR: essentially, genomic DNA from FVB wild type mouse (20ng) was used as template, and the following primers were used to amplify the promoter:

Hes5-promoter-1051-F CACAAAATGCTGAATGAAACTGG

Hes5-promoter-266-F CACCTGCTCCTCGGGGAGC

Hes5-promoter-72-R GCCTGGAGCTCTGGAGGCG

The PCR was performed using a proofreading polymerase (*Pfu*Turbo, Stratagene); the

fragments were purified, phosphorilated and cloned in pBlueScriptII pBSK vector, previously digested with EcoRV restriction enzyme. The cloned fragments were verified by restriction analysis and sequencing. The clones with the correct promoter sequence were sub-cloned in pGL3 (Clontech).

Murine genomic DNA was used as template, and the PCR reaction was performed as following:

Mix	Amount
DNA	20 ng (2μl)
10X Buffer	2μl
Primer Forward (10μM)	1μl
Primer Forward (10μM)	1μl
dNTPs (10μM)	1μl
*Pfu*Turbo	1μl
H$_2$O	12μl
Total	20μl

Amplification conditions:

Temperature	Time	Cycles
95°C	03:00	
95°C	00:30	
62°C	00:30	
72°C	2:00	30
72°C	5:00	
4°C	forever	

To mutagenize the promoter, we used the following primers:

BRE-mut-F CATTGTGATATCTACCAATTCACAGGCAATTTAGC

BRE-mut-R TGTGAATTGGTAGATATCACAATGGTCGCTC

ZBS-141-F AGCTGGGGATCCTGCCCACTCCTCTGGAAG

ZBS-141-R TGGGCAGGATCCCCAGCTGGGACCTGTTGCCCA

pGL3-Hes5-promoter were used as template, and a PCR reaction was performed as following:

Mix	Amount
DNA	30 ng (3µl)
10X Buffer	5µl
Primer Forward (10µM)	2,5µl
Primer Forward (10µM)	2,5µl
dNTPs (10µM)	5µl
*Pfu*Turbo	2µl
H$_2$O	30µl
Total	50µl

Amplification conditions:

Temperature	Time	Cycles
95°C	03:00	
95°C	00:30	
64°C	00:30	
72°C	10:00	30
72°C	5:00	
4°C	forever	

Transfection

Both P19 and C2C12 were transfected with Lipofectamine2000 according to the manufacturer's instructions (Invitrogen).

About 1x10^5 P19 cells were plated in one well of 6-well plate (Corning) in complete medium one day before the transfection. For each transfection, two mixes were prepared:

- Mix A: 150µl Opti-Mem (Invitrogen) and 6µl Lipo2000

- Mix B: 150µl Opti-Mem (Invitrogen) and 3µg DNA (total)

Mix B was mixed with Mix A in a 1.5ml eppendorf, and leave it at room temperature for about 20-30 minutes, to allow the formation of Lipo2000-DNA macromolecules.

In the meantime, cells were washed twice with PBS 1X, and then about 200µl of fresh and warmed DMEM medium, devoid of FBS and antibiotics, was added to the cells.

Finally, 300µl of the MixA-MixB solution were added drop by drop to the cells, and let them recover for 4 hours in the incubator ad 37°C. After that time, to avoid Lipo2000 toxicity, transfection solution was removed and fresh and warmed medium, DMEM with either 5%, 2% and R.A, or 1% R.A., depending on the experiment, was added to the cells.

The total amount of plasmid molecules transfected was kept constant in almost every experiment, but the amount of each plasmid varied depending on the experiment, and was adjusted considering the size of each construct. To reach the correct amount of plasmid, pBlue-ScriptII was added to the mixture.

Summary of the size of the construct transfected and the relative ratio:

Name	Size	Ratio
pBlue-Script II	3000	0,375
Flag-NICD	8100	1
6Myc-ZFP423	11000	1,25
FlagEBF1	8000	1
FlagEBF2	8000	1
FlagEBF3	8000	1
FlagPCAF	8000	1

In the experiment shown in figure 2.3, we transfected the following amount of DNA:

Sample	Plasmid	Amount
1	pBlue-ScriptII	1,125µg
2	Flag-NICD pBlue-ScriptII	1µg 0,75µg
3	6Myc-ZFP423 pBlue-ScriptII	1,25 0,7µg
4	Flag-NICD 6-MycZFP423 pBlue-ScriptII	1µg 0,6µg 0,56µg
5	Flag-NICD 6-MycZFP423 pBlue-ScriptII	1µg 1,25µg 0
6	Flag-NICD 6-MycZFP423 pBlue-ScriptII	1µg 2,5µg 0

The transfection of C2C12 was essentially made as for P19, except that we plated about 2×10^5 cells. Moreover, to increase transfection efficiency, 4µl of Plus Reagent (Invitrogen) was added to MixA, together with Lipo2000.

In each transfection experiment, an extra well was transfected with a plasmid encoding GFP protein (pCDNA3-GFP) to evaluate the transfection efficiency.

Reverse Transcription (RT)-PCR Assay

Total RNA was extracted with RNeasy MicroKit (Qiagen), according to the manufacturer's instructions. Total RNA was retro-transcribed as follows: 1-1,5 µg was adjusted to a final volume of 10µl with DEPC water and incubate at 65°C for 15 minutes, then transferred to ice; in a separate tube, 4µl of 5X First strand Buffer (Invitrogen), 2µl DTT 0,1M, 2µl dNTPs (10mM), 0,8µl Random Primers (500µM, Roche), 0,2µl RNasiOut (Invitrogen) and 1µl of cDNA MMLV-Retrotranscriptase (Invitrogen) were combined. This mixture was added to the RNA-water mixture and incubated at 37°C for 1 hour. The reaction was stopped by incubating the sample at 70°C for 10 minutes. The obtained cDNA was diluted one to ten, and 3µl was used in each real-time PCR sample. The following oligonucleotide primers were used for the RT-PCR:

- Flag-*Nicd*-for: TACAAAGACGATGACGATAAAGC;

- *Nicd*-Rev: CCTCAAACCGGAACTTCTTGG;

- m*Zfp423*-For: CACCCGCAGCTGTCCGAGAAGGC;

- m*Zfp423*-Rev: CTCCACAGAGGCGCTGGAGTCGGG;

- m*Gapdh*-For: CGCATCTTCTTGTGCAGTG;

- m*Gapdh*-Rev: GTTCAGCTCTGGGATGAC

mRNA quantitation was performed on a LighCycler480 instrument (Roche) following the manufacturer's protocol. Briefly, 10µl of the LightCycler480 SYBR Green I Master Mix (Roche) were mixed with 1µl of the forward primer and 1µl of the reverse primer, both diluted to a concentration of 10mM. This solution was mixed with the sample containing 3µl of the diluted cDNA and 5µl of water, in a final reaction volume of 20µl. We set the software with the following conditions:

Temperature	Time (min:sec)	Cycles
95°C	05:00	
95°C	00:30	
60°C	00:30	
72°C	00:13	45

After the amplification cycles, we always added the step to analyze the formation of unspecific amplicons (the so called *Tmelting curve Analysis*). We used the following oligonucleotides:

- - *Gapdh* (Vincent et al., 2002);

- - *Hes5*, *Hes1* primers (Jensen et al., 2000);

- - *Blbp* (Lowell et al., 2006);

- - *Nrarp* (Yun and Bevan, 2003);

- - *Zfp423* (Hata et al., 2000);

- - *Smad6* (Wang et al., 2007);

- - *Msx2* (Li et al., 2004).

Each gene was analyzed in triplicate, and each experiment was repeated at least three times. Data were exported in RTF format and the analysis was performed with the $\Delta\Delta$Ct method (Livak and Schmittgen, 2001) using Excel Datasheet (Microsoft).

RNA Interference

Single-stranded DNA oligos encoding the pre-miRNAs were annealed according to the manufacturer's instructions (Invitrogen). Pre-miRNA double-stranded oligos were cloned in pCDNA™6.2-GW/-EmGFP-miR vector (Invitrogen). A Pre-miRNA containing a non-targeting sequence (Invitrogen) was used as a negative control. The pre-miRNAs were transfected via Lipofectamine2000 (Invitrogen) according to the manufacturer's instructions. To test the efficacy of the preMiRNA, HEK293 cells were transfected with 6mycZFP423 and either a non-targeting pre-miRNA vector or ZFP423-specific pre-miRNA, and cell lysates were analyzed via Western Blot. Among the specific pre-miRNA tested (three pre-miRNA), we selected the most effective one (named OAZ-0) in abolishing protein expression. Transfected P19 cells sorted for GFP expression and lysed for RNA extraction with RNeasy MicroKit (Qiagen), according to the manufacturer's instructions.

Cell Sorting

Cells were sorted by the FACS Sorting Facility at Dibit. Briefly, the day of sorting, cells were rinsed twice with PBS, detached from the 6-well plates using trypsin/EDTA solution at 0,05%, then collected with DMEM and FBS, when needed, prewarmed at 37°C. Cells were centrifuged 3 minutes at 1300 RPM, then re-suspended in 500μl DMEM. FACS sorting parameters – essentially, cell size and autofluorescence –were set up using untransfected cells, and then transfected GFP-positive cells were sorted in a collection tube containing PBS. Soon after the sorting, cells were pelleted and immediately processed for the RNA extraction.

Luciferase Assay

The day before the transfection, P19 cells were plated in 6-well plates, and grown in 10% FBS. They were transfected with the indicated vectors, and cultured for 24 hours. C2C12 were plated in 12-well plates and, depending on the experiment, grown either in 10% FBS and DMEM, or 1% FBS and DMEM. After the transfection, the medium was substituted with fresh medium, either at 10% FBS or 1% FBS in DMEM, and the cells were treated, when indicated, with 100 ng/ml BMP4 (R&D System) for 6h before performing the luciferase assays. In the experiment with Noggin (R&D System), Noggin was added to the culture medium soon after the plating at 100ng/ml, and maintained in Noggin-added medium during the experiment. Luciferase assays were carried out according to the manufacturer's instructions (Promega). Each result is the average of three independent measurements, and each experiment has been repeated at least three times.

Immunoprecipitation and Western blots

COS7 and HEK293 cells were harvested 48 hours after transfection and then frozen at -80°C. For the co-immunoprecipitation experiments, cells were thawed at room temperature and lysed in 5 volumes of Extraction Buffer (10 mM Hepes pH 7.9; 400 mM NaCl; 5% glycerol, PMSF 1mM, Leupeptin 0,5mM , NaF 50mM, Pepstatin 1mM). Samples were centrifuged at 34000 rpm for 30 minutes at 4°C and supernatants collected. Protein concentration was determined by the BCA assay (Pierce). Part of the lysate (20%) was kept as positive input

control. Lysates were incubated with 10 μg of the indicated antibodies overnight, then 60 μl of Sepharose/protein G 50% slurry were added for 4 hours at 4°C. Resin was washed four times with Extraction Buffer. Protein complexes were eluted by addition of Sample Buffer (Tris-Cl 125 mM pH 6.8; 0.1 M 2-mercaptoethanol; 2% SDS; 20% glycerol; 25 mg/ml Bromphenol Blue), boiled for 15 minutes and separated on an SDS-polyacrylamide gel at 8%. Proteins were transferred on a PVDF membrane (Millipore). Western Blots were performed with the following antibodies: anti-myc (9E10, Santa Cruz Biotechnology), anti-Notch (E-20, sc-6014, Santa Cruz Biotechnology), anti-FLAG-M2 (Sigma-Aldrich), anti-RBPJ-k (H-50, sc-28713 Santa-Cruz Biotechnology), anti-βactin (A5441, Sigma). The secondary antibodies used were a goat anti-rabbit HRP-conjugated antibody (Bio-Rad), and sheep anti-mouse HRP-conjugated antibody (Amersham). Blots were developed with the LiteAblot substrate (EuroClone).

Immunofluorescence and image acquisition

Transfected cells were rinsed with PBS 1X and, then, fixed with PFA 4% for 20 minutes at room temperature. Cells were firstly permeabilized with a P-solution (10% Goat serum, 0,5% TritonX-100, PBS1X) for 10 minutes and then blocked in a blocking solution (15% Goat serum, 0,2% TritonX-100, PBS1X) for 1 hours. Primary antibody – anti-myc (9E10, Santa Cruz Biotechnology) – was diluted in blocking solution and hybridized for at least 2 hours at room temperature. Cell were washed 3 times with PBS1X, then the anti-mouse-TRITC (AlexaFluor), diluted (1:1000) in blocking solution, was added to the cells and left for 1 hours. Cells were rinsed 2 times with PBS, DAPI staining was performed, then cells were rinsed 3 times with PBS1X and, finally, mounted with an acqueous mounting media (Dako).

The images were acquired with a Leica Confocal microscopy at a magnification of 63X.

Animal Care

All experiments described in this paper were conducted in agreement with the stipulations of the San Raffaele Scientific Institute Animal Care and Use Committee, University of

Calgary guidelines, and the Guide to the Care and Use of Experimental Animals as outlined by the Canadian Council for Animal Care.

Tissue preparation

Pregnant mice were anesthetized with Avertin (Sigma). Embryos were fixed overnight by immersion with either 4% PFA. Tissues fixed with 4% PFA were rinsed three times in 1X PBS, cryoprotected in 30% sucrose overnight, embedded in OCT (Bioptica), and stored at −80°C, before sectioning on a cryotome (20 μm).

Xenopus embryo microinjection

Mouse *Zfp423* from pCDNA3-*Zfp423* was subcloned into the pCS2+ expression vector and used to make capped mRNA *in vitro* using the Message mMachine kit (Ambion). Also the following constructs were used as DNA templates to make capped mRNA : pCS2+X-Delta^{stu} (Chitnis and Kintner, 1996), pCS2+MT-XotchΔE (Referred to here as N^{act}) (Coffman et al., 1993), pCS2+Xebf2 (Pozzoli et al., 2001), pCS2+Xebf3 (Pozzoli et al., 2001), pCS2+nβgal (Chitnis et al., 1995) and pCS2+GFP (Chalfie et al., 1994). The full length *Xenopus Zfp423* (*XZfp423*) cDNA including part of 5'UTR was acquired by 5'RACE (Roche) using the sequence of image clone 6636947, and then by RT-PCR with Superscript II Reverse Transcriptase (Invitrogen) and PfuUltraII fusion HS DNA polymerse (Stratagene) (GenBank accession No. GQ421283). The sequence of our XZfp423 morpholino (Gene Tools) is TCCACTGTACCTCAAAACTAACCCC, which is complementary to the nucleotides −26 to −2. mRNA and morpholino were injected into one blastomere of 2-cell stage embryos in the following amounts: *Zfp423* (1ng for single injection and co-injection with *Delta^{stu}*, 600pg for co-injection with XotchΔE), *Delta^{stu}* (400pg), *XotchΔE* (100pg), *Xebf2* (100pg), *Xebf3* (100pg), *nβgal* (50pg) and XZfp423 morpholino (30ng). mRNA was injected into one dorsal blastomere of 16-cell stage embryos in the following amounts : *Zfp423* (300pg) and *Gfp* (200pg). mRNA for *nβgal* or *Gfp* was co-injected into all embryos as a tracer. Embryos were grown until neural plate stages and fixed in MEMFA for 30 minutes (Harland, 1991). X-gal staining was performed on the embryos injected with nβgal as described (Turner and

Weintraub, 1994).

In situ hybridization

For whole mount *in situ* hybridizations of *Xenopus* embryos, the following constructs were used to generate antisense RNA probes : pCMV-sport6-XZfp423 (Image clone 6636947, ATCC), pBS-ESR1 (Wettstein et al., 1997), pBS-Hairy1 (Dawson et al., 1995), and pBS-Nrarp (Lamar et al., 2001). Antisense RNA probes were generated *in vitro* using T7 or T3 RNA polymerase (Ambion) and labeled with digoxigeninin-11-UTP (Roche). Whole mount *in situ* hybridization was performed on the fixed and X-gal stained embryos as described (Harland, 1991) except using BM purple (Boehringer Mannheim) as the substrate for alkaline phosphatase.

In situ hybridization of whole mount mouse embryos and embryonic sections were performed as described (Chizhikov and Millen, 2004) and (www.ucl.ac.uk/~ucbzwdr/double in situ protocol.htm). Digoxygenin-labeled riboprobes were transcribed from plasmids containing *Zfp423, Hes1, Hes5*.

In the following section, I reported all the steps followed for *in situ* hybridization on embryonic section:

SLIDES PRE-TREATMENTS

All solutions and containers need to be RNAse free.

- Fix slides in 4% Paraformaldehyde in 1X PBS for 20' RT

- Wash 2 for 5' in 1X PBS

- Pre-incubate in Proteinase K Buffer for 5' (Proteinase K Buffer: 50mM Tris-HCl pH8/5mM EDTA pH8)

- Incubate at 30°C with Proteinase K at 0.5µg/ml in Proteinase K Buffer for 10' to 30' (the digestion time might have to be adjust for different tissues)

- Wash in 0.2% (w/v) glycine in 1X PBS for 30" to stop the digestion

- Wash 2 for 30" in 1X PBS

- Fix in 4% Paraformaldehyde in 1X PBS for 20' RT

- Wash 2 for 5' in 1X PBS

- Place slides in 0.1M triethanolamine-HCl (pH 8) for 5'

- Replace with 0.1M triethanolamine-HCl (pH 8) containing freshly added acetic anhydride (1/400 dilution; add the acetic anhydride to the triethanolamine-HCl, shake vigorously for a few seconds and use immediately). Incubate for 10', than repeat.

- Wash 2 for 5' in 2X SSC

- Incubate slides in pre-hybridization mix for 1-2 hours (pre-hybridization mix: 3XSSC/50% formamide)

HYBRIDIZATION

- Heat the Hybridization mix at 50°C for 10' (Hybridization mix: 1X Denhardt's solution, 50% deionized formamide, 3X SSC, 10% dextran sulfate, 500ug/ml t-RNA)

- Heat the probe at 75°C for 5', chill briefly on ice

- Add the DIG-labeled probe to the Hybridization mix at the concentation of 1µg/ml, vortex briefly

- Add to the slide an appropriate volume of diluted DIG-labeled probe (usually 180µl for 22X60mm coverslip), cover the sections with an HybriSlip coverslip (SIGMA cat# HS6024)

- Place slides in a humid container and incubate at 55-60°C overnight

POST-HYBRIDIZATION WASHES

For the following washing steps, solutions and containers do not have to be RNAse free. Heat the solutions before use.

SOLUTIONS:

- NTE: 0.5M NaCl, 10mM Tris-HCl (pH 8), 5mM EDTA (pH 8)

- Wash 1: 50% formamide/2X SSC

- Wash 2: 50% formamide/1X SSC

- Wash 2 for 30' at 60°C in Wash 1

- Wash 2 for 15' at 37°C in NTE

- Incubate at 37°C with RNAse A at 20µg/ml in NTE for 30'

- Wash 1 time for 15' at 37°C in NTE

- Wash 2 for 30' at 60°C in Wash 2

- 2X SSC 1 time for 10' at room temperature

BLOCKING AND ANTIBODY INCUBATION

SOLUTIONS

- TBS: 100mM Tris-HCl pH 7.5, 150mM NaCl

- Blocking solution: 10% Sheep serum in TBS

- NTM: 100mM NaCl, 100mM Tris-HCl pH9.5, 50mM $MgCl_2$

- Wash 2 for 15' in TBS

- Add 1ml of blocking solution on each slide, incubate for 1 hour

- Dry off the slide around the sections using tissue paper

- Circle the sections with Pap Pen

- Replace the blocking solution with anti-digoxygenin AP-coniugated antibody (Roche cat# 11 093 274 910) diluted 1:2000 in blocking solution

  - Incubate slides in a humid container at 4°C overnight

POST-ANTIBODY WASHES

SOLUTIONS

Staining buffer (10ml): 30µl of NBT (100 mg/ml in 75% Dimetilformamide), 30µl BCIP (50mg/ml in Dimetilformamide) in NTM. Prepare fresh and protect from light.

  - Wash 2 for 15' in TBS

  - Wash 2 for 10' in NTM

  - Add 1 ml of Staining buffer to the slides and incubate in the dark until the signal reaches a satisfactory intensity

- Block the colour reaction washing the slides 3 times for 10' in 1X PBS

- Mount the slides using an aqueous mounting medium

PREPARATION OF DIG-LABELED PROBE

TEMPLATE DIGESTION

- Prepare the template DNA by linearizing the cDNA vector with the appropriate restriction enzymes. Usually I digest 20µg of DNA in a final volume of 100µl.

- After 3 hours run a small aliquot of digestion (500 ng) on an agarose gel to check that the plasmid is fully linearized.

- Add 1 volume of phenol/chloroform (1:1), mix well and centrifuge for 5' at 13500 rpm.

- Take the upper phase, add 1/10 volume of 3M Na Acetate (pH 5.2) and mix well.

- Add 2.5 volumes of cold absolute ethanol, mix well and leave at –20°C for 2 hours.

- Centifuge at 13500 rpm for 20' at 4°C.

- Wash the pellet with cold 70% ethanol and resuspend in 20µl of water.

RIBOPROBE TRANSCRIPTION

- 1.5µg linearized cDNA

- 2µl 10X Buffer

- 2µl 10mM ATP

- 2µl 10mM CTP

- 2µl 10mM GTP

- 1.2µl 10mM UTP

- 0.8µl 10mM DIG-11-UTP (Roche cat #1209256)

- 1µl 250mM DTT

- 1µl RNAse inhibitor (=40 units, Roche)

- 1µl (=10 units) of the appropriate RNA polymerase (Roche)

- RNAse-free water to 20µl

- Incubate the reaction at 37°C for 1 hour.

- Add again 1µl (=10 units) of the appropriate RNA polymerase, leave 1 hour at 37°C.

- Run 1µl of the reaction on a gel for RNA (add 8 µl of RNA loading buffer to 1µl of the

reaction and incubate at 65°C for 15 minutes. Spin down and chill briefly on ice. Add 2 μl Ethidium bromide, 2 μl loading dye, mix well and load on a gel for RNA).

RIBOPROBE PRECIPITATION

- Make the final volume of the reaction up to 100μl with RNAse-free water.

- Add 1/10 volume of 3M Na Acetate (pH 5.2), 1μl of glycogen (10mg/ml) and mix well.

- Add 2.5 volumes of cold absolute ethanol, mix well and leave at –20°C overnight.

- Centifuge at 13500 rpm for 20' at 4°C.

- Wash the pellet with cold 70% ethanol and resuspend in 40μl of RNAse-free water.

- Run 2 μl of the DIG-labeled riboprobe on a gel for RNA (as described above). To quantify the riboprobe concentration, load 1 and 1.5 μg of total RNA.

- Dilute the riboprobe to 100 ng/μl with RNAse-free water and store at –80°C in small aliquots.

GEL FOR RNA (50ml)

Dissolve 0.5 gr of agarose in 44.2 ml of RNAse-free water. Cool to 60°C and then add 5ml of 10X MOPS and 0.8 ml of 37% formaldehyde. Cast the gel in a chemical hood and allow the gel to set for at least 30 minutes.

RNA LOADING BUFFER (1.5 ml)

1 ml deionized formamide

200 μl 10X MOPS

300 μl 37% formaldehyde

Store at –20°C in the dark.

In the following section, I reported all the steps followed for whole mount *in situ* hybridization:

EMBRYO DISSECTION AND PREPARATION

- Dissect embryops in a iced solution NaCl 0.9%

- Transfer the embryos in a 2ml eppendorf and fix them with PFA 4% dissolved in

PBS 1X at least 6 hours at 4°C;

- De-hydrate embryos as follows:

_ 25% MetOH in PBT 10' on ice

_ 50% MetOH in PBT 10' on ice

_75% MetOH in PBT 10' on ice

Wash twice in methanol.

Embryos can be stored in MetOH at -20°C up to 12 months.

1° DAY

- Put embryos in a 2ml eppendorf and re-hydrate them as follows:

75% MetOH in PBT 5' RT

50% MetOH in PBT 5' RT

25% MetOH in PBT 5' RT

- 2x5' in PBT, RT

- 6% H_2O_2 in PBT per 2-4 hours in rotation, RT

- 2x5' in PBT, RT. Make a small hole in the telencephalon with Pasteur pipette: this procedure is important mainly for embryos at E9.5-E10.5

- Permeabilize embryos with Proteinase K in PBT (10µg/ml) at 37°C (E7.5/8.5 embryos: 5-6'; E9.5 embryos: 8-10'; E10.5 embryos: 15')

- 2x5' glycine in PBT (2mg/ml)

- 5' in PBT

- Post-fix embryos with 4%PFA/0.2% glutaraldhyde in PBT, 20' RT

- Wash embryos in PBT

- 2x5' in PBT, RT

- 1:1 Hybridization Mix/PBT pre-warmed a 65°C. Wait until them embryos reach the floor of the eppendorf.

- Hybridization Mix pre-warmed a 65°C. Wait until them embryos reach the floor of the eppendorf.

- 3x1 hour in Hybridization Mix a 65°C

- Denature the probe at 65°C for 15'

- Add the probe to 1ml Hybridization Mix [1μg/ml]; for highly expressed genes, one cand add up to 250ng/ml of probe.

- Hybridize O/N a 65°C in rotation

Hybridization Mix (50ml)

25ml Formamide De-Ionized

12.5 ml 20X SSC

0.5ml 10% Tween-20

1ml 5% CHAPS

0.1ml eparina (50mg/ml)

0.1ml t-RNA (10mg/ml)

0.5ml EDTA 0.5M pH8

10.3ml H_2O

PBT

0.1% Tween-20 in 1X PBS

2° DAY

Transfer embryos into 8ml glass vial. Each washing step has to be done with samples rotating.

POST-HYBRIDIZATION WASHING

- Wash Solution 1, 2x30' a 65°C

- Wash 10' at 65°C with a mix 1:1 of Wash Solution 1 e 2

- Was 3x5' RT con Wash Solution 2

- Incubate with RNAse A (100μg/ml) in Wash Solution 2 per 30' a 37°C

- Wash 5' RT with Wash Solution 2

- Wash with Wash Solution 3, 2x30' a 65°C

- Wash 3x5' RT with TBST

Wash Solution 1

50% Formamide

5X SSC pH5

1% SDS

Wash Solution 2

0.5M NaCl

10mM Tris-HCl pH 7.5

0.1% Tween-20

Wash Solution 3

50% Formamide

2X SSC pH5

0.1% Tween-20

TBST

140mM NaCL

2.7mM KCl

25mM Tris-HCl pH 7.5

0.1% Tween-20

ANTIBODY INCUBATION

Transfer the embryos in a 2ml eppendorf

- Treat the embryos with a Blocking solution 10% Sheep Serum in TBST per 1-2

ore

- Antibody pre-absorption (receipt for per 3ml):

   _ Add 3mg of embryo powder a 0.5ml di TBST, 70°C per 30'

   _ Cool in ice for 2-3'

   _ Add 5µl of Sheep Serum and 1µl anti-Digoxygenin-AP antibody

   _ Put in rotation at 4°C for 1 hour

   _ Centrifuge at 2500g for 10' a 4°C

   _ Recover the supernatant and add it to 2.5ml di 1% Sheep Serum in TBST

- Remove the blocking solution form the embryos and substitute it with 1ml pre-absorbed antibody

- Incubate O/N at 4°C rotation

3° DAY

Transfer the embryos in 20ml glass vials.

- Wash 3x10' RT with TBST

- Wash 6x 1 ora RT with TBST

- Keep in rotation in TBST a 4°C O/N

4° DAY

- Wash 3x10' RT con TBST

- Wash 3x15' RT con NTMT

- Transfer the embryos in a 2ml eppendorf

- Incubate at dark with 1ml solution containing the substrat for the alkaline phosphatase (For 1ml: 3.5µl BCIP, 3.5µl NBT in NTMT)

- When you have obtained the desired color intensity, wash at least 5-6 times with PBT.

- Leave the embryos in 4%PFA at 4°C

NTMT

100mM NaCl

100mM tris-HCl pH9.5

50mM $MgCl_2$

0.1% Tween-20

Statistical Analysis

Statistical significance was determined by the Student *t* test with a threshold for significance set to *p*= 0.05. All results are plotted as the mean ± standard deviation.

Bibliography

Aaku-Saraste, E., Hellwig, A., and Huttner, W.B. (1996). Loss of occludin and functional tight junctions, but not ZO-1, during neural tube closure--remodeling of the neuroepithelium prior to neurogenesis. Dev Biol 180, 664-679.

Afrakhte, M., Moren, A., Jossan, S., Itoh, S., Sampath, K., Westermark, B., Heldin, C.H., Heldin, N.E., and ten Dijke, P. (1998). Induction of inhibitory Smad6 and Smad7 mRNA by TGF-beta family members. Biochem Biophys Res Commun 249, 505-511.

Akazawa, C., Sasai, Y., Nakanishi, S., and Kageyama, R. (1992). Molecular characterization of a rat negative regulator with a basic helix-loop-helix structure predominantly expressed in the developing nervous system. J Biol Chem 267, 21879-21885.

Alcaraz, W.A., Gold, D.A., Raponi, E., Gent, P.M., Concepcion, D., and Hamilton, B.A. (2006). Zfp423 controls proliferation and differentiation of neural precursors in cerebellar vermis formation. Proc Natl Acad Sci U S A 103, 19424-19429.

Alder, J., Cho, N.K., and Hatten, M.E. (1996). Embryonic precursor cells from the rhombic lip are specified to a cerebellar granule neuron identity. Neuron 17, 389-399.

Alder, J., Lee, K.J., Jessell, T.M., and Hatten, M.E. (1999). Generation of cerebellar granule neurons in vivo by transplantation of BMP-treated neural progenitor cells. Nat Neurosci 2, 535-540.

Ang, S.L., Jin, O., Rhinn, M., Daigle, N., Stevenson, L., and Rossant, J. (1996). A targeted mouse Otx2 mutation leads to severe defects in gastrulation and formation of axial mesoderm and to deletion of rostral brain. Development 122, 243-252.

Anthony, T.E., Mason, H.A., Gridley, T., Fishell, G., and Heintz, N. (2005). Brain lipid-binding protein is a direct target of Notch signaling in radial glial cells. Genes Dev 19, 1028-1033.

Avantaggiato, V., Acampora, D., Tuorto, F., and Simeone, A. (1996). Retinoic acid induces stage-specific repatterning of the rostral central nervous system. Dev Biol 175, 347-357.

Bae, S., Bessho, Y., Hojo, M., and Kageyama, R. (2000). The bHLH gene Hes6, an inhibitor of Hes1, promotes neuronal differentiation. Development 127, 2933-2943.

Baek, J.H., Hatakeyama, J., Sakamoto, S., Ohtsuka, T., and Kageyama, R. (2006). Persistent and high levels of Hes1 expression regulate boundary formation in the developing central nervous system. Development 133, 2467-2476.

Bai, C.B., Auerbach, W., Lee, J.S., Stephen, D., and Joyner, A.L. (2002). Gli2, but not Gli1, is required for initial Shh signaling and ectopic activation of the Shh pathway. Development 129, 4753-4761.

Bai, C.B., Stephen, D., and Joyner, A.L. (2004). All mouse ventral spinal cord patterning by hedgehog is Gli dependent and involves an activator function of Gli3. Dev Cell 6, 103-115.

Barrantes, I.B., Elia, A.J., Wunsch, K., Hrabe de Angelis, M.H., Mak, T.W., Rossant, J., Conlon, R.A., Gossler, A., and de la Pompa, J.L. (1999). Interaction between Notch signalling and Lunatic fringe during somite boundary formation in the mouse. Curr Biol 9, 470-480.

Basak, O., and Taylor, V. (2007). Identification of self-replicating multipotent progenitors in the embryonic nervous system by high Notch activity and Hes5 expression. Eur J Neurosci 25, 1006-1022.

Ben-Arie, N., Bellen, H.J., Armstrong, D.L., McCall, A.E., Gordadze, P.R., Guo, Q., Matzuk, M.M., and Zoghbi, H.Y. (1997). Math1 is essential for genesis of cerebellar granule neurons. Nature 390, 169-172.

Bermingham, N.A., Hassan, B.A., Price, S.D., Vollrath, M.A., Ben-Arie, N., Eatock, R.A., Bellen, H.J., Lysakowski, A., and Zoghbi, H.Y. (1999). Math1: an essential gene for the generation of inner ear hair cells. Science 284, 1837-1841.

Bessho, Y., Hirata, H., Masamizu, Y., and Kageyama, R. (2003). Periodic repression by the bHLH factor Hes7 is an essential mechanism for the somite segmentation clock. Genes Dev 17, 1451-1456.

Bessho, Y., Miyoshi, G., Sakata, R., and Kageyama, R. (2001a). Hes7: a bHLH-type re-

pressor gene regulated by Notch and expressed in the presomitic mesoderm. Genes Cells 6, 175-185.

Bessho, Y., Sakata, R., Komatsu, S., Shiota, K., Yamada, S., and Kageyama, R. (2001b). Dynamic expression and essential functions of Hes7 in somite segmentation. Genes Dev 15, 2642-2647.

Bland, C.E., Kimberly, P., and Rand, M.D. (2003). Notch-induced proteolysis and nuclear localization of the Delta ligand. J Biol Chem 278, 13607-13610.

Blaumueller, C.M., Qi, H., Zagouras, P., and Artavanis-Tsakonas, S. (1997). Intracellular cleavage of Notch leads to a heterodimeric receptor on the plasma membrane. Cell 90, 281-291.

Blumberg, B., Bolado, J., Jr., Moreno, T.A., Kintner, C., Evans, R.M., and Papalopulu, N. (1997). An essential role for retinoid signaling in anteroposterior neural patterning. Development 124, 373-379.

Bodmer, R., Carretto, R., and Jan, Y.N. (1989). Neurogenesis of the peripheral nervous system in Drosophila embryos: DNA replication patterns and cell lineages. Neuron 3, 21-32.

Boukhtouche, F., Janmaat, S., Vodjdani, G., Gautheron, V., Mallet, J., Dusart, I., and Mariani, J. (2006). Retinoid-related orphan receptor alpha controls the early steps of Purkinje cell dendritic differentiation. J Neurosci 26, 1531-1538.

Brayer, K.J., Kulshreshtha, S., and Segal, D.J. (2008). The protein-binding potential of C2H2 zinc finger domains. Cell Biochem Biophys 51, 9-19.

Briscoe, J., Pierani, A., Jessell, T.M., and Ericson, J. (2000). A homeodomain protein code specifies progenitor cell identity and neuronal fate in the ventral neural tube. Cell 101, 435-445.

Briscoe, J., Sussel, L., Serup, P., Hartigan-O'Connor, D., Jessell, T.M., Rubenstein, J.L., and Ericson, J. (1999). Homeobox gene Nkx2.2 and specification of neuronal identity by graded Sonic hedgehog signalling. Nature 398, 622-627.

Brodin, G., Ahgren, A., ten Dijke, P., Heldin, C.H., and Heuchel, R. (2000). Efficient TGF-beta induction of the Smad7 gene requires cooperation between AP-1, Sp1, and Smad proteins on the mouse Smad7 promoter. J Biol Chem 275, 29023-29030.

Brown, N.L., Patel, S., Brzezinski, J., and Glaser, T. (2001). Math5 is required for retinal ganglion cell and optic nerve formation. Development 128, 2497-2508.

Bruckner, K., Perez, L., Clausen, H., and Cohen, S. (2000). Glycosyltransferase activity of Fringe modulates Notch-Delta interactions. Nature 406, 411-415.

Cabrera, C.V., and Alonso, M.C. (1991). Transcriptional activation by heterodimers of the achaete-scute and daughterless gene products of Drosophila. EMBO J 10, 2965-2973.

Campbell, K., and Gotz, M. (2002). Radial glia: multi-purpose cells for vertebrate brain development. Trends Neurosci 25, 235-238.

Castella, P., Sawai, S., Nakao, K., Wagner, J.A., and Caudy, M. (2000). HES-1 repression of differentiation and proliferation in PC12 cells: role for the helix 3-helix 4 domain in transcription repression. Mol Cell Biol 20, 6170-6183.

Chae, T.H., Kim, S., Marz, K.E., Hanson, P.I., and Walsh, C.A. (2004). The hyh mutation uncovers roles for alpha Snap in apical protein localization and control of neural cell fate. Nat Genet 36, 264-270.

Chalfie, M., Tu, Y., Euskirchen, G., Ward, W.W., and Prasher, D.C. (1994). Green fluorescent protein as a marker for gene expression. Science 263, 802-805.

Chen, G., Fernandez, J., Mische, S., and Courey, A.J. (1999). A functional interaction between the histone deacetylase Rpd3 and the corepressor groucho in Drosophila development. Genes Dev 13, 2218-2230.

Chen, H., Thiagalingam, A., Chopra, H., Borges, M.W., Feder, J.N., Nelkin, B.D., Baylin, S.B., and Ball, D.W. (1997). Conservation of the Drosophila lateral inhibition pathway in human lung cancer: a hairy-related protein (HES-1) directly represses achaete-scute homo-

log-1 expression. Proc Natl Acad Sci U S A 94, 5355-5360.

Cheng, L.E., and Reed, R.R. (2007). Zfp423/OAZ participates in a developmental switch during olfactory neurogenesis. Neuron 54, 547-557.

Cheng, L.E., Zhang, J., and Reed, R.R. (2007). The transcription factor Zfp423/OAZ is required for cerebellar development and CNS midline patterning. Dev Biol 307, 43-52.

Chenn, A., and McConnell, S.K. (1995). Cleavage orientation and the asymmetric inheritance of Notch1 immunoreactivity in mammalian neurogenesis. Cell 82, 631-641.

Chesnutt, C., Burrus, L.W., Brown, A.M., and Niswander, L. (2004). Coordinate regulation of neural tube patterning and proliferation by TGFbeta and WNT activity. Dev Biol 274, 334-347.

Chitnis, A., Henrique, D., Lewis, J., Ish-Horowicz, D., and Kintner, C. (1995). Primary neurogenesis in Xenopus embryos regulated by a homologue of the Drosophila neurogenic gene Delta. Nature 375, 761-766.

Chitnis, A., and Kintner, C. (1996). Sensitivity of proneural genes to lateral inhibition affects the pattern of primary neurons in Xenopus embryos. Development 122, 2295-2301.

Chizhikov, V., and Millen, K.J. (2003). Development and malformations of the cerebellum in mice. Mol Genet Metab 80, 54-65.

Chizhikov, V.V., and Millen, K.J. (2004). Control of roof plate formation by Lmx1a in the developing spinal cord. Development 131, 2693-2705.

Coffman, C.R., Skoglund, P., Harris, W.A., and Kintner, C.R. (1993). Expression of an extracellular deletion of Xotch diverts cell fate in Xenopus embryos. Cell 73, 659-671.

Corradi, A., Croci, L., Broccoli, V., Zecchini, S., Previtali, S., Wurst, W., Amadio, S., Maggi, R., Quattrini, A., and Consalez, G.G. (2003). Hypogonadotropic hypogonadism and peripheral neuropathy in Ebf2-null mice. Development 130, 401-410.

Croci, C., Fasano, S., Superchi, D., Perani, L., Martellosio, A., Brambilla, R., Consalez, G., and Bongarzone, E.R. (2006a). Cerebellar neurons and glial cells are transducible by lentiviral vectors without decrease of cerebellar functions. Dev Neurosci 28, 216-221.

Croci, L., Chung, S.H., Masserdotti, G., Gianola, S., Bizzoca, A., Gennarini, G., Corradi, A., Rossi, F., Hawkes, R., and Consalez, G.G. (2006b). A key role for the HLH transcription factor EBF2COE2,O/E-3 in Purkinje neuron migration and cerebellar cortical topography. Development 133, 2719-2729.

Crozatier, M., Valle, D., Dubois, L., Ibnsouda, S., and Vincent, A. (1996). Collier, a novel regulator of Drosophila head development, is expressed in a single mitotic domain. Curr Biol 6, 707-718.

D'Ercole, A.J., Ye, P., Calikoglu, A.S., and Gutierrez-Ospina, G. (1996). The role of the insulin-like growth factors in the central nervous system. Mol Neurobiol 13, 227-255.

Dahlqvist, C., Blokzijl, A., Chapman, G., Falk, A., Dannaeus, K., Ibanez, C.F., and Lendahl, U. (2003). Functional Notch signaling is required for BMP4-induced inhibition of myogenic differentiation. Development 130, 6089-6099.

Darken, R.S., and Wilson, P.A. (2001). Axis induction by wnt signaling: Target promoter responsiveness regulates competence. Dev Biol 234, 42-54.

Davis, R.L., and Turner, D.L. (2001). Vertebrate hairy and Enhancer of split related proteins: transcriptional repressors regulating cellular differentiation and embryonic patterning. Oncogene 20, 8342-8357.

Dawson, S.R., Turner, D.L., Weintraub, H., and Parkhurst, S.M. (1995). Specificity for the hairy/enhancer of split basic helix-loop-helix (bHLH) proteins maps outside the bHLH domain and suggests two separable modes of transcriptional repression. Mol Cell Biol 15, 6923-6931.

de la Pompa, J.L., Wakeham, A., Correia, K.M., Samper, E., Brown, S., Aguilera, R.J., Nakano, T., Honjo, T., Mak, T.W., Rossant, J., et al. (1997). Conservation of the Notch signalling pathway in mammalian neurogenesis. Development 124, 1139-1148.

Dekker, E.J., Vaessen, M.J., van den Berg, C., Timmermans, A., Godsave, S., Holling, T., Nieuwkoop, P., Geurts van Kessel, A., and Durston, A. (1994). Overexpression of a cellular retinoic acid binding protein (xCRABP) causes anteroposterior defects in developing Xenopus embryos. Development 120, 973-985.

Ding, B., Liu, C.J., Huang, Y., Hickey, R.P., Yu, J., Kong, W., and Lengyel, P. (2006). p204 is required for the differentiation of P19 murine embryonal carcinoma cells to beating cardiac myocytes: its expression is activated by the cardiac Gata4, Nkx2.5, and Tbx5 proteins. J Biol Chem 281, 14882-14892.

Dubois, L., Bally-Cuif, L., Crozatier, M., Moreau, J., Paquereau, L., and Vincent, A. (1998). XCoe2, a transcription factor of the Col/Olf-1/EBF family involved in the specification of primary neurons in Xenopus. Curr Biol 8, 199-209.

Dunwoodie, S.L., Clements, M., Sparrow, D.B., Sa, X., Conlon, R.A., and Beddington, R.S. (2002). Axial skeletal defects caused by mutation in the spondylocostal dysplasia/pudgy gene Dll3 are associated with disruption of the segmentation clock within the presomitic mesoderm. Development 129, 1795-1806.

Egan, S.E., St-Pierre, B., and Leow, C.C. (1998). Notch receptors, partners and regulators: from conserved domains to powerful functions. Curr Top Microbiol Immunol 228, 273-324.

Englund, C., Fink, A., Lau, C., Pham, D., Daza, R.A., Bulfone, A., Kowalczyk, T., and Hevner, R.F. (2005). Pax6, Tbr2, and Tbr1 are expressed sequentially by radial glia, intermediate progenitor cells, and postmitotic neurons in developing neocortex. J Neurosci 25, 247-251.

Englund, C., Kowalczyk, T., Daza, R.A., Dagan, A., Lau, C., Rose, M.F., and Hevner, R.F. (2006). Unipolar brush cells of the cerebellum are produced in the rhombic lip and migrate through developing white matter. J Neurosci 26, 9184-9195.

Ericson, J., Rashbass, P., Schedl, A., Brenner-Morton, S., Kawakami, A., van Heyningen, V., Jessell, T.M., and Briscoe, J. (1997). Pax6 controls progenitor cell identity and neuronal fate in response to graded Shh signaling. Cell 90, 169-180.

Feder, J.N., Jan, L.Y., and Jan, Y.N. (1993). A rat gene with sequence homology to the Drosophila gene hairy is rapidly induced by growth factors known to influence neuronal differentiation. Mol Cell Biol 13, 105-113.

Fehon, R.G., Kooh, P.J., Rebay, I., Regan, C.L., Xu, T., Muskavitch, M.A., and Artavanis-Tsakonas, S. (1990). Molecular interactions between the protein products of the neurogenic loci Notch and Delta, two EGF-homologous genes in Drosophila. Cell 61, 523-534.

Fields, S., Ternyak, K., Gao, H., Ostraat, R., Akerlund, J., and Hagman, J. (2008). The 'zinc knuckle' motif of Early B cell Factor is required for transcriptional activation of B cell-specific genes. Mol Immunol 45, 3786-3796.

Fink, A.J., Englund, C., Daza, R.A., Pham, D., Lau, C., Nivison, M., Kowalczyk, T., and Hevner, R.F. (2006). Development of the deep cerebellar nuclei: transcription factors and cell migration from the rhombic lip. J Neurosci 26, 3066-3076.

Fode, C., Gradwohl, G., Morin, X., Dierich, A., LeMeur, M., Goridis, C., and Guillemot, F. (1998). The bHLH protein NEUROGENIN 2 is a determination factor for epibranchial placode-derived sensory neurons. Neuron 20, 483-494.

Fortini, M.E., and Artavanis-Tsakonas, S. (1994). The suppressor of hairless protein participates in notch receptor signaling. Cell 79, 273-282.

Frise, E., Knoblich, J.A., Younger-Shepherd, S., Jan, L.Y., and Jan, Y.N. (1996). The Drosophila Numb protein inhibits signaling of the Notch receptor during cell-cell interaction in sensory organ lineage. Proc Natl Acad Sci U S A 93, 11925-11932.

Fryer, C.J., Lamar, E., Turbachova, I., Kintner, C., and Jones, K.A. (2002). Mastermind mediates chromatin-specific transcription and turnover of the Notch enhancer complex. Genes Dev 16, 1397-1411.

Fryer, C.J., White, J.B., and Jones, K.A. (2004). Mastermind recruits CycC:CDK8 to phos-

phorylate the Notch ICD and coordinate activation with turnover. Mol Cell 16, 509-520.

Galileo, D.S., Gray, G.E., Owens, G.C., Majors, J., and Sanes, J.R. (1990). Neurons and glia arise from a common progenitor in chicken optic tectum: demonstration with two retroviruses and cell type-specific antibodies. Proc Natl Acad Sci U S A 87, 458-462.

Garcia-Bellido, A. (1979). Genetic Analysis of the Achaete-Scute System of DROSOPHILA MELANOGASTER. Genetics 91, 491-520.

Garcia-Dominguez, M., Poquet, C., Garel, S., and Charnay, P. (2003). Ebf gene function is required for coupling neuronal differentiation and cell cycle exit. Development 130, 6013-6025.

Garel, S., Garcia-Dominguez, M., and Charnay, P. (2000). Control of the migratory pathway of facial branchiomotor neurones. Development 127, 5297-5307.

Garel, S., Marin, F., Grosschedl, R., and Charnay, P. (1999). Ebf1 controls early cell differentiation in the embryonic striatum. Development 126, 5285-5294.

Garel, S., Marin, F., Mattei, M.G., Vesque, C., Vincent, A., and Charnay, P. (1997). Family of Ebf/Olf-1-related genes potentially involved in neuronal differentiation and regional specification in the central nervous system. Dev Dyn 210, 191-205.

Gavalas, A., Davenne, M., Lumsden, A., Chambon, P., and Rijli, F.M. (1997). Role of Hoxa-2 in axon pathfinding and rostral hindbrain patterning. Development 124, 3693-3702.

Georgia, S., Soliz, R., Li, M., Zhang, P., and Bhushan, A. (2006). p57 and Hes1 coordinate cell cycle exit with self-renewal of pancreatic progenitors. Dev Biol 298, 22-31.

Ghosh, B., and Leach, S.D. (2006). Interactions between hairy/enhancer of split-related proteins and the pancreatic transcription factor Ptf1-p48 modulate function of the PTF1 transcriptional complex. Biochem J 393, 679-685.

Gisler, R., Akerblad, P., and Sigvardsson, M. (1999). A human early B-cell factor-like protein participates in the regulation of the human CD19 promoter. Mol Immunol 36, 1067-1077.

Gisler, R., Jacobsen, S.E., and Sigvardsson, M. (2000). Cloning of human early B-cell factor and identification of target genes suggest a conserved role in B-cell development in man and mouse. Blood 96, 1457-1464.

Goebel, P., Janney, N., Valenzuela, J.R., Romanow, W.J., Murre, C., and Feeney, A.J. (2001). Localized gene-specific induction of accessibility to V(D)J recombination induced by E2A and early B cell factor in nonlymphoid cells. J Exp Med 194, 645-656.

Gonzalez, F., Romani, S., Cubas, P., Modolell, J., and Campuzano, S. (1989). Molecular analysis of the asense gene, a member of the achaete-scute complex of Drosophila melanogaster, and its novel role in optic lobe development. EMBO J 8, 3553-3562.

Gotz, M. (2003). Glial cells generate neurons--master control within CNS regions: developmental perspectives on neural stem cells. Neuroscientist 9, 379-397.

Grbavec, D., and Stifani, S. (1996). Molecular interaction between TLE1 and the carboxyl-terminal domain of HES-1 containing the WRPW motif. Biochem Biophys Res Commun 223, 701-705.

Greenwald, I. (1998). LIN-12/Notch signaling: lessons from worms and flies. Genes Dev 12, 1751-1762.

Grove, E.A., Williams, B.P., Li, D.Q., Hajihosseini, M., Friedrich, A., and Price, J. (1993). Multiple restricted lineages in the embryonic rat cerebral cortex. Development 117, 553-561.

Gulyas, B.J. (1975). A reexamination of cleavage patterns in eutherian mammalian eggs: rotation of blastomere pairs during second cleavage in the rabbit. J Exp Zool 193, 235-248.

Gupta-Rossi, N., Six, E., LeBail, O., Logeat, F., Chastagner, P., Olry, A., Israel, A., and Brou, C. (2004). Monoubiquitination and endocytosis direct gamma-secretase cleavage of activated Notch receptor. J Cell Biol 166, 73-83.

Hagman, J., Belanger, C., Travis, A., Turck, C.W., and Grosschedl, R. (1993). Cloning and functional characterization of early B-cell factor, a regulator of lymphocyte-specific gene

expression. Genes Dev 7, 760-773.

Hagman, J., Gutch, M.J., Lin, H., and Grosschedl, R. (1995). EBF contains a novel zinc co-ordination motif and multiple dimerization and transcriptional activation domains. EMBO J 14, 2907-2916.

Hagman, J., Travis, A., and Grosschedl, R. (1991). A novel lineage-specific nuclear factor regulates mb-1 gene transcription at the early stages of B cell differentiation. EMBO J 10, 3409-3417.

Hallonet, M.E., Teillet, M.A., and Le Douarin, N.M. (1990). A new approach to the development of the cerebellum provided by the quail-chick marker system. Development 108, 19-31.

Hamada, Y., Kadokawa, Y., Okabe, M., Ikawa, M., Coleman, J.R., and Tsujimoto, Y. (1999). Mutation in ankyrin repeats of the mouse Notch2 gene induces early embryonic lethality. Development 126, 3415-3424.

Harland, R.M. (1991). In situ hybridization: an improved whole-mount method for Xenopus embryos. Methods Cell Biol 36, 685-695.

Hartfuss, E., Forster, E., Bock, H.H., Hack, M.A., Leprince, P., Luque, J.M., Herz, J., Frotscher, M., and Gotz, M. (2003). Reelin signaling directly affects radial glia morphology and biochemical maturation. Development 130, 4597-4609.

Hartman, J., Muller, P., Foster, J.S., Wimalasena, J., Gustafsson, J.A., and Strom, A. (2004). HES-1 inhibits 17beta-estradiol and heregulin-beta1-mediated upregulation of E2F-1. Oncogene 23, 8826-8833.

Hashimoto, H., Itoh, M., Yamanaka, Y., Yamashita, S., Shimizu, T., Solnica-Krezel, L., Hibi, M., and Hirano, T. (2000). Zebrafish Dkk1 functions in forebrain specification and axial mesendoderm formation. Dev Biol 217, 138-152.

Hata, A., Lagna, G., Massague, J., and Hemmati-Brivanlou, A. (1998). Smad6 inhibits BMP/Smad1 signaling by specifically competing with the Smad4 tumor suppressor. Genes Dev 12, 186-197.

Hata, A., Seoane, J., Lagna, G., Montalvo, E., Hemmati-Brivanlou, A., and Massague, J. (2000). OAZ uses distinct DNA- and protein-binding zinc fingers in separate BMP-Smad and Olf signaling pathways. Cell 100, 229-240.

Hatakeyama, J., Bessho, Y., Katoh, K., Ookawara, S., Fujioka, M., Guillemot, F., and Kageyama, R. (2004). Hes genes regulate size, shape and histogenesis of the nervous system by control of the timing of neural stem cell differentiation. Development 131, 5539-5550.

Haubensak, W., Attardo, A., Denk, W., and Huttner, W.B. (2004). Neurons arise in the basal neuroepithelium of the early mammalian telencephalon: a major site of neurogenesis. Proc Natl Acad Sci U S A 101, 3196-3201.

Hayashi, H., Abdollah, S., Qiu, Y., Cai, J., Xu, Y.Y., Grinnell, B.W., Richardson, M.A., Topper, J.N., Gimbrone, M.A., Jr., Wrana, J.L., et al. (1997). The MAD-related protein Smad7 associates with the TGFbeta receptor and functions as an antagonist of TGFbeta signaling. Cell 89, 1165-1173.

Heisenberg, C.P., Tada, M., Rauch, G.J., Saude, L., Concha, M.L., Geisler, R., Stemple, D.L., Smith, J.C., and Wilson, S.W. (2000). Silberblick/Wnt11 mediates convergent extension movements during zebrafish gastrulation. Nature 405, 76-81.

Hevner, R.F., Hodge, R.D., Daza, R.A., and Englund, C. (2006). Transcription factors in glutamatergic neurogenesis: conserved programs in neocortex, cerebellum, and adult hippocampus. Neurosci Res 55, 223-233.

Hirata, H., Bessho, Y., Kokubu, H., Masamizu, Y., Yamada, S., Lewis, J., and Kageyama, R. (2004). Instability of Hes7 protein is crucial for the somite segmentation clock. Nat Genet 36, 750-754.

Hirata, H., Ohtsuka, T., Bessho, Y., and Kageyama, R. (2000). Generation of structurally and functionally distinct factors from the basic helix-loop-helix gene Hes3 by alternative first

exons. J Biol Chem 275, 19083-19089.

Hirata, H., Tomita, K., Bessho, Y., and Kageyama, R. (2001). Hes1 and Hes3 regulate maintenance of the isthmic organizer and development of the mid/hindbrain. EMBO J 20, 4454-4466.

Hirata, H., Yoshiura, S., Ohtsuka, T., Bessho, Y., Harada, T., Yoshikawa, K., and Kageyama, R. (2002). Oscillatory expression of the bHLH factor Hes1 regulated by a negative feedback loop. Science 298, 840-843.

Hojo, M., Ohtsuka, T., Hashimoto, N., Gradwohl, G., Guillemot, F., and Kageyama, R. (2000). Glial cell fate specification modulated by the bHLH gene Hes5 in mouse retina. Development 127, 2515-2522.

Hoshino, M. (2006). Molecular machinery governing GABAergic neuron specification in the cerebellum. Cerebellum 5, 193-198.

Hoshino, M., Nakamura, S., Mori, K., Kawauchi, T., Terao, M., Nishimura, Y.V., Fukuda, A., Fuse, T., Matsuo, N., Sone, M., et al. (2005). Ptf1a, a bHLH transcriptional gene, defines GABAergic neuronal fates in cerebellum. Neuron 47, 201-213.

Hsieh, J.J., Zhou, S., Chen, L., Young, D.B., and Hayward, S.D. (1999). CIR, a corepressor linking the DNA binding factor CBF1 to the histone deacetylase complex. Proc Natl Acad Sci U S A 96, 23-28.

Huang, Q., Raya, A., DeJesus, P., Chao, S.H., Quon, K.C., Caldwell, J.S., Chanda, S.K., Izpisua-Belmonte, J.C., and Schultz, P.G. (2004). Identification of p53 regulators by genome-wide functional analysis. Proc Natl Acad Sci U S A 101, 3456-3461.

Huang, S., Laoukili, J., Epping, M.T., Koster, J., Holzel, M., Westerman, B.A., Nijkamp, W., Hata, A., Asgharzadeh, S., Seeger, R.C., et al. (2009). ZNF423 is critically required for retinoic acid-induced differentiation and is a marker of neuroblastoma outcome. Cancer Cell 15, 328-340.

Huelsken, J., and Birchmeier, W. (2001). New aspects of Wnt signaling pathways in higher vertebrates. Curr Opin Genet Dev 11, 547-553.

Huttner, W.B., and Brand, M. (1997). Asymmetric division and polarity of neuroepithelial cells. Curr Opin Neurobiol 7, 29-39.

Iacopetti, P., Barsacchi, G., Tirone, F., Maffei, L., and Cremisi, F. (1994). Developmental expression of PC3 gene is correlated with neuronal cell birthday. Mech Dev 47, 127-137.

Iacopetti, P., Michelini, M., Stuckmann, I., Oback, B., Aaku-Saraste, E., and Huttner, W.B. (1999). Expression of the antiproliferative gene TIS21 at the onset of neurogenesis identifies single neuroepithelial cells that switch from proliferative to neuron-generating division. Proc Natl Acad Sci U S A 96, 4639-4644.

Imayoshi, I., Sakamoto, M., Ohtsuka, T., Takao, K., Miyakawa, T., Yamaguchi, M., Mori, K., Ikeda, T., Itohara, S., and Kageyama, R. (2008). Roles of continuous neurogenesis in the structural and functional integrity of the adult forebrain. Nat Neurosci 11, 1153-1161.

Inman, G.J., and Hill, C.S. (2002). Stoichiometry of active smad-transcription factor complexes on DNA. J Biol Chem 277, 51008-51016.

Irving, C., and Mason, I. (2000). Signalling by FGF8 from the isthmus patterns anterior hindbrain and establishes the anterior limit of Hox gene expression. Development 127, 177-186.

Ishibashi, M., Ang, S.L., Shiota, K., Nakanishi, S., Kageyama, R., and Guillemot, F. (1995). Targeted disruption of mammalian hairy and Enhancer of split homolog-1 (HES-1) leads to up-regulation of neural helix-loop-helix factors, premature neurogenesis, and severe neural tube defects. Genes Dev 9, 3136-3148.

Ishibashi, M., Moriyoshi, K., Sasai, Y., Shiota, K., Nakanishi, S., and Kageyama, R. (1994). Persistent expression of helix-loop-helix factor HES-1 prevents mammalian neural differentiation in the central nervous system. EMBO J 13, 1799-1805.

Ishibashi, M., Sasai, Y., Nakanishi, S., and Kageyama, R. (1993). Molecular characterization

of HES-2, a mammalian helix-loop-helix factor structurally related to Drosophila hairy and Enhancer of split. Eur J Biochem 215, 645-652.

Ishida, W., Hamamoto, T., Kusanagi, K., Yagi, K., Kawabata, M., Takehara, K., Sampath, T.K., Kato, M., and Miyazono, K. (2000). Smad6 is a Smad1/5-induced smad inhibitor. Characterization of bone morphogenetic protein-responsive element in the mouse Smad6 promoter. J Biol Chem 275, 6075-6079.

Iso, T., Chung, G., Hamamori, Y., and Kedes, L. (2002). HERP1 is a cell type-specific primary target of Notch. J Biol Chem 277, 6598-6607.

Iso, T., Sartorelli, V., Poizat, C., Iezzi, S., Wu, H.Y., Chung, G., Kedes, L., and Hamamori, Y. (2001). HERP, a novel heterodimer partner of HES/E(spl) in Notch signaling. Mol Cell Biol 21, 6080-6089.

Jarriault, S., and Greenwald, I. (2005). Evidence for functional redundancy between C. elegans ADAM proteins SUP-17/Kuzbanian and ADM-4/TACE. Dev Biol 287, 1-10.

Jennings, B., Preiss, A., Delidakis, C., and Bray, S. (1994). The Notch signalling pathway is required for Enhancer of split bHLH protein expression during neurogenesis in the Drosophila embryo. Development 120, 3537-3548.

Jensen, J., Pedersen, E.E., Galante, P., Hald, J., Heller, R.S., Ishibashi, M., Kageyama, R., Guillemot, F., Serup, P., and Madsen, O.D. (2000). Control of endodermal endocrine development by Hes-1. Nat Genet 24, 36-44.

Jogi, A., Persson, P., Grynfeld, A., Pahlman, S., and Axelson, H. (2002). Modulation of basic helix-loop-helix transcription complex formation by Id proteins during neuronal differentiation. J Biol Chem 277, 9118-9126.

Jones-Villeneuve, E.M., McBurney, M.W., Rogers, K.A., and Kalnins, V.I. (1982). Retinoic acid induces embryonal carcinoma cells to differentiate into neurons and glial cells. J Cell Biol 94, 253-262.

Kageyama, R., Ohtsuka, T., and Kobayashi, T. (2007). The Hes gene family: repressors and oscillators that orchestrate embryogenesis. Development 134, 1243-1251.

Kageyama, R., Ohtsuka, T., and Kobayashi, T. (2008). Roles of Hes genes in neural development. Dev Growth Differ 50 Suppl 1, S97-103.

Kao, H.Y., Ordentlich, P., Koyano-Nakagawa, N., Tang, Z., Downes, M., Kintner, C.R., Evans, R.M., and Kadesch, T. (1998). A histone deacetylase corepressor complex regulates the Notch signal transduction pathway. Genes Dev 12, 2269-2277.

Kiecker, C., and Niehrs, C. (2001). A morphogen gradient of Wnt/beta-catenin signalling regulates anteroposterior neural patterning in Xenopus. Development 128, 4189-4201.

Kimmel, R.A., Turnbull, D.H., Blanquet, V., Wurst, W., Loomis, C.A., and Joyner, A.L. (2000). Two lineage boundaries coordinate vertebrate apical ectodermal ridge formation. Genes Dev 14, 1377-1389.

Kokubo, H., Lun, Y., and Johnson, R.L. (1999). Identification and expression of a novel family of bHLH cDNAs related to Drosophila hairy and enhancer of split. Biochem Biophys Res Commun 260, 459-465.

Kosodo, Y., Roper, K., Haubensak, W., Marzesco, A.M., Corbeil, D., and Huttner, W.B. (2004). Asymmetric distribution of the apical plasma membrane during neurogenic divisions of mammalian neuroepithelial cells. EMBO J 23, 2314-2324.

Koyano-Nakagawa, N., Kim, J., Anderson, D., and Kintner, C. (2000). Hes6 acts in a positive feedback loop with the neurogenins to promote neuronal differentiation. Development 127, 4203-4216.

Krebs, L.T., Deftos, M.L., Bevan, M.J., and Gridley, T. (2001). The Nrarp gene encodes an ankyrin-repeat protein that is transcriptionally regulated by the notch signaling pathway. Dev Biol 238, 110-119.

Krishna, S.S., Majumdar, I., and Grishin, N.V. (2003). Structural classification of zinc fingers: survey and summary. Nucleic Acids Res 31, 532-550.

Ku, M., Howard, S., Ni, W., Lagna, G., and Hata, A. (2006). OAZ regulates bone morphogenetic protein signaling through Smad6 activation. J Biol Chem 281, 5277-5287.

Ku, M.C., Stewart, S., and Hata, A. (2003). Poly(ADP-ribose) polymerase 1 interacts with OAZ and regulates BMP-target genes. Biochem Biophys Res Commun 311, 702-707.

Kudrycki, K., Stein-Izsak, C., Behn, C., Grillo, M., Akeson, R., and Margolis, F.L. (1993). Olf-1-binding site: characterization of an olfactory neuron-specific promoter motif. Mol Cell Biol 13, 3002-3014.

Kurooka, H., and Honjo, T. (2000). Functional interaction between the mouse notch1 intracellular region and histone acetyltransferases PCAF and GCN5. J Biol Chem 275, 17211-17220.

Lamar, E., Deblandre, G., Wettstein, D., Gawantka, V., Pollet, N., Niehrs, C., and Kintner, C. (2001). Nrarp is a novel intracellular component of the Notch signaling pathway. Genes Dev 15, 1885-1899.

Lamar, E., and Kintner, C. (2005). The Notch targets Esr1 and Esr10 are differentially regulated in Xenopus neural precursors. Development 132, 3619-3630.

Lee, B.M., Xu, J., Clarkson, B.K., Martinez-Yamout, M.A., Dyson, H.J., Case, D.A., Gottesfeld, J.M., and Wright, P.E. (2006). Induced fit and "lock and key" recognition of 5S RNA by zinc fingers of transcription factor IIIA. J Mol Biol 357, 275-291.

Lee, J.C., Smith, S.B., Watada, H., Lin, J., Scheel, D., Wang, J., Mirmira, R.G., and German, M.S. (2001). Regulation of the pancreatic pro-endocrine gene neurogenin3. Diabetes 50, 928-936.

Leimeister, C., Externbrink, A., Klamt, B., and Gessler, M. (1999). Hey genes: a novel subfamily of hairy- and Enhancer of split related genes specifically expressed during mouse embryogenesis. Mech Dev 85, 173-177.

Leimeister, C., Schumacher, N., Steidl, C., and Gessler, M. (2000). Analysis of HeyL expression in wild-type and Notch pathway mutant mouse embryos. Mech Dev 98, 175-178.

Lekven, A.C., Thorpe, C.J., Waxman, J.S., and Moon, R.T. (2001). Zebrafish wnt8 encodes two wnt8 proteins on a bicistronic transcript and is required for mesoderm and neurectoderm patterning. Dev Cell 1, 103-114.

Leyns, L., Bouwmeester, T., Kim, S.H., Piccolo, S., and De Robertis, E.M. (1997). Frzb-1 is a secreted antagonist of Wnt signaling expressed in the Spemann organizer. Cell 88, 747-756.

Li, H., Malbon, C.C., and Wang, H.Y. (2004). Gene profiling of Frizzled-1 and Frizzled-2 signaling: expression of G-protein-coupled receptor chimeras in mouse F9 teratocarcinoma embryonal cells. Mol Pharmacol 65, 45-55.

Liberg, D., Sigvardsson, M., and Akerblad, P. (2002). The EBF/Olf/Collier family of transcription factors: regulators of differentiation in cells originating from all three embryonal germ layers. Mol Cell Biol 22, 8389-8397.

Lim, R.W., Varnum, B.C., and Herschman, H.R. (1987). Cloning of tetradecanoyl phorbol ester-induced 'primary response' sequences and their expression in density-arrested Swiss 3T3 cells and a TPA non-proliferative variant. Oncogene 1, 263-270.

Lin, D., Edwards, A.S., Fawcett, J.P., Mbamalu, G., Scott, J.D., and Pawson, T. (2000). A mammalian PAR-3-PAR-6 complex implicated in Cdc42/Rac1 and aPKC signalling and cell polarity. Nat Cell Biol 2, 540-547.

Lin, H., and Grosschedl, R. (1995). Failure of B-cell differentiation in mice lacking the transcription factor EBF. Nature 376, 263-267.

Lin, S.E., Oyama, T., Nagase, T., Harigaya, K., and Kitagawa, M. (2002). Identification of new human mastermind proteins defines a family that consists of positive regulators for notch signaling. J Biol Chem 277, 50612-50620.

Litingtung, Y., and Chiang, C. (2000). Specification of ventral neuron types is mediated by an antagonistic interaction between Shh and Gli3. Nat Neurosci 3, 979-985.

Liu, A., Li, J., Marin-Husstege, M., Kageyama, R., Fan, Y., Gelinas, C., and Casaccia-Bonnefil, P. (2006). A molecular insight of Hes5-dependent inhibition of myelin gene expression: old partners and new players. EMBO J 25, 4833-4842.

Livak, K.J., and Schmittgen, T.D. (2001). Analysis of relative gene expression data using real-time quantitative PCR and the 2(-Delta Delta C(T)) Method. Methods 25, 402-408.

Lobe, C.G. (1997). Expression of the helix-loop-helix factor, Hes3, during embryo development suggests a role in early midbrain-hindbrain patterning. Mech Dev 62, 227-237.

Low, S.H., Li, X., Miura, M., Kudo, N., Quinones, B., and Weimbs, T. (2003). Syntaxin 2 and endobrevin are required for the terminal step of cytokinesis in mammalian cells. Dev Cell 4, 753-759.

Lowell, S., Benchoua, A., Heavey, B., and Smith, A.G. (2006). Notch promotes neural lineage entry by pluripotent embryonic stem cells. PLoS Biol 4, e121.

Lu, D., Searles, M.A., and Klug, A. (2003). Crystal structure of a zinc-finger-RNA complex reveals two modes of molecular recognition. Nature 426, 96-100.

Lutolf, S., Radtke, F., Aguet, M., Suter, U., and Taylor, V. (2002). Notch1 is required for neuronal and glial differentiation in the cerebellum. Development 129, 373-385.

Ma, Q., Chen, Z., del Barco Barrantes, I., de la Pompa, J.L., and Anderson, D.J. (1998). neurogenin1 is essential for the determination of neuronal precursors for proximal cranial sensory ganglia. Neuron 20, 469-482.

Ma, Q., Fode, C., Guillemot, F., and Anderson, D.J. (1999). Neurogenin1 and neurogenin2 control two distinct waves of neurogenesis in developing dorsal root ganglia. Genes Dev 13, 1717-1728.

Machold, R., and Fishell, G. (2005). Math1 is expressed in temporally discrete pools of cerebellar rhombic-lip neural progenitors. Neuron 48, 17-24.

Machold, R.P., Kittell, D.J., and Fishell, G.J. (2007). Antagonism between Notch and bone morphogenetic protein receptor signaling regulates neurogenesis in the cerebellar rhombic lip. Neural Dev 2, 5.

Maden, M. (1996). Retinoids in patterning: chimeras win by a knockout. Curr Biol 6, 790-793.

Maier, M.M., and Gessler, M. (2000). Comparative analysis of the human and mouse Hey1 promoter: Hey genes are new Notch target genes. Biochem Biophys Res Commun 275, 652-660.

Malatesta, P., Hack, M.A., Hartfuss, E., Kettenmann, H., Klinkert, W., Kirchhoff, F., and Gotz, M. (2003). Neuronal or glial progeny: regional differences in radial glia fate. Neuron 37, 751-764.

Malatesta, P., Hartfuss, E., and Gotz, M. (2000). Isolation of radial glial cells by fluorescent-activated cell sorting reveals a neuronal lineage. Development 127, 5253-5263.

Malgaretti, N., Pozzoli, O., Bosetti, A., Corradi, A., Ciarmatori, S., Panigada, M., Bianchi, M.E., Martinez, S., and Consalez, G.G. (1997). Mmot1, a new helix-loop-helix transcription factor gene displaying a sharp expression boundary in the embryonic mouse brain. J Biol Chem 272, 17632-17639.

Marin, F., and Puelles, L. (1995). Morphological fate of rhombomeres in quail/chick chimeras: a segmental analysis of hindbrain nuclei. Eur J Neurosci 7, 1714-1738.

Martinez, S., Crossley, P.H., Cobos, I., Rubenstein, J.L., and Martin, G.R. (1999). FGF8 induces formation of an ectopic isthmic organizer and isthmocerebellar development via a repressive effect on Otx2 expression. Development 126, 1189-1200.

Masamizu, Y., Ohtsuka, T., Takashima, Y., Nagahara, H., Takenaka, Y., Yoshikawa, K., Okamura, H., and Kageyama, R. (2006). Real-time imaging of the somite segmentation clock: revelation of unstable oscillators in the individual presomitic mesoderm cells. Proc Natl Acad Sci U S A 103, 1313-1318.

Massari, M.E., and Murre, C. (2000). Helix-loop-helix proteins: regulators of transcription

in eucaryotic organisms. Mol Cell Biol 20, 429-440.

Matter-Sadzinski, L., Puzianowska-Kuznicka, M., Hernandez, J., Ballivet, M., and Matter, J.M. (2005). A bHLH transcriptional network regulating the specification of retinal ganglion cells. Development 132, 3907-3921.

McBurney, M.W., Jones-Villeneuve, E.M., Edwards, M.K., and Anderson, P.J. (1982). Control of muscle and neuronal differentiation in a cultured embryonal carcinoma cell line. Nature 299, 165-167.

McBurney, M.W., and Rogers, B.J. (1982). Isolation of male embryonal carcinoma cells and their chromosome replication patterns. Dev Biol 89, 503-508.

McCarthy, M., Turnbull, D.H., Walsh, C.A., and Fishell, G. (2001). Telencephalic neural progenitors appear to be restricted to regional and glial fates before the onset of neurogenesis. J Neurosci 21, 6772-6781.

McGill, M.A., and McGlade, C.J. (2003). Mammalian numb proteins promote Notch1 receptor ubiquitination and degradation of the Notch1 intracellular domain. J Biol Chem 278, 23196-23203.

Meyers, E.N., Lewandoski, M., and Martin, G.R. (1998). An Fgf8 mutant allelic series generated by Cre- and Flp-mediated recombination. Nat Genet 18, 136-141.

Miller, J., McLachlan, A.D., and Klug, A. (1985). Repetitive zinc-binding domains in the protein transcription factor IIIA from Xenopus oocytes. EMBO J 4, 1609-1614.

Millet, S., Campbell, K., Epstein, D.J., Losos, K., Harris, E., and Joyner, A.L. (1999). A role for Gbx2 in repression of Otx2 and positioning the mid/hindbrain organizer. Nature 401, 161-164.

Mishra-Gorur, K., Rand, M.D., Perez-Villamil, B., and Artavanis-Tsakonas, S. (2002). Down-regulation of Delta by proteolytic processing. J Cell Biol 159, 313-324.

Miyata, T., Kawaguchi, A., Okano, H., and Ogawa, M. (2001). Asymmetric inheritance of radial glial fibers by cortical neurons. Neuron 31, 727-741.

Miyata, T., Kawaguchi, A., Saito, K., Kawano, M., Muto, T., and Ogawa, M. (2004). Asymmetric production of surface-dividing and non-surface-dividing cortical progenitor cells. Development 131, 3133-3145.

Mizuguchi, R., Sugimori, M., Takebayashi, H., Kosako, H., Nagao, M., Yoshida, S., Nabeshima, Y., Shimamura, K., and Nakafuku, M. (2001). Combinatorial roles of olig2 and neurogenin2 in the coordinated induction of pan-neuronal and subtype-specific properties of motoneurons. Neuron 31, 757-771.

Morales, D., and Hatten, M.E. (2006). Molecular markers of neuronal progenitors in the embryonic cerebellar anlage. J Neurosci 26, 12226-12236.

Mumm, J.S., Schroeter, E.H., Saxena, M.T., Griesemer, A., Tian, X., Pan, D.J., Ray, W.J., and Kopan, R. (2000). A ligand-induced extracellular cleavage regulates gamma-secretase-like proteolytic activation of Notch1. Mol Cell 5, 197-206.

Murata, K., Hattori, M., Hirai, N., Shinozuka, Y., Hirata, H., Kageyama, R., Sakai, T., and Minato, N. (2005). Hes1 directly controls cell proliferation through the transcriptional repression of p27Kip1. Mol Cell Biol 25, 4262-4271.

Nadarajah, B., and Parnavelas, J.G. (2002). Modes of neuronal migration in the developing cerebral cortex. Nat Rev Neurosci 3, 423-432.

Nakagawa, O., Nakagawa, M., Richardson, J.A., Olson, E.N., and Srivastava, D. (1999). HRT1, HRT2, and HRT3: a new subclass of bHLH transcription factors marking specific cardiac, somitic, and pharyngeal arch segments. Dev Biol 216, 72-84.

Nakao, A., Afrakhte, M., Moren, A., Nakayama, T., Christian, J.L., Heuchel, R., Itoh, S., Kawabata, M., Heldin, N.E., Heldin, C.H., et al. (1997). Identification of Smad7, a TGFbeta-inducible antagonist of TGF-beta signalling. Nature 389, 631-635.

Nakashima, K., Takizawa, T., Ochiai, W., Yanagisawa, M., Hisatsune, T., Nakafuku, M., Miyazono, K., Kishimoto, T., Kageyama, R., and Taga, T. (2001). BMP2-mediated alteration in

the developmental pathway of fetal mouse brain cells from neurogenesis to astrocytogenesis. Proc Natl Acad Sci U S A 98, 5868-5873.

Nguyen, V., Chokas, A.L., Stecca, B., and Ruiz i Altaba, A. (2005). Cooperative requirement of the Gli proteins in neurogenesis. Development 132, 3267-3279.

Nishimura, M., Isaka, F., Ishibashi, M., Tomita, K., Tsuda, H., Nakanishi, S., and Kageyama, R. (1998). Structure, chromosomal locus, and promoter of mouse Hes2 gene, a homologue of Drosophila hairy and Enhancer of split. Genomics 49, 69-75.

Noctor, S.C., Flint, A.C., Weissman, T.A., Dammerman, R.S., and Kriegstein, A.R. (2001). Neurons derived from radial glial cells establish radial units in neocortex. Nature 409, 714-720.

Noctor, S.C., Martinez-Cerdeno, V., Ivic, L., and Kriegstein, A.R. (2004). Cortical neurons arise in symmetric and asymmetric division zones and migrate through specific phases. Nat Neurosci 7, 136-144.

Ohsako, S., Hyer, J., Panganiban, G., Oliver, I., and Caudy, M. (1994). Hairy function as a DNA-binding helix-loop-helix repressor of Drosophila sensory organ formation. Genes Dev 8, 2743-2755.

Ohtsuka, T., Imayoshi, I., Shimojo, H., Nishi, E., Kageyama, R., and McConnell, S.K. (2006). Visualization of embryonic neural stem cells using Hes promoters in transgenic mice. Mol Cell Neurosci 31, 109-122.

Ohtsuka, T., Ishibashi, M., Gradwohl, G., Nakanishi, S., Guillemot, F., and Kageyama, R. (1999). Hes1 and Hes5 as notch effectors in mammalian neuronal differentiation. EMBO J 18, 2196-2207.

Oswald, F., Kostezka, U., Astrahantseff, K., Bourteele, S., Dillinger, K., Zechner, U., Ludwig, L., Wilda, M., Hameister, H., Knochel, W., et al. (2002). SHARP is a novel component of the Notch/RBP-Jkappa signalling pathway. EMBO J 21, 5417-5426.

Overstreet, E., Fitch, E., and Fischer, J.A. (2004). Fat facets and Liquid facets promote Delta endocytosis and Delta signaling in the signaling cells. Development 131, 5355-5366.

Panin, V.M., Papayannopoulos, V., Wilson, R., and Irvine, K.D. (1997). Fringe modulates Notch-ligand interactions. Nature 387, 908-912.

Paroush, Z., Finley, R.L., Jr., Kidd, T., Wainwright, S.M., Ingham, P.W., Brent, R., and Ish-Horowicz, D. (1994). Groucho is required for Drosophila neurogenesis, segmentation, and sex determination and interacts directly with hairy-related bHLH proteins. Cell 79, 805-815.

Pascual, M., Abasolo, I., Mingorance-Le Meur, A., Martinez, A., Del Rio, J.A., Wright, C.V., Real, F.X., and Soriano, E. (2007). Cerebellar GABAergic progenitors adopt an external granule cell-like phenotype in the absence of Ptf1a transcription factor expression. Proc Natl Acad Sci U S A 104, 5193-5198.

Peiffer, D.A., Von Bubnoff, A., Shin, Y., Kitayama, A., Mochii, M., Ueno, N., and Cho, K.W. (2005). A Xenopus DNA microarray approach to identify novel direct BMP target genes involved in early embryonic development. Dev Dyn 232, 445-456.

Pepinsky, R.B., Zeng, C., Wen, D., Rayhorn, P., Baker, D.P., Williams, K.P., Bixler, S.A., Ambrose, C.M., Garber, E.A., Miatkowski, K., et al. (1998). Identification of a palmitic acid-modified form of human Sonic hedgehog. J Biol Chem 273, 14037-14045.

Pierani, A., Brenner-Morton, S., Chiang, C., and Jessell, T.M. (1999). A sonic hedgehog-independent, retinoid-activated pathway of neurogenesis in the ventral spinal cord. Cell 97, 903-915.

Porter, J.A., von Kessler, D.P., Ekker, S.C., Young, K.E., Lee, J.J., Moses, K., and Beachy, P.A. (1995). The product of hedgehog autoproteolytic cleavage active in local and long-range signalling. Nature 374, 363-366.

Porter, J.A., Young, K.E., and Beachy, P.A. (1996). Cholesterol modification of hedgehog signaling proteins in animal development. Science 274, 255-259.

Pozzoli, O., Bosetti, A., Croci, L., Consalez, G.G., and Vetter, M.L. (2001). Xebf3 is a regulator of neuronal differentiation during primary neurogenesis in Xenopus. Dev Biol 233, 495-512.

Prasad, B.C., Ye, B., Zackhary, R., Schrader, K., Seydoux, G., and Reed, R.R. (1998). unc-3, a gene required for axonal guidance in Caenorhabditis elegans, encodes a member of the O/E family of transcription factors. Development 125, 1561-1568.

Rebay, I., Fleming, R.J., Fehon, R.G., Cherbas, L., Cherbas, P., and Artavanis-Tsakonas, S. (1991). Specific EGF repeats of Notch mediate interactions with Delta and Serrate: implications for Notch as a multifunctional receptor. Cell 67, 687-699.

Redies, C., and Takeichi, M. (1996). Cadherins in the developing central nervous system: an adhesive code for segmental and functional subdivisions. Dev Biol 180, 413-423.

Reifers, F., Bohli, H., Walsh, E.C., Crossley, P.H., Stainier, D.Y., and Brand, M. (1998). Fgf8 is mutated in zebrafish acerebellar (ace) mutants and is required for maintenance of midbrain-hindbrain boundary development and somitogenesis. Development 125, 2381-2395.

Rhyu, M.S., Jan, L.Y., and Jan, Y.N. (1994). Asymmetric distribution of numb protein during division of the sensory organ precursor cell confers distinct fates to daughter cells. Cell 76, 477-491.

Romanow, W.J., Langerak, A.W., Goebel, P., Wolvers-Tettero, I.L., van Dongen, J.J., Feeney, A.J., and Murre, C. (2000). E2A and EBF act in synergy with the V(D)J recombinase to generate a diverse immunoglobulin repertoire in nonlymphoid cells. Mol Cell 5, 343-353.

Ross, D.A., Hannenhalli, S., Tobias, J.W., Cooch, N., Shiekhattar, R., and Kadesch, T. (2006). Functional analysis of Hes-1 in preadipocytes. Mol Endocrinol 20, 698-705.

Ross, D.A., Rao, P.K., and Kadesch, T. (2004). Dual roles for the Notch target gene Hes-1 in the differentiation of 3T3-L1 preadipocytes. Mol Cell Biol 24, 3505-3513.

Rouault, J.P., Falette, N., Guehenneux, F., Guillot, C., Rimokh, R., Wang, Q., Berthet, C., Moyret-Lalle, C., Savatier, P., Pain, B., et al. (1996). Identification of BTG2, an antiproliferative p53-dependent component of the DNA damage cellular response pathway. Nat Genet 14, 482-486.

Sapir, A., Assa-Kunik, E., Tsruya, R., Schejter, E., and Shilo, B.Z. (2005). Unidirectional Notch signaling depends on continuous cleavage of Delta. Development 132, 123-132.

Sasai, Y., Kageyama, R., Tagawa, Y., Shigemoto, R., and Nakanishi, S. (1992). Two mammalian helix-loop-helix factors structurally related to Drosophila hairy and Enhancer of split. Genes Dev 6, 2620-2634.

Sasaki, H., Hui, C., Nakafuku, M., and Kondoh, H. (1997). A binding site for Gli proteins is essential for HNF-3beta floor plate enhancer activity in transgenics and can respond to Shh in vitro. Development 124, 1313-1322.

Sasaki, H., Nishizaki, Y., Hui, C., Nakafuku, M., and Kondoh, H. (1999). Regulation of Gli2 and Gli3 activities by an amino-terminal repression domain: implication of Gli2 and Gli3 as primary mediators of Shh signaling. Development 126, 3915-3924.

Sauer, M.E., and Walker, B.E. (1959). Radioautographic study of interkinetic nuclear migration in the neural tube. Proc Soc Exp Biol Med 101, 557-560.

Scardigli, R., Schuurmans, C., Gradwohl, G., and Guillemot, F. (2001). Crossregulation between Neurogenin2 and pathways specifying neuronal identity in the spinal cord. Neuron 31, 203-217.

Schroeter, E.H., Kisslinger, J.A., and Kopan, R. (1998). Notch-1 signalling requires ligand-induced proteolytic release of intracellular domain. Nature 393, 382-386.

Schuurmans, C., Armant, O., Nieto, M., Stenman, J.M., Britz, O., Klenin, N., Brown, C., Langevin, L.M., Seibt, J., Tang, H., et al. (2004). Sequential phases of cortical specification involve Neurogenin-dependent and -independent pathways. EMBO J 23, 2892-2902.

Sekiya, T., and Zaret, K.S. (2007). Repression by Groucho/TLE/Grg proteins: genomic site recruitment generates compacted chromatin in vitro and impairs activator binding in vivo.

Mol Cell 28, 291-303.

Selkoe, D., and Kopan, R. (2003). Notch and Presenilin: regulated intramembrane proteolysis links development and degeneration. Annu Rev Neurosci 26, 565-597.

Seoane, J., Le, H.V., Shen, L., Anderson, S.A., and Massague, J. (2004). Integration of Smad and forkhead pathways in the control of neuroepithelial and glioblastoma cell proliferation. Cell 117, 211-223.

Seto, E., Lewis, B., and Shenk, T. (1993). Interaction between transcription factors Sp1 and YY1. Nature 365, 462-464.

Shen, Q., Zhong, W., Jan, Y.N., and Temple, S. (2002). Asymmetric Numb distribution is critical for asymmetric cell division of mouse cerebral cortical stem cells and neuroblasts. Development 129, 4843-4853.

Shi, Y., Wang, Y.F., Jayaraman, L., Yang, H., Massague, J., and Pavletich, N.P. (1998). Crystal structure of a Smad MH1 domain bound to DNA: insights on DNA binding in TGF-beta signaling. Cell 94, 585-594.

Shim, S., Bae, N., and Han, J.K. (2002). Bone morphogenetic protein-4-induced activation of Xretpos is mediated by Smads and Olf-1/EBF associated zinc finger (OAZ). Nucleic Acids Res 30, 3107-3117.

Shim, S., Lee, S.K., and Han, J.K. (2000). A novel family of retrotransposons in Xenopus with a developmentally regulated expression. Genesis 26, 198-207.

Sidman, R.L., Miale, I.L., and Feder, N. (1959). Cell proliferation and migration in the primitive ependymal zone: an autoradiographic study of histogenesis in the nervous system. Exp Neurol 1, 322-333.

Sigvardsson, M., O'Riordan, M., and Grosschedl, R. (1997). EBF and E47 collaborate to induce expression of the endogenous immunoglobulin surrogate light chain genes. Immunity 7, 25-36.

Smith, E.M., Akerblad, P., Kadesch, T., Axelson, H., and Sigvardsson, M. (2005). Inhibition of EBF function by active Notch signaling reveals a novel regulatory pathway in early B-cell development. Blood 106, 1995-2001.

Smoller, D., Friedel, C., Schmid, A., Bettler, D., Lam, L., and Yedvobnick, B. (1990). The Drosophila neurogenic locus mastermind encodes a nuclear protein unusually rich in amino acid homopolymers. Genes Dev 4, 1688-1700.

Solecki, D.J., Liu, X.L., Tomoda, T., Fang, Y., and Hatten, M.E. (2001). Activated Notch2 signaling inhibits differentiation of cerebellar granule neuron precursors by maintaining proliferation. Neuron 31, 557-568.

Sonneveld, E., van den Brink, C.E., Tertoolen, L.G., van der Burg, B., and van der Saag, P.T. (1999). Retinoic acid hydroxylase (CYP26) is a key enzyme in neuronal differentiation of embryonal carcinoma cells. Dev Biol 213, 390-404.

Stifani, S., Blaumueller, C.M., Redhead, N.J., Hill, R.E., and Artavanis-Tsakonas, S. (1992). Human homologs of a Drosophila Enhancer of split gene product define a novel family of nuclear proteins. Nat Genet 2, 119-127.

Stopa, M., Benes, V., Ansorge, W., Gressner, A.M., and Dooley, S. (2000). Genomic locus and promoter region of rat Smad7, an important antagonist of TGFbeta signaling. Mamm Genome 11, 169-176.

Streit, A., Berliner, A.J., Papanayotou, C., Sirulnik, A., and Stern, C.D. (2000). Initiation of neural induction by FGF signalling before gastrulation. Nature 406, 74-78.

Strutt, D.I., Weber, U., and Mlodzik, M. (1997). The role of RhoA in tissue polarity and Frizzled signalling. Nature 387, 292-295.

Stuckmann, I., Weigmann, A., Shevchenko, A., Mann, M., and Huttner, W.B. (2001). Ephrin B1 is expressed on neuroepithelial cells in correlation with neocortical neurogenesis. J Neurosci 21, 2726-2737.

Sun, J., Kamei, C.N., Layne, M.D., Jain, M.K., Liao, J.K., Lee, M.E., and Chin, M.T.

(2001a). Regulation of myogenic terminal differentiation by the hairy-related transcription factor CHF2. J Biol Chem 276, 18591-18596.

Sun, L., Liu, A., and Georgopoulos, K. (1996). Zinc finger-mediated protein interactions modulate Ikaros activity, a molecular control of lymphocyte development. EMBO J 15, 5358-5369.

Sun, Y., Nadal-Vicens, M., Misono, S., Lin, M.Z., Zubiaga, A., Hua, X., Fan, G., and Greenberg, M.E. (2001b). Neurogenin promotes neurogenesis and inhibits glial differentiation by independent mechanisms. Cell 104, 365-376.

Swiatek, P.J., Lindsell, C.E., del Amo, F.F., Weinmaster, G., and Gridley, T. (1994). Notch1 is essential for postimplantation development in mice. Genes Dev 8, 707-719.

Takebayashi, K., Sasai, Y., Sakai, Y., Watanabe, T., Nakanishi, S., and Kageyama, R. (1994). Structure, chromosomal locus, and promoter analysis of the gene encoding the mouse helix-loop-helix factor HES-1. Negative autoregulation through the multiple N box elements. J Biol Chem 269, 5150-5156.

Takizawa, T., Ochiai, W., Nakashima, K., and Taga, T. (2003). Enhanced gene activation by Notch and BMP signaling cross-talk. Nucleic Acids Res 31, 5723-5731.

Tamagnone, L., and Comoglio, P.M. (2000). Signalling by semaphorin receptors: cell guidance and beyond. Trends Cell Biol 10, 377-383.

Tamamaki, N., Nakamura, K., Okamoto, K., and Kaneko, T. (2001). Radial glia is a progenitor of neocortical neurons in the developing cerebral cortex. Neurosci Res 41, 51-60.

Tang, S.J., Hoodless, P.A., Lu, Z., Breitman, M.L., McInnes, R.R., Wrana, J.L., and Buchwald, M. (1998). The Tlx-2 homeobox gene is a downstream target of BMP signalling and is required for mouse mesoderm development. Development 125, 1877-1887.

Tarabykin, V., Stoykova, A., Usman, N., and Gruss, P. (2001). Cortical upper layer neurons derive from the subventricular zone as indicated by Svet1 gene expression. Development 128, 1983-1993.

Tarassishin, L., Yin, Y.I., Bassit, B., and Li, Y.M. (2004). Processing of Notch and amyloid precursor protein by gamma-secretase is spatially distinct. Proc Natl Acad Sci U S A 101, 17050-17055.

Temple, S. (1989). Division and differentiation of isolated CNS blast cells in microculture. Nature 340, 471-473.

Tian, X., Hansen, D., Schedl, T., and Skeath, J.B. (2004). Epsin potentiates Notch pathway activity in Drosophila and C. elegans. Development 131, 5807-5815.

Travis, A., Hagman, J., Hwang, L., and Grosschedl, R. (1993). Purification of early-B-cell factor and characterization of its DNA-binding specificity. Mol Cell Biol 13, 3392-3400.

Tsai, R.Y., and Reed, R.R. (1997). Cloning and functional characterization of Roaz, a zinc finger protein that interacts with O/E-1 to regulate gene expression: implications for olfactory neuronal development. J Neurosci 17, 4159-4169.

Tsai, R.Y., and Reed, R.R. (1998). Identification of DNA recognition sequences and protein interaction domains of the multiple-Zn-finger protein Roaz. Mol Cell Biol 18, 6447-6456.

Turner, D.L., and Weintraub, H. (1994). Expression of achaete-scute homolog 3 in Xenopus embryos converts ectodermal cells to a neural fate. Genes Dev 8, 1434-1447.

Uemura, T., Shepherd, S., Ackerman, L., Jan, L.Y., and Jan, Y.N. (1989). numb, a gene required in determination of cell fate during sensory organ formation in Drosophila embryos. Cell 58, 349-360.

Van Doren, M., Bailey, A.M., Esnayra, J., Ede, K., and Posakony, J.W. (1994). Negative regulation of proneural gene activity: hairy is a direct transcriptional repressor of achaete. Genes Dev 8, 2729-2742.

Vetrivel, K.S., Cheng, H., Lin, W., Sakurai, T., Li, T., Nukina, N., Wong, P.C., Xu, H., and Thinakaran, G. (2004). Association of gamma-secretase with lipid rafts in post-Golgi and endosome membranes. J Biol Chem 279, 44945-44954.

Villares, R., and Cabrera, C.V. (1987). The achaete-scute gene complex of D. melanogaster: conserved domains in a subset of genes required for neurogenesis and their homology to myc. Cell 50, 415-424.

Vincent, V.A., DeVoss, J.J., Ryan, H.S., and Murphy, G.M., Jr. (2002). Analysis of neuronal gene expression with laser capture microdissection. J Neurosci Res 69, 578-586.

von Bubnoff, A., Peiffer, D.A., Blitz, I.L., Hayata, T., Ogata, S., Zeng, Q., Trunnell, M., and Cho, K.W. (2005). Phylogenetic footprinting and genome scanning identify vertebrate BMP response elements and new target genes. Dev Biol 281, 210-226.

Wallace, V.A. (1999). Purkinje-cell-derived Sonic hedgehog regulates granule neuron precursor cell proliferation in the developing mouse cerebellum. Curr Biol 9, 445-448.

Wallberg, A.E., Pedersen, K., Lendahl, U., and Roeder, R.G. (2002). p300 and PCAF act cooperatively to mediate transcriptional activation from chromatin templates by notch intracellular domains in vitro. Mol Cell Biol 22, 7812-7819.

Walsh, C., and Cepko, C.L. (1993). Clonal dispersion in proliferative layers of developing cerebral cortex. Nature 362, 632-635.

Wang, M.M., and Reed, R.R. (1993). Molecular cloning of the olfactory neuronal transcription factor Olf-1 by genetic selection in yeast. Nature 364, 121-126.

Wang, Q., Wei, X., Zhu, T., Zhang, M., Shen, R., Xing, L., O'Keefe, R.J., and Chen, D. (2007). Bone morphogenetic protein 2 activates Smad6 gene transcription through bone-specific transcription factor Runx2. J Biol Chem 282, 10742-10748.

Wang, S.S., Betz, A.G., and Reed, R.R. (2002). Cloning of a novel Olf-1/EBF-like gene, O/E-4, by degenerate oligo-based direct selection. Mol Cell Neurosci 20, 404-414.

Wang, S.S., Tsai, R.Y., and Reed, R.R. (1997). The characterization of the Olf-1/EBF-like HLH transcription factor family: implications in olfactory gene regulation and neuronal development. J Neurosci 17, 4149-4158.

Wang, S.W., Kim, B.S., Ding, K., Wang, H., Sun, D., Johnson, R.L., Klein, W.H., and Gan, L. (2001). Requirement for math5 in the development of retinal ganglion cells. Genes Dev 15, 24-29.

Wang, W., and Struhl, G. (2004). Drosophila Epsin mediates a select endocytic pathway that DSL ligands must enter to activate Notch. Development 131, 5367-5380.

Warming, S., Rachel, R.A., Jenkins, N.A., and Copeland, N.G. (2006). Zfp423 is required for normal cerebellar development. Mol Cell Biol 26, 6913-6922.

Wassarman, K.M., Lewandoski, M., Campbell, K., Joyner, A.L., Rubenstein, J.L., Martinez, S., and Martin, G.R. (1997). Specification of the anterior hindbrain and establishment of a normal mid/hindbrain organizer is dependent on Gbx2 gene function. Development 124, 2923-2934.

Weigmann, A., Corbeil, D., Hellwig, A., and Huttner, W.B. (1997). Prominin, a novel microvilli-specific polytopic membrane protein of the apical surface of epithelial cells, is targeted to plasmalemmal protrusions of non-epithelial cells. Proc Natl Acad Sci U S A 94, 12425-12430.

Weisheit, G., Gliem, M., Endl, E., Pfeffer, P.L., Busslinger, M., and Schilling, K. (2006). Postnatal development of the murine cerebellar cortex: formation and early dispersal of basket, stellate and Golgi neurons. Eur J Neurosci 24, 466-478.

Wettstein, D.A., Turner, D.L., and Kintner, C. (1997). The Xenopus homolog of Drosophila Suppressor of Hairless mediates Notch signaling during primary neurogenesis. Development 124, 693-702.

White, J.A., Ramshaw, H., Taimi, M., Stangle, W., Zhang, A., Everingham, S., Creighton, S., Tam, S.P., Jones, G., and Petkovich, M. (2000). Identification of the human cytochrome P450, P450RAI-2, which is predominantly expressed in the adult cerebellum and is responsible for all-trans-retinoic acid metabolism. Proc Natl Acad Sci U S A 97, 6403-6408.

Wightman, B., Baran, R., and Garriga, G. (1997). Genes that guide growth cones along the

C. elegans ventral nerve cord. Development 124, 2571-2580.

Willert, K., Brown, J.D., Danenberg, E., Duncan, A.W., Weissman, I.L., Reya, T., Yates, J.R., 3rd, and Nusse, R. (2003). Wnt proteins are lipid-modified and can act as stem cell growth factors. Nature 423, 448-452.

Williams, B.P., and Price, J. (1995). Evidence for multiple precursor cell types in the embryonic rat cerebral cortex. Neuron 14, 1181-1188.

Wilson, L., Gale, E., Chambers, D., and Maden, M. (2004). Retinoic acid and the control of dorsoventral patterning in the avian spinal cord. Dev Biol 269, 433-446.

Wilson, S.I., Graziano, E., Harland, R., Jessell, T.M., and Edlund, T. (2000). An early requirement for FGF signalling in the acquisition of neural cell fate in the chick embryo. Curr Biol 10, 421-429.

Wingate, R.J., and Hatten, M.E. (1999). The role of the rhombic lip in avian cerebellum development. Development 126, 4395-4404.

Wodarz, A., and Huttner, W.B. (2003). Asymmetric cell division during neurogenesis in Drosophila and vertebrates. Mech Dev 120, 1297-1309.

Wu, L., Sun, T., Kobayashi, K., Gao, P., and Griffin, J.D. (2002). Identification of a family of mastermind-like transcriptional coactivators for mammalian notch receptors. Mol Cell Biol 22, 7688-7700.

Yang, X.J., Ogryzko, V.V., Nishikawa, J., Howard, B.H., and Nakatani, Y. (1996). A p300/CBP-associated factor that competes with the adenoviral oncoprotein E1A. Nature 382, 319-324.

Yedvobnick, B., Smoller, D., Young, P., and Mills, D. (1988). Molecular analysis of the neurogenic locus mastermind of Drosophila melanogaster. Genetics 118, 483-497.

Yokota, Y. (2001). Id and development. Oncogene 20, 8290-8298.

Yoon, J.W., Kita, Y., Frank, D.J., Majewski, R.R., Konicek, B.A., Nobrega, M.A., Jacob, H., Walterhouse, D., and Iannaccone, P. (2002). Gene expression profiling leads to identification of GLI1-binding elements in target genes and a role for multiple downstream pathways in GLI1-induced cell transformation. J Biol Chem 277, 5548-5555.

Yun, K., Fischman, S., Johnson, J., Hrabe de Angelis, M., Weinmaster, G., and Rubenstein, J.L. (2002). Modulation of the notch signaling by Mash1 and Dlx1/2 regulates sequential specification and differentiation of progenitor cell types in the subcortical telencephalon. Development 129, 5029-5040.

Yun, T.J., and Bevan, M.J. (2003). Notch-regulated ankyrin-repeat protein inhibits Notch1 signaling: multiple Notch1 signaling pathways involved in T cell development. J Immunol 170, 5834-5841.

Zhong, W., Feder, J.N., Jiang, M.M., Jan, L.Y., and Jan, Y.N. (1996). Asymmetric localization of a mammalian numb homolog during mouse cortical neurogenesis. Neuron 17, 43-53.

Zhong, W., Jiang, M.M., Schonemann, M.D., Meneses, J.J., Pedersen, R.A., Jan, L.Y., and Jan, Y.N. (2000). Mouse numb is an essential gene involved in cortical neurogenesis. Proc Natl Acad Sci U S A 97, 6844-6849.

Zinyk, D.L., Mercer, E.H., Harris, E., Anderson, D.J., and Joyner, A.L. (1998). Fate mapping of the mouse midbrain-hindbrain constriction using a site-specific recombination system. Curr Biol 8, 665-668.

Zordan, P., Croci, L., Hawkes, R., and Consalez, G.G. (2008). Comparative analysis of proneural gene expression in the embryonic cerebellum. Dev Dyn 237, 1726-1735.

Thanks to...